ESCOLA DE CIÊNCIAS
PROGRAMA DE PÓS-GRADUAÇÃO EM BIOLOGIA CELULAR E MOLECULAR
DOUTORADO EM BIOLOGIA CELULAR E MOLECULAR

HENRIQUE BREGOLIN DIAS

# AVALIAÇÃO DO EFEITO DA FRUTOSE-1,6-BISFOSFATO NA PREVENÇÃO DA FIBROSE PULMONAR EXPERIMENTAL

Porto Alegre
2019

HENRIQUE BREGOLIN DIAS

# AVALIAÇÃO DO EFEITO DA FRUTOSE-1,6-BISFOSFATO NA PREVENÇÃO DA FIBROSE PULMONAR EXPERIMENTAL

Tese apresentada ao Curso de Pós-Graduação stricto sensu Doutorado em Biologia Celular e Molecular da Pontifícia Universidade Católica do Rio Grande do Sul como requisito parcial para obtenção do grau de Doutor em Biologia Celular e Molecular.

Orientador: Prof. Dr. Márcio V. F. Donadio

Co-orientador: Prof. Dr. Jarbas R. de Oliveira

Porto Alegre

2019

**FICHA CATALOGRÁFICA**

## Ficha Catalográfica

D541a Dias, Henrique Bregolin

Avaliação do efeito da Frutose-1,6-bisfosfato na prevenção da fibrose pulmonar experimental / Henrique Bregolin Dias . – 2019.
127.
Tese (Doutorado) – Programa de Pós-Graduação em Biologia Celular e Molecular, PUCRS.

Orientador: Prof. Dr. Márcio Vinícius Fagundes Donadio.
Co-orientador: Prof. Dr. Jarbas Rodrigues de Oliveira.

1. fibrose pulmonar. 2. frutose-1,6-bisfosfato. 3. bleomicina. 4. fibroblasto. 5. matriz extracelular. I. Donadio, Márcio Vinícius Fagundes. II. de Oliveira, Jarbas Rodrigues. III. Título.

Elaborada pelo Sistema de Geração Automática de Ficha Catalográfica da PUCRS
com os dados fornecidos pelo(a) autor(a).
Bibliotecária responsável: Salete Maria Sartori CRB-10/1363

*“**A vida é sofrimento**.”*

***Sidarta Gautama***

## AGRADECIMENTOS

Durante esses quatro anos, cruzei pelo caminho de muitas pessoas que, de alguma forma, sabendo ou não, me ensinaram pequenas ou grandes lições que guardarei para sempre.

Aos meus orientadores, Prof. Dr. Márcio Vinícius Fagundes Donadio e Prof. Dr. Jarbas Rodrigues de Oliveira. Obrigado por me aceitarem como aluno há 13 anos atrás na iniciação científica, por me ajudarem a publicar meu primeiro artigo, por sempre acreditarem em mim, pelas broncas e pelo estímulo durante todos esses anos.

À Dra. Shioko Kimura, que, mesmo sem me conhecer, me aceitou como aluno em seu laboratório, sendo sempre exigente e desejando o meu desenvolvimento pessoal e profissional. Por sempre contribuir com críticas valiosas e por me ensinar tanto. Por me abrir as portas do seu laboratório e por confiar em mim.

À Profa. Dr. Fernanda Bordignon Nunes, pelas ideias, conselhos, parceria, monitorias, histórias, torcida, novas parcerias, por todas as discussões e contribuições durantes nossos encontros ao longo desses anos.

Aos colegas dos Laboratórios de Biofísica Celular e Inflamação, de Respirologia Pediátrica e de Atividade Física em Pediatria da PUCRS e do Laboratório de Metabolismo do NCI, por todo auxílio e pelas risadas ao longo desse período. Em especial ao Renan Jost, por começar essa caminhada comigo, me ajudar a desenvolver e padronizar a técnica de indução de fibrose pulmonar, pelas longas discussões, caronas, preocupações, idas e vindas ao IPB, frustrações, alegrias e, principalmente pela amizade. A Gabriele Krause, pelos conselhos, conversas, cafés, artigos, jantas, GOT, sopas, pela companhia durante os experimentos e pela amizade.

À CAPES pela bolsa de Doutorado Sanduíche.

Aos meus pais, Salete e Zeca, e meu irmão Rafael, pelo amor e apoio incondicional nas horas de dúvida e pela grande saudade.

A todos, que de uma forma ou outra estiveram comigo durante essa etapa, meu mais sincero obrigado!

## RESUMO

Fibrose pulmonar (FP) é o resultado de um processo de lesão crônica no qual fibroblastos se tornam ativados e passam a secretar e depositar grandes quantidades de matriz extracelular (ECM). Este fato leva uma dificuldade na degradação da ECM, seguido por rigidez tecidual, perda de função tecidual e morte. A frutose-1,6-bisfosfato é um metabólito intermediário da rota glicolítica que vem sendo estudada há vários anos e tem demonstrado ações protetoras em diferentes tipos celulares e tecidos. Há evidências de que a FBP é capaz de prevenir o desenvolvimento da FP induzida por bleomicina (BLM) em camundongos, mas o mecanismo pelo qual isso acontece ainda é desconhecido. Assim, o objetivo deste estudo foi avaliar os efeitos da FBP sobre a prevenção e/ou regulação do processo fibrótico em um modelo experimental de FP *in vivo* e em células pulmonares *in vitro*. Para isso, tratamos animais que receberam BLM intratraqueal com FBP por 14 dias. Ainda, utilizamos culturas primárias de fibroblastos e miofibroblastos pulmonares extraídos de camundongos saudáveis e fibróticos, respectivamente. Analisamos, a função pulmonar, a expressão gênica de subtipos de colágenos e outros componentes importantes no processo fibrotico, assim como as taxas de proliferação, contração e migração celular, além das proteínas envolvidas na degradação da ECM. No modelo de FP, a FBP foi capaz de melhorar significativamente a função pulmonar, como demonstrado pela redução do depósito de colágeno e diminuição da expressão de genes relacionados à ECM, como colágeno e fibronectina. *In vitro*, miofibroblastos tratados com FBP por 3 dias demonstraram uma menor taxa de proliferação, contração e migração, o que são indícios de desativação e reversão fenotípica. Além disso, a FBP também diminui a expressão de genes e proteínas relacionados à ECM, como colágeno, fibronectina e actina de músculo liso α em cultura primária de miofibroblastos. MMP1, uma colagenase responsável pela degradação da ECM, teve sua expressão aumentada, enquanto a TIMP-1, um inibidor da MMP1, diminuiu. MMP2, que está associada ao aumento da invasão do tecido por miofibroblastos, também teve sua expressão diminuída. Nossos resultados demonstram que a FBP pode prevenir o desenvolvimento de FP induzida por BLM através da redução da produção e depósito de colágeno e outros componentes de ECM e isso pode ser mediado através do aumento da produção de MMP1 e diminuição da TIMP-1, o que promoveria uma degradação efetiva da ECM depositada no tecido.



**Palavras-chave:** fibrose pulmonar; bleomicina; frutose-1,6-bisfosfato; matriz extracelular; fibroblasto.

## ABSTRACT

Pulmonary fibrosis (PF) is the result of chronic injury where fibroblasts become activated and secrete large amounts of extracellular matrix (ECM), leading to impaired ECM degradation followed by tissue stiffness, loss of lung function and death. Fructose-1,6-bisphosphate is a metabolite from glycolytic pathway that has been studied for many years and showing beneficial actions in different cell lines and tissues. In a recent study from our laboratory, FBP was able to prevent the development of FP bleomycin (BLM)-induced on mice, but the underlying mechanism is still unknown. In this way, the objective of this study was to evaluate the effects of FBP under prevention and regulation of fibrotic process in PF mouse model and lung fibroblasts. In this way, we treated mice that received BLM intratracheally with FBP for 14 days. We also extracted lung fibroblasts and myofibroblasts from healthy and fibrotic animals, respectively. We analyzed lung function, gene expression of collagen subtypes and other important components of ECM, as well proliferation, contraction and migration rates, and proteins involved in ECM degradation. In PF mice model, lung function was improved by FBP as revealed by reduced collagen deposition and downregulation of ECM gene expression such as collagens and fibronectin. Myofibroblasts treated with FBP for 3 days *in vitro* showed decreased proliferation, contraction, and migration, which are characteristic of myofibroblast to fibroblast phenotype reversal. ECM-related genes and proteins such as collagens, fibronectin and α-smooth muscle actin, were downregulated in FBP-treated myofibroblasts *in vitro*. Moreover, MMP1, responsible for ECM degradation, and TIMP-1, a MMP1 inhibitor, were up and down regulated, respectively. MMP2, which is associated with fibroblast invasion on tissue, also was downregulated. These results demonstrate that FBP may prevent bleomycin-induced PF development through reduced expression of collagen and other ECM components mediated by a reduced TIMP-1 and increased MMP1 production, which would allow a better ECM degradation.



**Keywords:** pulmonary fibrosis; bleomycin; fructose-1,6-bisphosphate; extracellular matrix; fibroblast**.**

**LISTA DE FIGURAS**

CAPÍTULO I

Figura 1 – Representação de um pulmão saudável e outro com fibrose pulmonar idiopática (FPI).

Figura 2 – Mortalidade por fibrose pulmonar idiopática (FPI) no Brasil.

Figura 3 – Imagens de tomografia computadorizada de alta resolução (TCAR) demonstrando padrões de pneumonia intersticial usual (PIU).

Figura 4 – Histopatológico mostrando padrão de pneumonia intersticial usual (PIU).

## LISTA DE SIGLAS

α-SMA – Actina de Músculo Liso α

ATP – Adenosina Trifosfato

BLM – Bleomicina

BLMH – Bleomicina Hidrolase

CAT – Catalase

Col-1 – Colágeno Tipo 1

ECM – Matriz Extracelular

EMT – Transição Epitélio-Mesenquimal

eNOS – Óxido Nítrico Sintase Epitelial

ERK – Quinase Regulada por Sinal Extracelular

FBP – Frutose-1,6-bisfosfato

FDA – Food and Drug Administration

FGF – Fator de Crescimento de Fibroblasto

Fn1 – Fibronectina

FP – Fibrose Pulmonar

FPI – Fibrose Pulmonar Idiopática

GPx – Glutationa Peroxidase

HSC – Células Estreladas Epáticas

IL-10 – Interleucina 10

IT – Intra-traqueal

LBA – Lavado Broncoalveolar

LOX – Lisil Oxidase

MMP – Metaloproteinase de Matriz

MMP1 – Metaloproteinase de Matriz 1

MMP2 – Metaloproteinase de Matriz 2

NO – Óxido Nítrico

p38 MAPK - Proteína Quinase Ativada por Mitógeno P38

PDGF – Fator de Crescimento Derivado de Plaqueta

PFK - Fosfofrutoquinase

PIU – Pneumonia Intersticial Usual

PPAR-γ – Receptor Ativado por Proliferadores de Peroxissoma Gama

ROS – Espécies Reativas de Oxigênio

SIM – Sistema de Informação de Mortalidade

SOD – Superóxido Dismutase

TBARS – Espécies Reativas ao Ácido Tiobarbitúrico

TCAR – Tomografia Computadorizada de Alta Resolução

TGF-β1 – Fator de Crescimento Transformante β1

TIMP – Inibidor De Metaloproteinase Tecidual

TIMP-1 – Inibidor De Metaloproteinase Tecidual 1

TIMP-4 – Inibidor De Metaloproteinase Tecidual 4

TNF-α – Fator de Necrose Tumoral α

VEGF – Fator de Crescimento Vascular Endotelial

# SUMÁRIO

**CAPÍTULO I** ..... **12**

**INTRODUÇÃO** ..... **13**

1.1 Fibrose e Fibrose Pulmonar Idiopática ..... 13

1.2 Epidemiologia ..... 14

1.3 Diagnóstico e Aspectos Clínicos ..... 17

1.4 Aspectos Moleculares e Regulação da Matriz Extracelular na FPI ..... 20

1.5 Tratamento ..... 23

1.6 Modelo Experimental de Fibrose Pulmonar em Camundongos com Bleomicina ..... 24

1.7 Frutose-1,6-bisfosfato ..... 26

1.8 Frutose-1,6-bisfosfato e Fibrose ..... 30

**JUSTIFICATIVA** ..... **32**

**OBJETIVOS** ..... **33**

1.9 Objetivo Geral ..... 33

1.10 Objetivos Específicos ..... 33

**CAPÍTULO II** ..... **34**

**ARTIGO ORIGINAL** ..... 35

**CAPÍTULO III** ..... **55**

**CONSIDERAÇÕES FINAIS** ..... **56**

**REFERÊNCIAS** ..... **61**

**ANEXO I – CARTA DE APROVAÇÃO DO COMITÊ DE ÉTICA PARA O USO DE ANIMAIS** ..... **69**

**ANEXO II – CARTADE APROVAÇÃO DO COMITÊ DE ÉTICA DO NCI** ..... **70**

**ANEXO III** ..... **72**

# CAPÍTULO I

INTRODUÇÃO

# INTRODUÇÃO

## 1.1 Fibrose e Fibrose Pulmonar Idiopática

Fibrose é o acúmulo excessivo de componentes de matriz extracelular (ECM) que ocorre ao redor do tecido inflamado e o resultado patológico de muitas doenças inflamatórias crônicas que podem levar a uma área cicatricial permanente, perda de função tecidual e morte. A fibrose pode ser ocasionada por inúmeros processos genéticos desregulados, infecções persistentes, exposição frequente a toxinas, agentes químicos, hipertensão, diabetes, obesidade, entre outros (1). Um evento fundamental no processo fibrótico é a ativação de fibroblastos em miofibroblastos, um processo denominado transição epitélio-mesenquimal (EMT) (2). No entanto, outras células podem se diferenciar em miofibroblastos e contribuir para o estabelecimento da fibrose, como protofibroblastos, fibrócitos derivados da medula óssea, células epiteliais e mesenquimais. Com o tempo, se a causa primária da lesão não é eliminada, os processos inflamatórios existentes se tornam crônicos e desregulados, gerando um aumento da produção e depósito totalmente desordenado de ECM por fibroblastos ativados. Além de sintetizar ECM, miofibroblastos são células altamente contráteis, o que contribui ainda mais para o aumento da rigidez tecidual e para a consecutiva perda de função do órgão que é observada em estágios mais avançados e terminais de fibrose. Por esses motivos, fibroblastos e miofibroblastos são as principais células responsáveis pelo remodelamento tecidual que ocorre durante a fibrose (Figura 1) (3).

Fibrose pulmonar (FP) idiopática (FPI) é uma forma crônica e progressiva de pneumonia intersticial que ocorre majoritariamente em idosos por causas desconhecidas e com pouquíssimas opções de tratamento, sendo que nenhum reverte o quadro fibrótico já estabelecido (4). O resultado desse processo é a perda da elasticidade pulmonar e da área de superfície alveolar. Isso leva à anormalidades na função pulmonar, à troca gasosa ineficiente (5, 6), diminuição da capacidade vital forçada (CVF), da capacidade de difusão e dessaturação de oxigênio (7). A FPI apresenta um prognóstico bastante ruim. Após o diagnóstico, somente 20 a 30% dos pacientes apresentam sobrevida maior que 5 anos (8, 9) e a taxa de declínio da capacidade vital forçada é bastante acentuada entre pacientes não tratados (10). Vários fatores externos estão associados ao desenvolvimento de FPI, como inalação de substâncias tóxicas, envolvimento de vírus e mesmo refluxo gastroesofágico, entretanto os processos exatos pelos quais a FPI se desenvolve ainda não estão claramente definidos (11).

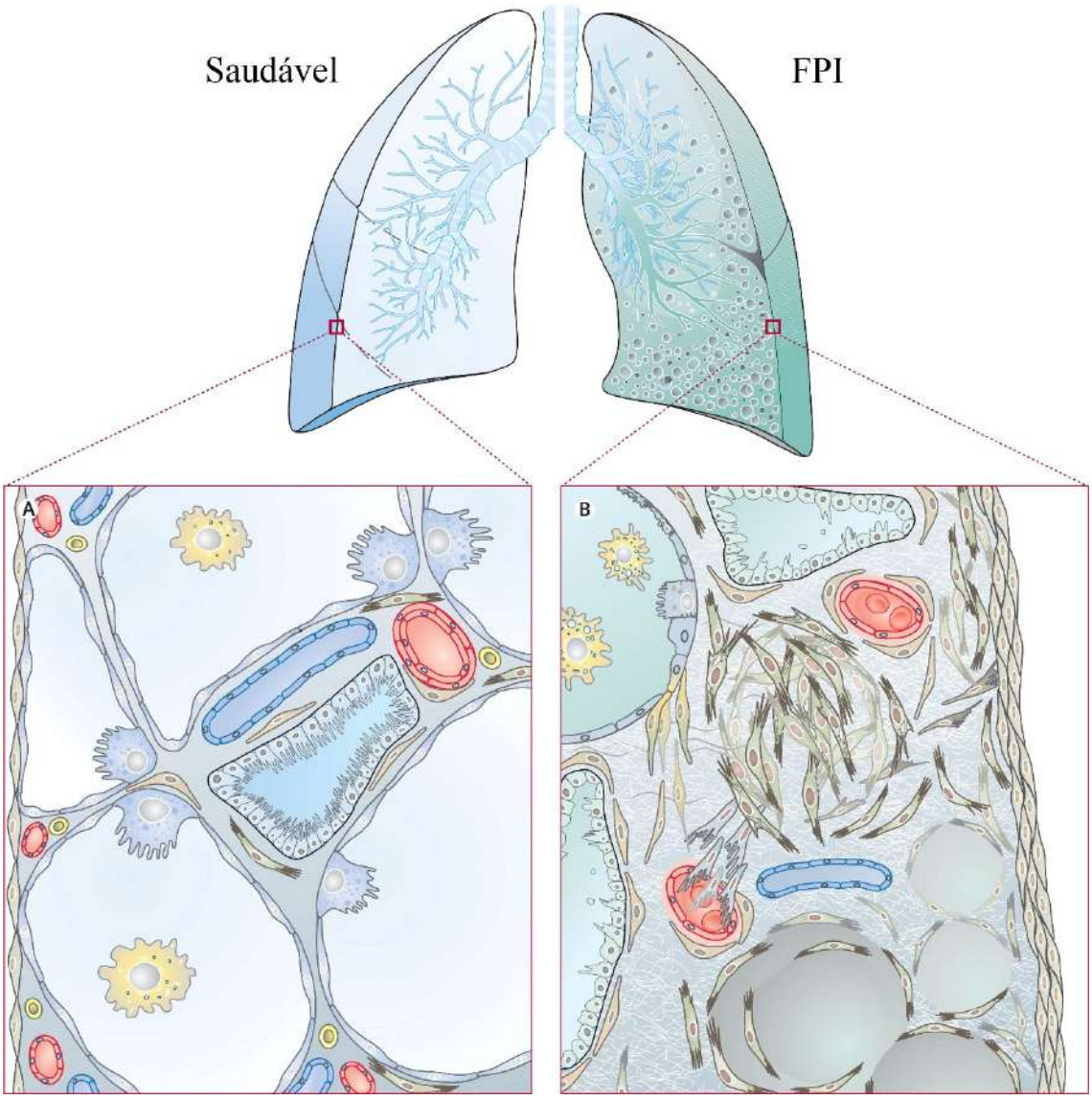


**Figura 1. Representação de um pulmão saudável e outro com FPI.** Enquanto o pulmão saudável apresenta arquitetura macroscópica e microscópica normal, o pulmão com FPI adquire um padrão heterogêneo, com regiões normais e fibróticas ao longe de áreas de faveolamento e com espessamento subpleural na região inferior. *A)* Estrutura alveolar com paredes alveolares preservadas e camada celular epitelial intacta. *B)* Epitélio danificado com espessamento da camada pleural e aumento da proliferação e migração de fibroblastos ativados por TEM que contribuem para o foco fibrótico (12).

## 1.2 Epidemiologia

A FPI é uma doença na qual, por seu caráter crônico, os sintomas irão se manifestar majoritariamente após os 50 anos de idade e com o quadro fibrótico já bastante avançado. A dispneia, uma das principais queixas relatadas por pacientes com FPI normalmente se

estabelece na sexta ou sétima décadas de vida. Consequentemente, o diagnóstico nos estágios iniciais da doença é extremamente difícil. Assim, a partir do início dos sintomas e a confirmação do diagnóstico pelo quadro clínico apresentado, uma incessante corrida é necessária para tentar retardar o avanço do processo fibrótico, visto que a reversão do quadro ainda não é possível com as medicações disponíveis no mercado (13).

A FPI está associada a inúmeros fatores de risco. Idade avançada, sexo masculino, diferentes interações genéticas hereditárias e não hereditárias, encurtamento de telômeros, estresse oxidativo, disfunção de surfactante, fatores epigenéticos, desregulação proteolítica, disfunção mitocondrial e secreção de mediadores pró fibróticos aumentada, como o TGF-β1, têm sido reportados em pacientes e aumentam o risco de FPI. Tabagismo também é um fator de risco fortemente associado à FPI, podendo coexistir com a presença de enfisema pulmonar. Ainda, algumas atividades envolvendo o contato direto com animais, por causa do contato com patógenos responsáveis por zoonoses, e agricultura, pela exposição a agrotóxicos, podem levar ao desenvolvimento de FPI e outras doenças. A relação com alguns vírus e patógenos, como vírus *Epstein-Barr*, adenovírus, herpes e hepatite C ainda não é totalmente clara. Embora não se saiba se o quadro fibrótico possa ser causado exclusivamente por esses agentes, existe a suspeita de que possa ser agravado pelos mesmos. Surpreendentemente, refluxo gastroesofágico tem sido um fator bastante associado à FPI. Pacientes com essa doença têm propensão a aspirar micropartículas do conteúdo gástrico que causam dano ao epitélio alveolar. Um estudo restrospectivo mostrou que pacientes com FPI que receberam tratamento para o refluxo apresentaram uma menor mortalidade em comparação a pacientes sem tratamento. Por último, largos agregados linfocíticos relacionados a auto-imunidade têm sido descritos em pacientes com FPI, o que sugere um quebra na tolerância imunológica (14).

A FPI possui muitas características e limitações que são compartilhadas com outras doenças, o que faz com quem sua epidemiologia não seja facilmente desvendada. A tentativa de classificar uniformemente os aspectos da FPI é relativamente recente. O primeiro consenso internacional para o diagnóstico de FPI foi publicado somente no ano 2000 (15), enquanto a resolução que orientava uma classificação e diferenciação mais precisa da FPI veio em 2002 para auxiliar na distinção da FPI dentre 6 outras formas de pneumonias intersticiais (16). Apesar de ser uma doença considerada rara, suas taxas de incidência e prevalência vem aumentando a cada ano. Isso se deve, provavelmente, à melhor possibilidade de diagnóstico com equipamentos e técnicas modernas, e à melhor diferenciação e classificação correta da

doença, visto que existem mais de 150 tipos de doenças intersticiais pulmonares conhecidas, dentre as quais a FPI é a mais comum e uma das mais agressivas (17).

Nos Estados Unidos, com um gasto de 25.000 USD por paciente ao ano, a FPI representa um custo maior que o câncer de mama e outras doenças que são consideradas graves (18). Ainda no mesmo país, estimou-se que 34.000 pessoas são diagnosticadas com FPI por ano. Esse número foi considerado abaixo da realidade devido a algumas limitações apresentadas no estudo, como a dificuldade do diagnóstico, atrasos nos registros dos planos de saúde, a interrupção da investigação sobre a doença de base pela não continuidade do atendimento no serviço de saúde primário e pacientes com doenças intersticiais pulmonares que o diagnóstico preciso não foi confirmado e que poderia ser FPI (19). Japão, Peru, Bolívia, Chile e alguns países do oeste europeu são os locais nos quais se apresentam as maiores taxas de FPI no mundo (14). No Reino Unido, 5.000 casos são estimados e 5.000 mortes são relatadas anualmente, o que significa que mais pessoas irão morrer por causa de FPI do que devido a câncer de ovário, linfoma, leucemia ou câncer renal. Congruente com outros estudos, a incidência é maior em homens idosos, sendo que a sobrevida de pacientes com fibrose comprovada por biópsia é de aproximadamente 5.5 anos (20).

No Brasil, dados epidemiológicos sobre a FPI que sejam detalhados e que reflitam o real quadro dessa doença são escassos. Isso dificulta a elaboração de políticas de saúde eficazes, visto que o impacto da FPI não é contemplado, já que ainda não existem dados confiáveis de incidência, prevalência e número total de pacientes afetados. Em 2015, na tentativa de se averiguar a prevalência de FPI no nosso país, Baddini-Martinez e Pereira analisaram dados de dois estudos realizados nos EUA. No primeiro, haviam relatórios e estimativas provenientes de comunidades de ancestralidade latina, enquanto o segundo continha a análise de um grande banco de dados de companhias de planos de saúde. Com isso, os dois pesquisadores extrapolaram esses números para realizar uma estimativa da realidade Brasileira. De acordo com suas análises, a incidência anual prevista de novos casos de FPI foi de 6.841 a 9.997 casos por 100.000 habitantes, enquanto a prevalência variou de 9.986 a 16.019 casos por 100.000 habitantes. Obviamente, essa extrapolação tem a tendência de mascarar a nossa realidade e um estudo com dados provenientes de nosso país deveria ser conduzido. Além disso, devido à grande extensão do nosso país, a análise epidemiológica entre regiões distintas também foi recomendada por esses autores (21). Em um artigo mais recente, uma avaliação realizada através da coleta de dados do Sistema da Informação de Mortalidade (SIM) entre os

anos 1979 e 2014 mostrou que o Brasil segue as tendências globais em relação ao aumento de casos de FPI (Figura 2A). As causas desse aumento são a possibilidade do diagnóstico correto com a melhora na tecnologia dos tomógrafos empregados e a disponibilidade do uso da tomografia computadorizada de alta resolução (TCAR), a discussão de casos em grupos multidisciplinares e o aumento da população com idade superior a 60 anos. Ainda, a análise de gênero demonstrou que a mortalidade é maior em homens do que em mulheres até a faixa de 85 anos, quando a mortalidade se iguala (Figura 2B) (22).

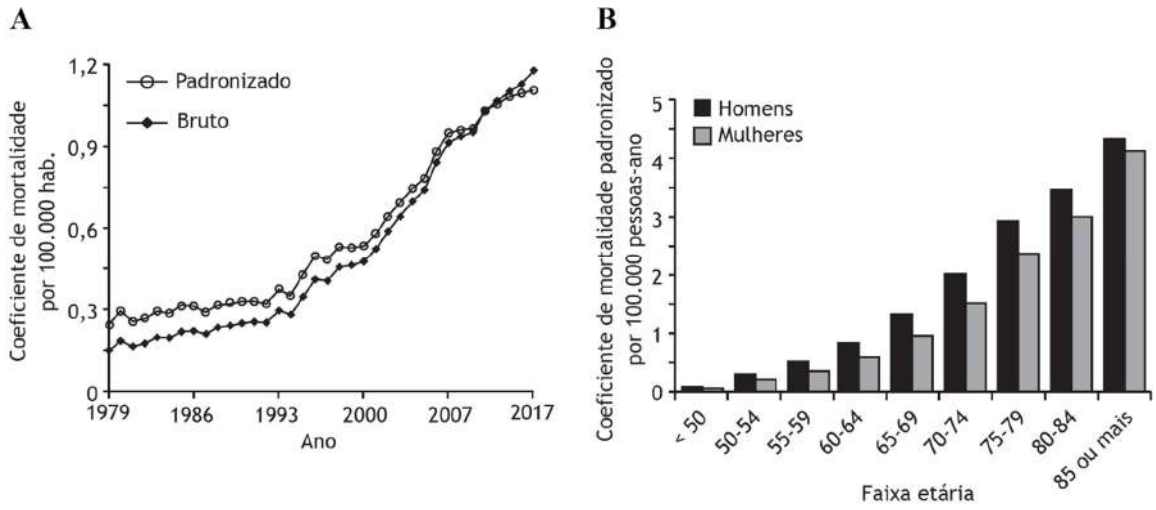


**Figura 2. Mortalidade por FPI no Brasil.** Dado coletados dos períodos entre 1979 e 2914 no Brasil no Sistema de Informação de Mortalidade (SIM). *A)* Coeficiente de mortalidade bruto (♦) e padronizado (○) e padronizado por FPI+Símiles, onde símiles significa a probabilidade de inclusão de dados errôneos no SIM. *B)* Taxa de mortalidade padronizado por gênero e faixa etária. Todas as faixas são significativamente diferentes entre homens e mulheres exceto "85 anos ou mais" (22).

### 1.3 Diagnóstico e Aspectos Clínicos

O diagnóstico precoce é de extrema importância, visando evitar que possíveis terapias com potencial lesivo para o pulmão sejam utilizadas e que o tratamento adequado possa ser iniciado o mais brevemente possível. O atraso do encaminhamento de pacientes com suspeita de FPI a um centro especializado pode ser ocasionado pela demora do paciente ao consultar um médico por causa da dispneia ou tosse, os quais são os primeiros sintomas que podem ser constatados no atendimento primário. Além disso, crepitações inspiratórias, que são percebidas na ausculta pulmonar, podem passar desapercebidas pelo médico sem experiência. Ainda, a

ausência de informações clínicas consideradas relevantes, como tabagismo, histórico ocupacional e informações sobre uso de medicações prévias, pode resultar em uma anamnese inapropriada e ocasionar o atraso no encaminhamento do paciente para um centro especializado (23).

Em seus guias, a *American Thoracic Society*, juntamente com a *European Respiratory Society*, *Japanese Respiratory Society* e *Latin American Thoracic Society*, recomendam que a presença de FPI deve ser considerada em todos os pacientes adultos que apresentarem dispneia e/ou tosse crônica, crepitações inspiratórias e/ou baqueteamento digital que ocorram sem causa específica ou mesmo devido a outros sintomas que sugiram uma doença multissistêmica. O uso de TCAR é altamente recomendado, visto que permite uma melhor definição dos padrões morfológicos pulmonares obtidos nas imagens e na observação da presença ou não de padrão de pneumonia intersticial usual (PIU), que é observado tanto no exame histopatológico, quanto no radiológico (24).

No exame radiológico, uma das principais características do padrão PIU observadas através da TCAR é o faveolamento. Faveolamento é um agrupamento cístico que se dispõem em camadas na região subpleural, com diâmetro tipicamente consistente (3-10mm), paredes espessas e bem definidas. Representa o estágio final do processo fibrótico com a destruição de espaços aéreos distais e possui esse nome por se assemelhar a favos de mel (25) (Figura 3). Usualmente, juntamente com o faveolamento, também se observam bronquiectasias e/ou bronquiolectasias de tração concomitantemente com a presença de opacidades reticulares de predomínio periférico e basal (26). Bronquiectasias de tração são dilatações ou espessamento permanente do calibre dos brônquios com usual espessamento do parênquima circunjacente à via aérea, resultante de alguma enfermidade pulmonar produtora de fibrose. Bronquiolectasias são semelhantes à bronquiectasia, porém ocorrem em bronquíolos, que possuem menor calibre (27).

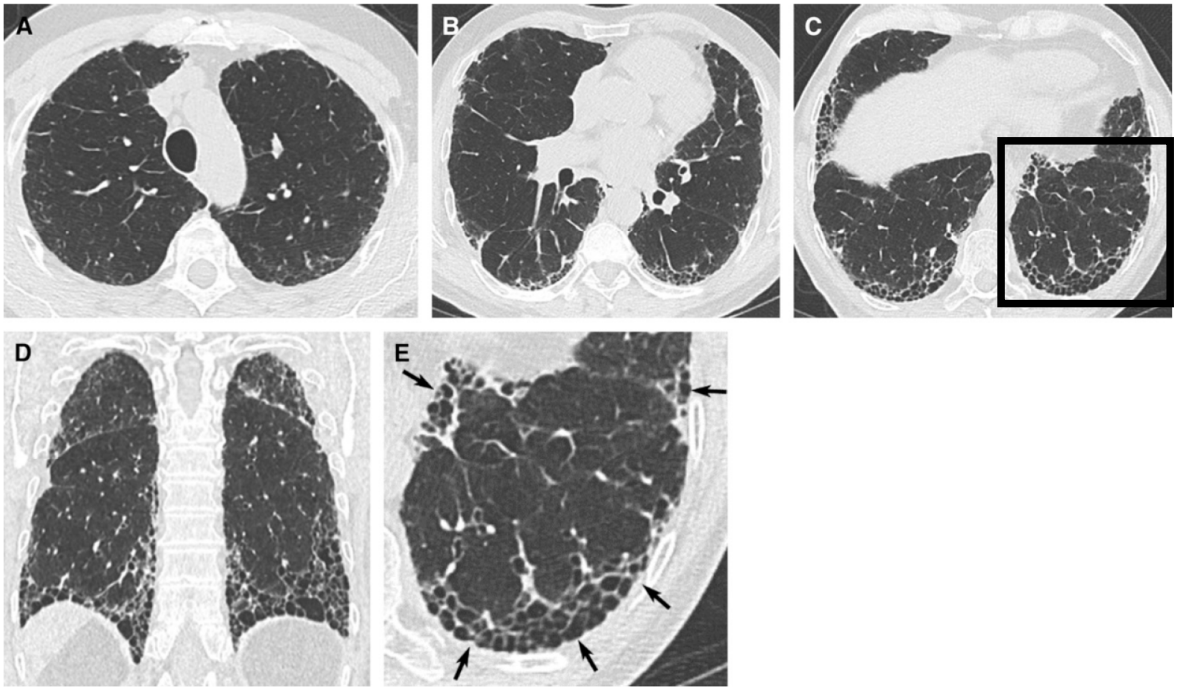


**Figura 3. Imagens de tomografia computadorizada de alta resolução (TCAR) demonstrando padrões de pneumonia intersticial usual (PIU).** *A-C*) seção transversal e (*D*) reconstrução coronal ilustrando a presença de faveolamento com predominância subpleural e basal e presença de opacidade reticular. *E)* visão em detalhe do quadro em *C* mostrando típicas características de faveolamento, consistindo de espaços agrupados com paredes bem definidas, diâmetros variáveis e vistos em única ou múltiplas camadas (setas) (24).

No achado histopatológico, deve-se buscar critérios que confirmem o padrão PIU. Esse, se caracteriza pela aparência de uma fibrose densa e desorganizada que causa remodelamento da arquitetura tecidual, frequentemente resultando em alterações típicas de faveolamento e alternando com áreas de parênquima menos afetadas. Nas regiões de faveolamento, em nível microscópico, existe a presença de espaços aéreos fibróticos que são frequentemente revestidos por epitélio bronquiolar e preenchido com muco e células inflamatórias. A presença de inflamação é, normalmente, moderada com infiltrado linfocítico e hiperplasia do epitélio dos bronquíolos. A zona fibrótica é composta majoritariamente de colágeno com a presença de fibroblastos e miofibroblastos em alta taxa de proliferação (27).

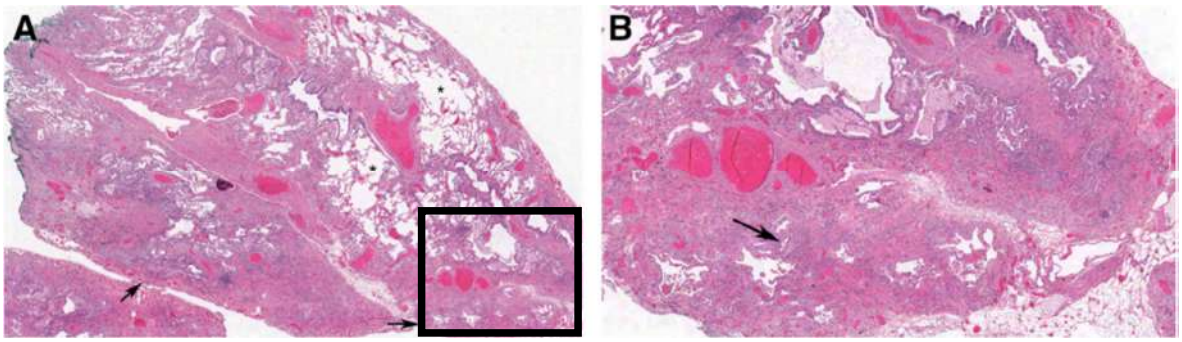


**Figura 4. Análise histopatológica mostrando padrão de pneumonia intersticial usual (PIU).** A) imagem mostrando padrão PIU clássico, correspondente com fibrose pulmonar idiopática (FPI), com presença de alta densidade fibrótica, distorção da arquitetura tecidual com faveolamento microscópico (flechas) justaposto com parênquima relativamente pouco afetado (*). *B)* Área em detalhe do quadro em *A,* mostra cicatriz subpleural com alterações características de faveolamento e foco fibroblástico (setas) (24).

A progressiva diminuição da função pulmonar leva a uma piora da qualidade de vida e é um indicador clínico importante na FPI (28, 29), refletindo mudanças na qualidade e aumento da quantidade de ECM acumulada durante a fibrogênese, o que leva ao enrijecimento do tecido (30). Com isso, pacientes com FPI apresentam perda progressiva da função pulmonar e consequente óbito. Em resumo, o diagnóstico de FPI pode ser confirmado quando outras causas conhecidas de doenças pulmonares intersticiais puderem ser excluídas, quando o padrão PIU for observado na TCAR e na presença de padrões histopatológicos característicos em pacientes que tiverem amostras de biópsia coletadas (24).

## 1.4 Aspectos Moleculares e Regulação da Matriz Extracelular na FPI

Tão importante quanto a regulação da produção e depósito, a degradação da ECM é fundamental para a resolução da fibrose e reestabelecimento do tecido saudável. Tanto em modelos experimentais quanto em humanos, existe um desequilíbrio extremamente significativo na produção e atividade de proteínas que são responsáveis pela reciclagem da ECM, gerada durante o processo fibrótico. Após a fonte primária da lesão ser retirada ou interrompida, fibroblastos que foram ativados entram em apoptose, devendo ser eliminados por células imunes ou desdiferenciar para que processos normais referentes à cicatrização ocorram de maneira controlada. Porém, no processo crônico, fibroblastos permanecem sendo ativados continuamente e depositando ECM no tecido. Além da composição química e estabilidade da estrutura tridimensional, propriedades mecânicas da ECM podem regular o fenótipo celular, sinalização e ativação de moléculas pró fibróticas. Existem estudos relacionando a

deformabilidade do parênquima tecidual e composição da ECM com a função e diferenciação de fibroblastos devido à interação da ECM com proteínas de adesão focal transmembrana, como integrinas. Forças mecânicas externas e internas podem ser transmitidas para o citoesqueleto, gerar sinais bioquímicos e estimular fatores de transcrição que vão alterar a conformação de proteínas importantes na regulação da diferenciação de fibroblastos, assim ativando-os (31).

O fator de crescimento transformante β1 (TGF-β1) é uma citocina envolvida em inúmeros processos fisiológicos, como embriogênese, imunidade, carcinogênese, cicatrização, proliferação e migração celular (32). Após sua síntese, o TGF-β1 é secretado e armazenado ligado à ECM como uma molécula inativa. Após lesão tecidual, o estresse mecânico e geração de espécies reativas de oxigênio (ROS) podem ativar o TGF-β1 (33), o que faz com que fibroblastos saudáveis se diferenciem em miofibroblastos. Por sua vez, esses miofibroblastos irão aumentar sua própria produção de ROS, liberando mais TGF-β1, induzindo a ativação de quinases reguladas por sinais extracelulares (ERK) e a expressão de actina de músculo liso α (α-SMA) em um círculo vicioso (34). TGF-β1 é a principal citocina indutora de fibrose (35, 36) e sua produção, quando aumentada, está relacionada à progressão de fibrose hepática, cardíaca, renal e pulmonar. A sinalização do TGF-β1 se dá através da ligação do TGF-β1 a seus receptores, o receptor de TGF-β1 tipo I e II, o que induz a ativação de proteínas Smad. Essa ativação leva à formação de complexos heteroméricos entre Smad2, Smad3 e Smad4 e a translocação desse complexo ao núcleo, onde podem direcionar a transcrição de genes relacionados à proliferação, diferenciação e produção de ECM, como , fibronectina (Fn1), além da α-SMA (37). A proteína Smad7, que parece ser ativada pelo fator de necrose tumoral alfa (TNF-α), ao contrário, inibe a formação desses heterocomplexos e, por isso, impede a sinalização do TGF-β1 (36, 38).

Estudos anteriores relacionam diretamente os níveis de produção e depósito de colágeno e outros componentes de ECM com a severidade do quadro (39). Após sua síntese, monômeros de colágeno polimerizam em sua forma fibrilar que, então, são unidos por ligações covalentes pela enzima lisil oxidase (LOX). Esse processo de maturação do colágeno é fundamental para a estabilidade da sua estrutura e das suas propriedades mecânicas e físicas (40) e, quando desregulado, confere uma maior resistência à proteólise do colágeno, que é realizado pela metaloproteinase de matriz (MMP) 1 (MMP1), aumento da rigidez tecidual e diminuição da elasticidade do tecido (30, 39, 41). Em modelos animais de fibrose hepática, o

aumento na rigidez do tecido precede a ativação de fibroblastos e acúmulo de colágeno. Isso indica que alterações precoces na mecânica tecidual podem ser suficientes para estimular cascatas de contração e a ligação do colágeno fibrilar pela LOX pode ser um dos fatores responsáveis por essas mudanças iniciais (42). A Fn1, outro importante componente de ECM que pode ter ação quimioatratora para fibroblastos, também é vista nas fases iniciais do desenvolvimento de FP em modelos animais e não somente nos estágios finais quando o quadro fibrótico já está estabelecido (43).

A α-SMA é um dos marcadores clássicos da diferenciação de fibroblasto em miofibroblasto e um dos componentes de ECM mais importantes em qualquer processo fibrótico. A síntese de α-SMA por miofibroblastos gera uma força de contração pelo menos duas vezes maior que outras isoformas de actina, o que é fundamental no processo normal de cicatrização, visto que a tensão mecânica necessária no reparo do dano e a carga suportada pelo tecido para reestabelecer sua estrutura é maior do que no tecido saudável. Ao menos três eventos são necessários para a geração de miofibroblastos que sejam totalmente diferenciados e capazes de expressar α-SMA. São eles o acúmulo de TGF-β1 biologicamente ativo, a presença de proteínas de ECM específicas e estresse extracelular proveniente do constante remodelamento da ECM circundante aos fibroblastos. Um passo fundamental para a formação da nova ECM é a estruturação da Fn1, que é mediada por miofibroblastos e dependente da ligação de dímeros de Fn1 a integrinas. Isso resulta em um formato fibrilar que irá servir de base para a ligação de colágeno e outros componentes de ECM, como a própria α-SMA, já que a expressão dessa pode afetar a estruturação da Fn1 fibrilar e modular a geração da força de contração máxima que a célula poderá suportar. Ainda, a estruturação da Fn1 em fibriblas é realizada de um modo muito mais eficaz e rápido por miofibroblastos do que por fibroblastos e esse efeito é diretamente relacionado com o aumento da expressão de genes relacionados à capacidade de contração celular (44).

As MMPs formam uma família de proteínas endopeptidases dependente de $Zn^{+2}$ que estão envolvidas na degradação e remodelamento da ECM em várias condições fisiológicas e patológicas (45). MMPs e seus inibidores, inibidores de metaloproteinase tecidual (TIMP), têm sido implicados na patogênese da FPI. MMP1 é uma colagenase e responsável por degradar uma das moléculas de ECM mais importantes e presente no quadro fibrótico (46). TIMPs estão distribuídos amplamente e em grandes quantidades no parênquima pulmonar de pacientes e animais com FP. Isso contribui para que o colágeno e outros componentes de ECM não sejam

degradados apropriadamente e se acumulem, contribuindo para a rigidez do tecido pulmonar afetado, perda de função e consequente ineficiência na habilidade de trocas gasosas e metabólicas, o que, por fim, leva à morte. Surpreendentemente, algumas MMPs promovem, ao invés de inibir, o desenvolvimento de FP através da promoção de EMT, aumento dos níveis ou atividade de mediadores pró-fibróticos, promovendo migração anormal de células epiteliais, migração de fibrócitos e outros processos de reparo celular aberrantes (47). Em animais submetidos à indução de fibrose com bleomicina (BLM), tanto a expressão quanto os níveis de metaloproteinase de matriz 2 (MMP2) aumentam gradativamente com o passar do tempo. Isso pode levar à desestabilização da membrana de células epiteliais, facilitando a invasão de fibroblastos a espaços alveolares, fazendo com que esse aumento esteja relacionado à severidade do quadro fibrótico (48).

## 1.5 Tratamento

As opções de tratamento para a FPI ainda são escassas. Dois medicamentos, nintedanibe e pirfenidona, foram recentemente aprovados para uso em humanos pelo *Food and Drug Administration* (FDA) dos Estados Unidos e são considerados seguros e efetivos no tratamento da FPI. Nintedanibe é um inibidor da tirosina-quinase que pode estimular migração e proliferação de fibroblastos pulmonares e tem como alvo receptores do fator de crescimento vascular endotelial (VEGF), do fator de crescimento de fibroblasto (FGF) e do fator de crescimento derivado de plaquetas (PDGF), que estão envolvidos na sinalização transmembrana e transdução de sinais intracelulares. A pirfenidona inibe citocinas inflamatórias em nível pós-transcricional e aumenta a produção de interleucina 10 (IL-10), que é anti-inflamatória, inibe a proliferação de fibroblastos induzida por PDGF e FGF e inibe a síntese de pró-colágeno estimulada por TGF-β1 (24). Aliás, o bloqueio de citocinas pró-fibróticas tem sido buscado como uma alternativa de tratamento, tendo o TGF-β1 como alvo principal. Porém, a administração de drogas e anticorpos inibidores dessa citocina tem demonstrado pouca eficácia quando aplicados sozinhos, o que sugere que a inibição de uma citocina não é suficiente para o sucesso do tratamento.

Em um estudo clínico de fase 3, analisando 555 pacientes, 47% deles apresentaram CVF estável (diminuição <10%) ou sobrevida maior que um ano de tratamento (49). Outro estudo, analisando o efeito do nintedanibe, mostrou que, de 80 pacientes, 59% apresentaram

melhora ou estabilidade no quadro fibrótico, enquanto 41% foram a óbito durante o período observacional do estudo (50). Quando comparados, pacientes em uso de nintedanibe apresentaram perda de peso significativamente maior em relação a pacientes em uso de pirfenidona (51). Ainda, o uso conjunto de diferentes fármacos abrem novas possibilidades de tratamento. Um estudo reportou a diminuição da CVF em 44% dos pacientes que usaram pirfenidona e em 87% de pacientes que associaram perfenidona e N-acetilcisteína, um antioxidante (52). Ainda, *in vitro*, a combinação de pirfenidona e interferon-γ mostrou um possível efeito sinérgico entre dois fármacos, inibindo a proliferação, diferenciação e migração de fibroblastos induzida por TGF-β1 e PDGF. Porém, um estudo japonês relatou um pequeno, porém significativo aumento no número de efeitos adversos e uma diminuição da biodisponibilidade do nintedanibe quando administrado em conjunto com a pirfenidona (53). Assim, mais estudos que avaliem os efeitos concomitantes de diferentes possíveis agentes são necessários.

Características da FPI incluem lesões e hiperplasia de células epiteliais alveolares, acúmulo de células inflamatórias, hiperplasia de fibroblastos, depósito e acúmulo de ECM. Apesar da presença de células inflamatórias no foco fibrótico, o papel que a inflamação desempenha no processo da FP ainda é incerto, visto que pacientes não respondem a terapias com agentes imunossupressores, como azatioprina e prednisona. Ao contrário, pacientes tratados com essa classe de fármacos apresentaram uma mortalidade maior e foram hospitalizados por exacerbações mais frequentemente que pacientes controles (54). Embora os exatos mecanismos ainda não sejam totalmente elucidados, esse fato põe em dúvida se a inflamação tem algum papel como protagonista do processo fibrótico que ocorre no pulmão. A eficácia apresentada pelo nintedanibe e pirfenidona, apesar de não reverterem a fibrose já instaurada, demonstram que a FPI é passível de tratamento e que é de extrema importância que a pesquisa por novas moléculas seja realizada, pois o transplante pulmonar ainda permanece como o único tratamento definitivo.

## 1.6 Modelo Experimental de Fibrose Pulmonar em Camundongos com Bleomicina

Nenhum animal desenvolve fibrose pulmonar espontaneamente como acontece em humanos. Isso faz com que a indução de fibrose com toxinas ou agentes químicos seja

necessária para que possamos estudar os aspectos e mecanismos moleculares que estão presentes no estabelecimento e resolução do processo fibrótico no pulmão. Obviamente, modelos experimentais e humanos apresentam diferenças intrínsecas, mas, ainda assim, são uma alternativa de grande relevância para o estudo dos efeitos de drogas que possam ter um papel antifibrótico em ensaios pré-clínicos.

A bleomicina (BLM) é um agente antineoplásico usado para tratar inúmeros tipos de câncer, como linfomas, carcinoma de testículos, ovários e cabeça. O principal mecanismo anticâncer da BLM ocorre através da indução de estresse oxidativo e clivagem de DNA. Porém, apresenta uma alta toxicidade pulmonar, pois a enzima bleomicina hidrolase (BLMH), que inativa a BLM quase não é produzida nesse órgão (55, 56). Por causa dessa toxicidade no pulmão, a BLM é o agente mais comumente utilizado para a indução de fibrose pulmonar experimental (56, 57) em ratos e camundongos. As lesões induzidas por esse agente incluem inflamação, dano epitelial com hiperplasia reativa e apoptose, alterações da membrana basal e fibrose heterogênea (58). Embora esse modelo seja facilmente reproduzível, a administração de BLM leva a um rápido estabelecimento do quadro fibrótico que não simula perfeitamente o quadro clínico em pacientes, o que é uma limitação presente em todos os modelos experimentais disponíveis (56, 57). Além disso, existe um consenso de que a fibrose pulmonar induzida por BLM se resolve, ou seja, regride, a partir do 28º dia após a administração (55). Porém, apesar do dano agudo, Limjunyawong e colaboradores observaram que, mesmo depois de seis meses de uma única administração intra-traqueal (IT) de 5 U/kg de BLM, animais ainda apresentavam várias alterações estruturais e funcionais, como diminuição do volume, aumento da rigidez pulmonar, dificuldade nas trocas gasosas, aumento de células inflamatórias e deposição de colágeno, quando comparados ao grupo controle, sugerindo que o quadro fibrótico se mantém mesmo depois de um longo período após a administração do fármaco (59).

Diferentes linhagens de camundongo respondem de diferentes modos ao estímulo fibrótico induzido pela BLM. Santos-Silva e colaboradores, em um estudo comparando três cepas distintas (BALB/c, DBA/2 e C57BL/6), encontraram várias diferenças entre elas. Por exemplo, a taxa de sobrevida após administração IT de BLM variou entre 50, 80 e 100% para C57BL/6, DBA/2 e BALB/c, respectivamente. Além disso, uma diferença significativa na expressão e atividade de marcadores de estresse oxidativo, como superóxido dismutase (SOD), catalase (CAT), glutationa peroxidase (GPx), espécies reativas ao ácido tiobarbitúrico (TBARS) e óxido nítrico (NO) também foi constatada entre as cepas. Visto que a BLM age

como uma fonte de ROS, a maior atividade antioxidante da SOD observada em camundongos BALB/c pode estar associada com a resistência à fibrose induzida por BLM nessa cepa (60). Apesar disso, um estudo analisando a resposta à BLM entre diferentes cepas encontrou graus semelhantes de fibrose e apoptose entre C57BL/6 e NMRI (61). Em células mesoteliais pulmonares, a BLM diminui níveis de expressão de citoqueratina 8 e E-caderina, aumentando a motilidade e migração celular, expressão de colágeno tipo 1 (Col-1), α-SMA e induzindo mudanças morfológicas para um fenótipo semelhante a miofibroblasto. Todas essas mudanças são características de EMT e a sinalização do TGF-β1 via Smad2/3 é fundamental para esse processo (62).

### 1.7 Frutose-1,6-bisfosfato

A Frutose-1,6-bisfosfato (FBP) é um intermediário glicolítico de alto potencial energético produzido pela enzima fosfofrutoquinase (PFK), que catalisa a fosforilação da frutose-6-fosfato. As propriedades protetoras deste açúcar têm sido demonstradas em uma variedade de condições patológicas por nosso grupo, incluindo sepse e imunomodulação (63, 64). Além disso, outros grupos demonstraram suas ações como agente neuroprotetor, anti-isquêmico e antioxidante (65), em uma variedade de tecidos, como fígado (66-68), rim (69), cérebro (70, 71), pulmão (72-74), músculo (75) e intestino (76). Rigobello e Galzigna realizaram um dos primeiros estudos que avaliaram o comportamento farmacocinético após a administração da FBP. Usando FBP marcada, eles viram que o rim apresentava os maiores níveis de radiação, enquanto o cérebro os menores, sugerindo uma distribuição ou mesmo captação não homogênea da FBP administrada (77).

Durante anos, os mecanismos pelos quais a FBP pudesse entrar nas células foram investigados e essa hipótese sempre foi controversa. Com a síntese de [$C^{13}$]FBP, detectável por ressonância nuclear magnética, Hardin e Robert viram que [$C^{13}$]lactato era produzido por células após sofrerem hipóxia, o que indicava que a FBP era metabolizada após entrar na célula e servia como intermediário glicolítico (75). Por possuir dois grupos fosfatos na sua molécula, Sano e colaboradores sugeriram que a FBP não pode cruzar a membrana plasmática intacta. Assim, seria necessária a ação de fosfatases no meio extracelular e a obtenção de frutose, que poderia, então, como uma molécula mais simples, atravessar a membrana, porém essa hipótese não foi confirmada (78). Anos mais tarde, em outro estudo, Hardin e colaboradores não viram

indícios de que a FBP fosse convertida a frutose no meio extracelular, mas sim de que era transportada para o meio intracelular e metabolizada a $CO_2$ e lactato, confirmando que a FBP pode cruzar a membrana celular intacta. Além disso, relataram que a forma linear da FBP utiliza um transportador dicarboxilado para entrar na célula. Esse efeito é inibido quando o fumarato está presente, o que indica uma competição pelo mesmo sistema de transporte (79). Além disso, foi descrito que a FBP poderia causar uma instabilidade na membrana plasmática através da interação com o cálcio que estabiliza fosfolipídeos da membrana. Isso aumentaria temporariamente a fluidez da bicamada lipídica e permitiria que a FBP entrasse na célula (80). Ainda, dados indicam que o processo de entrada da FBP na célula é dependente de energia, visto que astrócitos são capazes de captar esse açúcar a 37°C, o que não acontece a 0°C (81). Desde então, a captação da FBP tem sido demonstrada em diferentes tecidos e células, mas o exato mecanismo pelo qual ela é capaz de cruzar a membrana com seus dois grupos fosfato intactos permanece como alvo de discussão.

Em relação à toxicidade da FBP, Nunes e colaboradores mostraram que a dose letal média desse açúcar em ratos é de aproximadamente 1,0g/kg quando administrada em *bolus* por via endovenosa e que esse efeito pode ser ocasionado pelo aumento de fosfato que é liberado quando a FBP é hidrolisada (82). Em outro trabalho, a administração de até 4,0 g/kg de FBP por via intraperitoneal em ratos neonatos não teve qualquer indício de toxicidade nem de alterações estruturais de órgãos como coração, fígado, pulmões e rins (83). Normalmente, testes realizados em roedores utilizam doses que variam de 100 a 1000 mg/kg de FBP (84). Em ratos, níveis plasmáticos de FBP atingem seu pico duas horas após a administração de 500mg/kg por via intraperitoneal, saltando de 15µg/mL para 35µg/mL. Decorridas 6 horas, os níveis de FBP diminuem em mais da metade, mas ainda continuam acima da concentração basal e permanecem estabilizados por, no mínimo, 3 dias, mostrando que os efeitos de uma única dose podem ser duradouros. Apesar de, nesse mesmo artigo, o pico de acúmulo de FBP ocorrer 1 hora após a administração em órgãos como fígado e rim, o pulmão não foi analisado (85). Ainda que saibamos que a FBP pode exercer efeitos protetores no tecido pulmonar, não se sabe exatamente como a FBP é capaz de influenciar esse órgão.

Muitos estudos mostram que a FBP possui ação protetora contra radicais livres (86) em modelos *in vitro* com células expostas a peróxido de hidrogênio (87), impedindo a produção de malondialdeído, um indicador de peroxidação lipídica (78) e reduzindo a formação de produtos de oxidação de proteínas (88). Em hepatócitos lesados com galactosamina, a FBP

aumenta a relação glutationa oxidada/glutationa reduzida que é um importante sistema antioxidante celular (89). Outro possível mecanismo pelo qual a FBP exerce sua atividade protetora é pela capacidade de quelar íons divalentes, como $Fe^{+2}$ (90, 91), que é responsável pela geração de ROS na reação de Fenton.

A PFK é o principal ponto de regulação na glicólise e sua atividade diminui drasticamente em um ambiente celular hipóxico ou com dano por causa do baixo pH do meio. Com isso, a fosfofrutoquinase diminui drasticamente sua capacidade de gerar FBP e a rota glicolítica é inibida, fazendo com que os níveis de adnosina trifosfato (ATP) celular caiam drasticamente. Isso leva à despolarização celular e a entrada de grandes quantidades de $Ca^{2+}$ por canais voltagem-dependentes. Principalmente em neurônios, a entrada de $Ca^{2+}$ resulta na ativação de cascatas de sinalização de morte celular. A administração exógena de FBP pode impedir esse processo por dois mecanismos. Primeiro, a FBP, ao entrar na célula, pode pular a etapa regulada pela PFK, fazendo com que a glicólise, assim como a produção de ATP seja restaurada, o que reestabelece o equilíbrio iônico e diminui a concentração de $Ca^{+2}$ intracelular. Segundo, a habilidade de FBP de se ligar ao $Ca^{2+}$, outro íon divalente, poderia impedir a sinalização tóxica desse cátion e exercer um efeito crucial para a estabilidade e sobrevivência celular (65, 92, 93).

Ainda, a FBP apresenta atividades imunomodulatórias, visto que a ativação de neutrófilos (94) e proliferação de linfócitos *in vitro* (64, 95) é inibida por esse açúcar, o que pode ser resultado da inibição da produção de NO e proteína quinase ativada por mitógeno p38 (p38 MAPK) (96). Em modelos *in vivo* de lesão pulmonar induzida por carragenina (97) e zimosan (72), a FBP foi capaz de exercer atividades anti-inflamatórias, diminuindo a migração de leucócitos e a produção de NO. Em um recente trabalho realizado por nosso laboratório, a administração de FBP no momento da indução de sepse experimental em camundongos foi capaz de, no cérebro, impedir a formação de radicais livres, aumentar a concentração de catalase e diminuir os níveis de S100β, uma proteína que é utilizada como marcador de lesão. Ainda, foi capaz de manter o metabolismo cerebral em níveis semelhantes aos dos animais controles (98).

Existem evidências que a FBP pode exercer suas propriedades anti-inflamatórias através da adenosina. Sola e colaboradores mostraram que a infusão de FBP aumenta os níveis de adenosina, diminuindo o acúmulo de xantina durante o período de isquemia, inibindo o

recrutamento de neutrófilos e subsequente geração de ROS durante a reperfusão. Com a administração de adenosina deaminase, que converte a adenosina a um metabólito inativo, a FBP teve seu efeito protetor bloqueado (94). Valério e colaboradores mostraram que a FBP diminui a hiperalgesia em camundongos após a injeção intraplantar de carragenina e que esse efeito pode ser mediado especificamente através da ativação do receptor de adenosina A1. Animais que receberam FBP antes da injeção de carragenina tiveram uma sensibilidade diminuída à dor causada pela inflamação e esse efeito foi inibido quando, antes da administração da FBP, os animais receberam DPCPX, um antagonista seletivo do receptor de adenosina A1. Além disso, viram que animais que receberam FBP tiveram seus níveis plasmáticos de adenosina aumentados e que a administração direta de adenosina tinha efeitos semelhantes aos da FBP em diminuir a hiperalgesia (84). Ainda avaliando a relação da FBP-adenosina, Veras e colaboradores utilizaram um modelo de artrite induzida por zymosan e viram que a FBP, uma vez mais, foi capaz de atenuar a inflamação. Além disso, a FBP foi capaz de aumentar os níveis de ATP sérico, além da adenosina extracelular, com sua concentração máxima atingida 24h após a administração de FBP. Ainda, relataram que esse aumento da adenosina é dependente de CD39 e CD73, que são ectonucleotidades que degradam o ATP extracelular em etapas sequenciais até adenosina. Porém, dessa vez, a FBP foi responsável pela ativação de um subtipo diferente de receptor, o receptor de adenosina A2a (99).

Alguns estudos com a administração de FBP já foram realizados em humanos com lesão miocárdica (100, 101) e acidente vascular cerebral isquêmico (102). Em um desses estudos, Markov e colaboradores demonstraram que a infusão endovenosa de 5g de FBP não altera a pressão arterial, diminui os níveis de piruvato e lactato e aumenta o consumo de carboidratos, enquanto diminui a utilização de lipídeos para a geração de energia em indivíduos saudáveis (103). Ainda, FBP foi administrada de modo seguro em pacientes com doença pulmonar obstrutiva crônica, onde melhorou a força de contração muscular, melhorando a respiração desses pacientes (104). Em outro estudo, em pacientes com insuficiência cardíaca congestiva, a administração de 125mg/kg resultou em uma modesta melhora na performance ventricular esquerda quando comparada ao grupo placebo (105).

## 1.8 Frutose-1,6-bisfosfato e Fibrose

Pelo fato da fibrose pulmonar ainda não ter uma alternativa de tratamento que reverta o quadro fibrótico, novos estudos se fazem necessários para entender os mecanismos subjacentes a essa doença e testar novas moléculas que possam agir contra o seu avanço. As HSC são fibroblastos residentes do fígado que acumulam vitamina A em seu citoplasma em gotículas de lipídeo que podem ser coradas e visualizadas facilmente ao microscópio. Durante a lesão hepática e à medida que essas células vão sendo ativadas, ocorre perda da habilidade de estocar vitamina A, perdem as gotículas de lipídeos e vão adquirindo características de miofibroblastos, com maior contratilidade, produção de TGF-β1, proliferação, etc. Porém, as HSC possuem a peculiar característica de sofrerem um processo de desativação, ou reversão fenotípica, quando expostas a moléculas que induzam proteção antioxidante. Em um estudo do nosso laboratório, utilizamos a FBP no cultivo celular de uma linhagem de células estreladas hepáticas (HSC) chamada GRX. Após 7 dias de tratamento, de Mesquita e colaboradores relataram uma drástica redução na taxa proliferação e um significativo aumento na quantidade de lipídeo armazenado no citoplasma dessas células. Esse efeito foi acompanhado por um aumento na expressão do receptor ativado por proliferadores de peroxissoma gama (PPAR-γ), que é um fator de transcrição envolvido no metabolismo, e pela diminuição da expressão e produção de Col-1 e TGF-β1 (106).

Em outro trabalho, expusemos essas células a uma solução de ferro e vimos que isso aumentava a taxa de proliferação celular, diminuía a quantidade de lipídeo intracelular, aumentava a expressão de colágeno e diminuía a de PPAR-γ. Esses efeitos foram revertidos com sucesso pelo co-tratamento com FBP que, como confirmado por nossos experimentos, pode quelar o ferro presente no meio de cultivo. Ainda, vimos que a FBP, apesar de dados indicarem possuir um efeito antioxidante, não parece ser uma molécula com propriedades antioxidantes, visto sua incapacidade de captar o radical livre DPPH (107).

Em um outro artigo publicado por nosso laboratório, vimos que a administração de FBP via IP foi capaz de prevenir o desenvolvimento de FP induzida por BLM em camundongos, a perda de função pulmonar e, *in vitro*, reduzir a taxa de proliferação de fibroblastos pulmonares pela indução de senescência celular (108). Apesar de termos demonstrado que a FBP é capaz de proteger o pulmão em diferentes modelos experimentais e contra o desenvolvimento da FP,

os mecanismos envolvidos nesse processo ainda não foram elucidados e novos estudos se fazem necessários.

## JUSTIFICATIVA

Estudos recentes apontam a FBP como uma molécula com um grande efeito terapêutico em inúmeras doenças. No entanto, o conjunto de evidências sobre esse açúcar ainda é incipiente. A FBP apresenta diferentes propriedades protetoras em diferentes órgãos e em diferentes modelos experimentais, mas as melhores condições para seu potencial farmacológico ainda não foram exploradas. Apesar da busca por novas terapias, ainda não existem tratamentos que revertam o quadro fibrótico na FPI. Um fator bastante importante é o remodelamento tecidual que ocorre no processo fibrótico, visto que mudanças na rigidez, composição e estrutura da ECM podem estimular a ativação de fibroblastos em miofibroblastos e propagar indefinidamente a fibrose no tecido. Neste sentido, a FBP já demonstrou potencial na prevenção de fibrose pulmonar experimental e é importante que os mecanismos pelos quais esse açúcar exerce esses efeitos sejam melhor investigados.

# OBJETIVOS

## 1.9 Objetivo Geral

Avaliar os efeitos da FBP sobre a prevenção e/ou regulação do processo fibrótico em um modelo experimental de FP *in vivo* e em células pulmonares *in vitro*.

## 1.10 Objetivos Específicos

Avaliar o efeito da FBP sobre:

- a morfologia do parênquima pulmonar de camundongos submetidos à FP;

- a deposição de componentes de matriz extracelular no parênquima pulmonar de camundongos submetidos à FP;

- parâmetros de função pulmonar de camundongos submetidos à FP;

- a expressão gênica de componentes de ECM nos pulmões de camundongos submetidos à FP;

- a proliferação, contração e migração de fibroblastos e miofibroblastos pulmonares extraídos de camundongos e mantidos em cultivo primário;

- a expressão gênica de diferentes componentes de ECM em fibroblastos e miofibroblastos pulmonares extraídos de camundongos e mantidos em cultivo primário;

- a expressão de MMP´s e TIMP´s de fibroblastos e miofibroblastos pulmonares extraídos de camundongos e mantidos em cultivo primário.

# CAPÍTULO II

ARTIGO ORIGINAL

**Fructose-1,6-bisphosphate prevents pulmonary fibrosis by regulating extracellular matrix deposition and inducing phenotype reversal of lung myofibroblasts.**

Os resultados do presente trabalho foram publicados no periódico ***PlosOne*** e estão formatados de acordo com as normas de submissão do mesmo.

Fator de Impacto: 2.776

PLOS ONE

RESEARCH ARTICLE

# Fructose-1,6-bisphosphate prevents pulmonary fibrosis by regulating extracellular matrix deposition and inducing phenotype reversal of lung myofibroblasts

**Henrique Bregolin Dias**[1,2], **Jarbas Rodrigues de Oliveira**[1], **Márcio Vinícius Fagundes Donadio**[1], **Shioko Kimura**[2]*

**1** Laboratory of Cellular Biophysics and Inflammation, PUCRS, Porto Alegre, RS, Brazil, **2** Laboratory of Metabolism, Center for Cancer Research, National Cancer Institute, National Institutes of Health, Bethesda, MD, United States of America

* kimuras@mail.nih.gov



OPEN ACCESS

**Citation:** Dias HB, de Oliveira JR, Donadio MVF, Kimura S (2019) Fructose-1,6-bisphosphate prevents pulmonary fibrosis by regulating extracellular matrix deposition and inducing phenotype reversal of lung myofibroblasts. PLoS ONE 14(9): e0222202. https://doi.org/10.1371/journal.pone.0222202

**Editor:** Oliver Eickelberg, University of Colorado School of Medicine, UNITED STATES

**Received:** March 15, 2019

**Accepted:** August 23, 2019

**Published:** September 11, 2019



**Data Availability Statement:** All relevant data are within the manuscript and its Supporting Information files.

**Funding:** This study was supported by the National Cancer Institute Intramural Research Program, Center for Cancer Research, National Institutes of Health (ZIA BC 010449 to SK) (https://www.cancer.gov), and in part by the Coordenação de Aperfeiçoamento de Pessoal de Nivel Superior – Brasil (CAPES) (http://www.capes.gov.br) –

## Abstract

Pulmonary fibrosis (PF) is the result of chronic injury where fibroblasts become activated and secrete large amounts of extracellular matrix (ECM), leading to impaired fibroblasts degradation followed by stiffness and loss of lung function. Fructose-1,6-bisphosphate (FBP), an intermediate of glycolytic pathway, decreases PF development, but the underlying mechanism is unknown. To address this issue, PF was induced *in vivo* using a mouse model, and pulmonary fibroblasts were isolated from healthy and fibrotic animals. In PF model mice, lung function was improved by FBP as revealed by reduced collagen deposition and downregulation of ECM gene expression such as collagens and fibronectin. Fibrotic lung fibroblasts (FLF) treated with FBP for 3 days *in vitro* showed decreased proliferation, contraction, and migration, which are characteristic of myofibroblast to fibroblast phenotype reversal. ECM-related genes and proteins such as collagens, fibronectin and α-smooth muscle actin, were also downregulated in FBP-treated FLF. Moreover, matrix metalloproteinase (MMP) 1, responsible for ECM degradation, was produced only in fibroblasts obtained from healthy lungs (HLF) and FBP did not alter its expression. On the other hand, tissue inhibitor of metalloproteinase (TIMP)-1, a MMP1 inhibitor, and MMP2, related to fibroblast tissue-invasion, were predominantly produced by FLF and FBP was able to downregulate its expression. These results demonstrate that FBP may prevent bleomycin-induced PF development through reduced expression of collagen and other ECM components mediated by a reduced TIMP-1 and MMP2 expression.

## Introduction

Pulmonary fibrosis (PF) is a chronic and progressive lung disease with scarring of lung interstitium and progressive decline of lung function. With an overall survival rate of 20% after 5 years of diagnosis, there is currently no treatment to reverse the fibrotic state and lung

Finance Code 001 – through a scholarship awarded to Dias, HB. The funders had no role in study design, data collection and analysis, decision to publish, or preparation of the manuscript.

**Competing interests:** The authors have declared that no competing interests exist.

transplant remains the best option [1, 2]. In the fibrotic tissue, a remarkable characteristic is the fibrotic foci, where active fibroblast to myofibroblast differentiation occurs. This leads to the production and deposition of the extracellular matrix (ECM) components collagen and fibronectin, and α-smooth muscle actin (α-SMA), an actin isoform responsible for cell-generated mechanical tension [3, 4]. In addition, ECM degradation by metalloproteinases (MMP) is compromised by increased production of its inhibitors, tissue inhibitor of metalloproteinase (TIMP) [5]. Thus, fibroblasts and myofibroblasts are regarded as the main source of ECM present in the fibrotic process [6]. Fibroblast activation can occur in response to growth factors after tissue damage, with increasing cell migration to the wound focus, contractility, and acquiring a high proliferative phenotype [7].

Fructose-1,6-bisphophate (FBP), an intermediate of glycolytic pathway, has shown protective effects in a wide range of pathological situations, including sepsis [8] and acute lung injury [9]. FBP has demonstrated anti-oxidant activity both *in vitro* and *in vivo*. However, conflicting results were also reported regarding this effect [10–13]. An earlier study found that activated liver myofibroblasts, or hepatic stellate cells, underwent a phenotype reversal associated with quiescence, decreased proliferation, and accumulation of lipid droplets when treated *in vitro* with FBP, all of which are characteristics of normal healthy fibroblast [14]. This protective effect of FBP was maintained even when these cells were concomitantly exposed to high doses of free iron, that sustains activation of stellate cells [15]. A previous study on lung fibrosis showed that FBP can prevent bleomycin-induced fibrosis development in mice [16], however, the molecular basis of this effect remains unknown. The aim of this study was to determine how FBP prevents and/or regulates the fibrotic process using an animal model of PF induced by bleomycin *in vivo* and primary fibroblasts isolated from healthy and fibrotic lungs of mice *in vitro*.

## Materials and methods

### Pulmonary fibrosis animal model

Male mice (eight week old, C57Bl/6N, 25-30g) maintained in a 12h light-dark cycle with water and chow *ad libitum*, were divided into four groups; 1) Bleomycin (BLM) group: received intratracheally (IT) 1.2U/kg BLM (Sigma-Aldrich) on day 0 [17], 2) control group: received IT an equal volume of saline on day 0, 3) BLM + FBP group; BLM IT on day 0 and thereafter daily intraperitoneal injection (ip) of 500 mg/kg FBP [16, 18] for 14 days, and 4) FBP group: saline IT on day 0 and thereafter daily ip of FBP. Weight and mortality were monitored daily for 14 days. Intratracheal intubation was carried out using the BioLITE system (BioTex, Inc., Houston, TX). Mice were anesthetized with ketamine (100 mg/kg) and xylazine (10 mg/kg) by ip injection, and a catheter, with the aid of the light of an optical fiber, was inserted into the trachea located between the arytenoid cartilages. The optical fiber light guide was removed with maintaining the catheter in a steady position in the trachea and 50 μl of BLM was added to the catheter. The quick suction of the solution through the catheter indicated its correct location in the trachea. All animal studies were performed after approval by the National Cancer Institute Animal Care and Use Committee.

### Lung function

On day 14, the mice were anesthetized with ketamine (100 mg/kg) and xylazine (20 mg/kg), tracheotomized, cannulated and subjected to lung function analysis with the Legacy FlexiVent System (SCIREQ, Montreal, Canada). To prevent spontaneous breathing during data acquisition and to avoid any interference in the analysis, the mice received the paralytic rocuronium bromide (0.5 mg/kg IP) and were kept ventilated for 5 min at 150 breaths/min before the tests,

with a tidal volume of 10 mL/kg and 3 cm $H_2O$ of positive end-expiratory pressure (PEEP). Through broadband (multifrequency) forced oscillation and, with a constant Phase Model parameter, different compartment of lungs were analyzed and the following measurements obtained: tissue elastance (H), which reflects parenchyma stiffness and is measured by energy conservation in the lungs; tissue damping (G) which indicates tissue resistance, is measured by the energy dissipation in the lungs, and reflects the peripheral airways; and Newtonian resistance (Rn), which is the raw resistance of the conducting central airways. For whole thorax measurement, the single frequency forced oscillation maneuver (Snapshot perturbation) was used to obtain values for: compliance (C), which is the easiness with which lungs can be extended; resistance (R), that reflects dynamic lung resistance; and elastance (E), which is the distensibility of the lungs, chest walls and airways, given by elastic rigidity of the lungs. Each perturbation was repeated three times per mouse with a 30 second interval between each measurement.

## Bronchoalveolar lavage fluid (BALF)

After analysis of lung function, the animals were exsanguinated by cardiac puncture and 1 mL of PBS was slowly injected to the lungs through the catheter and immediately aspirated. Samples were centrifuged, supernatant was stored at -80˚C and the pellet was resuspended in 250 μl of PBS. The total number of cells were assessed by direct counting in hemocytometer with the Trypan blue exclusion method. For cell differentiation analysis, 200 μL of cell suspension was added in a cytospin slide chamber (Shandon EZ Double Cytofunnel, Thermo Scientific, USA), spun at 800 rpm for 5 min in a Cytospin 4 (Thermo Scientific, USA) and stained with Stain Set Diff-Quik (Siemens Healthcare Diagnosis Inc., Newark, NJ, USA). Percentages of macrophages, neutrophils and lymphocytes were obtained and adjusted by total cell number.

## Lung histological analysis

After BALF collection, the right lungs were tied, collected, quick frozen in liquid nitrogen and stored in -80˚C for quantitative RT-PCR (qRT-PCR). For histological analysis, left lungs were inflated under 20 cm $H_2O$ and fixed overnight in 10% phosphate buffered formalin, dehydrated and embedded in paraffin. Sections of 4 μm were stained with hematoxylin and eosin (H&E) or Picro Sirius Red (PS) for collagen fibers. Sections were made from different portions of lung, so that the analysis was congruent with the fibrotic stage of the whole lung. To develop a modified Ashcroft Score, 30 fields in each lung of every mouse was visualized and classified according to Hübner and coworkers [19]. For PS, images from lung sections were obtained with BZ-X7000 Analyzer (Keyence, Japan) and the area of the tissue stained with PS was accessed with Image Pro Plus® 6.0 software (Media Cybernetics, Inc., Rockville, MD, USA).

## Lung fibroblasts primary culture

Mouse whole lungs were minced and digested with 1 mg/ml collagenase (Gibco, Invitrogen) in RPMI-1640 medium with 2% antibiotic/antimycotic (Lonza) at 37˚C. After 1h, dispersed cells were centrifuged, washed in PBS, seeded in 10-$cm^2$ dishes with RPMI-1640 containing 1% antibiotic/antimycotic + 10% fetal bovine serum (FBS), and placed in a cell culture incubator. Media was replaced every day until cells reached confluence. Lung fibroblast primary cultures were obtained from healthy (HLF) and fibrotic (FLF) mice. All experiments were carried out using cells between passages 4 and 8.

## Cell proliferation

Fibroblasts were seeded into 96-well plates ($2x10^3$ cell/well) and treated with 0.6 or 1.25 mM FBP dissolved in complete growth media. After 24, 48 and 72 h, media was removed and 10% of Cell Counting Kit-8 (CCK8) (DOJINDO, USA) in RPMI-1640 was added to the wells and allowed to react for 2 h. Absorbance was measured at 450 nm.

## Culture insert migration analysis

Fibroblasts were pre-treated with FBP for 72 h and $10^4$ cells were seeded on cell culture inserts with 8 μm pore size (Falcon, USA) with 1% FBS in RPMI-1640 (low serum media). The insert was placed inside a well of a 24-well plate that contained 20% FBS in RPMI-1640 that was used as chemoattractant to stimulate cells to migrate to the bottom of the insert. FBP was added into the media of the upper chamber at 0 (control), 0.6, or 1.25 mM to examine the effect of FBP on cell migration. After 24 h, the cells inside the insert were mechanically removed and those that migrated to the bottom of the insert were incubated with 10% CCK8 solution in RPMI-1640. The absorbance was obtained, and the migration rate was adjusted by healthy control absorbance.

## Cell contraction in collagen gel assay

Collagen solution (Advanced BioMatrix, USA) was impregnated with $10^5$ cells dissolved in RPMI-1640 media at a final concentration of 0.75 mg/ml collagen, added to a 24-well plate and left to polymerize at 37˚C for 1 h. The gels were then detached and soaked in 600 μL of complete growth media containing 0 (control), 0.6, or 1.25 mM FBP and incubated for 24 h. Photographs were taken and the surface area of the gel was measured using ImageJ (http://rsb.info.nih.gov/ij) with the area of an empty well considered the initial area occupied by the gel.

## RNA extraction and quantitative RT-PCR

Total RNA was isolated using TRIzol (Invitrogen), and was converted to cDNA using Superscript II reverse transcriptase (Invitrogen, USA). Quantitative RT-PCR (qRT-PCR) was performed with ABI Prism 7900 Sequence Detection System (Applied Biosystems, Foster City, CA) using SYBR Green FastMix (Quanta Biosciences, Gaithersburg, MD). GAPDH was used as a normalization gene and the standard curve method was used to calculate the relative expression. The PCR conditions used were 50˚C for 2 min and 95˚C for 10 min followed by 95˚C for 15 s and 60˚C for 40 s for 40 cycles. Primers used for qRT-PCR analysis are shown in S1 Table.

## Western blotting

Total protein was obtained using cold RIPA lysis buffer (Millipore, USA) with protease inhibitor cocktail (Roche Diagnosis, Indianapolis IN), fractionated by SDS-PAGE and transferred to a PVDF membrane using a transfer apparatus according to the manufacturer's instructions (Bio-Rad, Hercules, CA). After blocking with 5% nonfat milk in TBS (Tris-buffered saline, pH 7.4) for 1 h, the membrane was washed thrice in TBST (TBS + 0.1% Tween 20) and incubated with the following primary antibodies; anti-α-smooth muscle actin (α-SMA, dilution 1:2000), anti-Collagen type 1 (1:1000), anti-MMP1 (1:500), anti-MMP2 (1:500), anti-TIMP-1 (1:500), anti-TIMP-4 (1:500), and anti-β-actin (1:5000). All antibodies were obtained from Proteintech Group-Fisher Scientific, (Hampton, NH). Membranes were washed three times and incubated with HRP linked anti-Rabbit IgG antibody (1:1000, Cell Signaling, USA) for 1 h. Bands were

revealed with SuperSignal West Dura kit (Thermo Scientific, Waltham, MA), visualized with ChemiDoc MP Imaging System (Bio-Rad), and normalized by intensity of β-actin bands.

### Statistical analysis

Data were reported as mean ± SD. Analysis of survival was performed by Kaplan-Meier analysis with log-rank (Mantel-Cox). Comparison between two groups was performed by unpaired two-tailed student's *t*-test. Multigroup comparisons were performed by One-way or Two-way ANOVA, as indicated in each separate analysis, followed by Tukey's post hoc test using Prism Software (GraphPad Software, v.7, San Diego, CA). A $p$ value $<0.05$ was considered statistically significant in all analysis. Replicates consisted of at least three independent experiments that were performed at different days. The numbers of biological replicates are indicated in each figure legend.

## Results

### Fructose-1,6-bisphosphate prevents pulmonary fibrosis development and collagen deposition in the lungs

Weight loss and mortality are well-known characteristics of the BLM-induced PF model once the fibrotic process starts. BLM induced a statistically significant decrease of body weight in the BLM and BLM+FBP groups when compared to the control and FBP groups ($p<0.001$) (Fig 1A). However, weight loss of the BLM+FBP-treated group was significantly smaller than BLM group ($p<0.001$). All mice from control and FBP groups survived until the end of induction period (14 days). On the other hand, mice from BLM group presented a survival rate of only 38%, which is significantly lower than the 58% found in BLM+FBP group.

To evaluate the extent of PF damage and collagen deposition induced by BLM and the effects of FBP treatment, Ashcroft score and morphometric analysis were performed, which evaluates parenchyma changes and collagen deposition, respectively (Fig 1B). The group that was treated with FBP once a day (BLM+FBP), when compared with non-treated (BLM) mice, had a decreased Ashcroft score, while no changes on lung architecture was observed in the control and FBP-only groups. BLM group also presented a significantly increased percentage of collagen area in the lungs, while a decreased percentage of alveoli space. In comparison, FBP treatment was able to prevent these effects, decreasing the amount of deposited collagen on the parenchyma and preserving the alveolar structure. Although BLM group showed a tendency for increases in cellular area, this value was not different from other groups. The representative histological images of lung sections stained with HE and PS showed a decreased distortion in lung architecture in the BLM+FBP group when compared with mice that received BLM only (Fig 1C). Taken together, these results show that daily treatment with FBP (500 mg/kg) can prevent body weight loss, increase survival and restore the lung architecture of mice with PF induced by BLM.

### Fructose-1,6-bisphosphate decreases inflammatory cell migration and improves lung function

BLM induces a strong inflammatory response in lungs and, consequently, many leucocytes are recruited to the tissue. BALF was collected to evaluate whether FBP influences immune cell migration. The total number of cells in the lung was significantly increased in animals that received BLM when compared to control, FBP, and BLM+FBP groups (Fig 2A). This effect was due to an increased number of neutrophils and lymphocytes, however the number of macrophages did not differ between the groups.

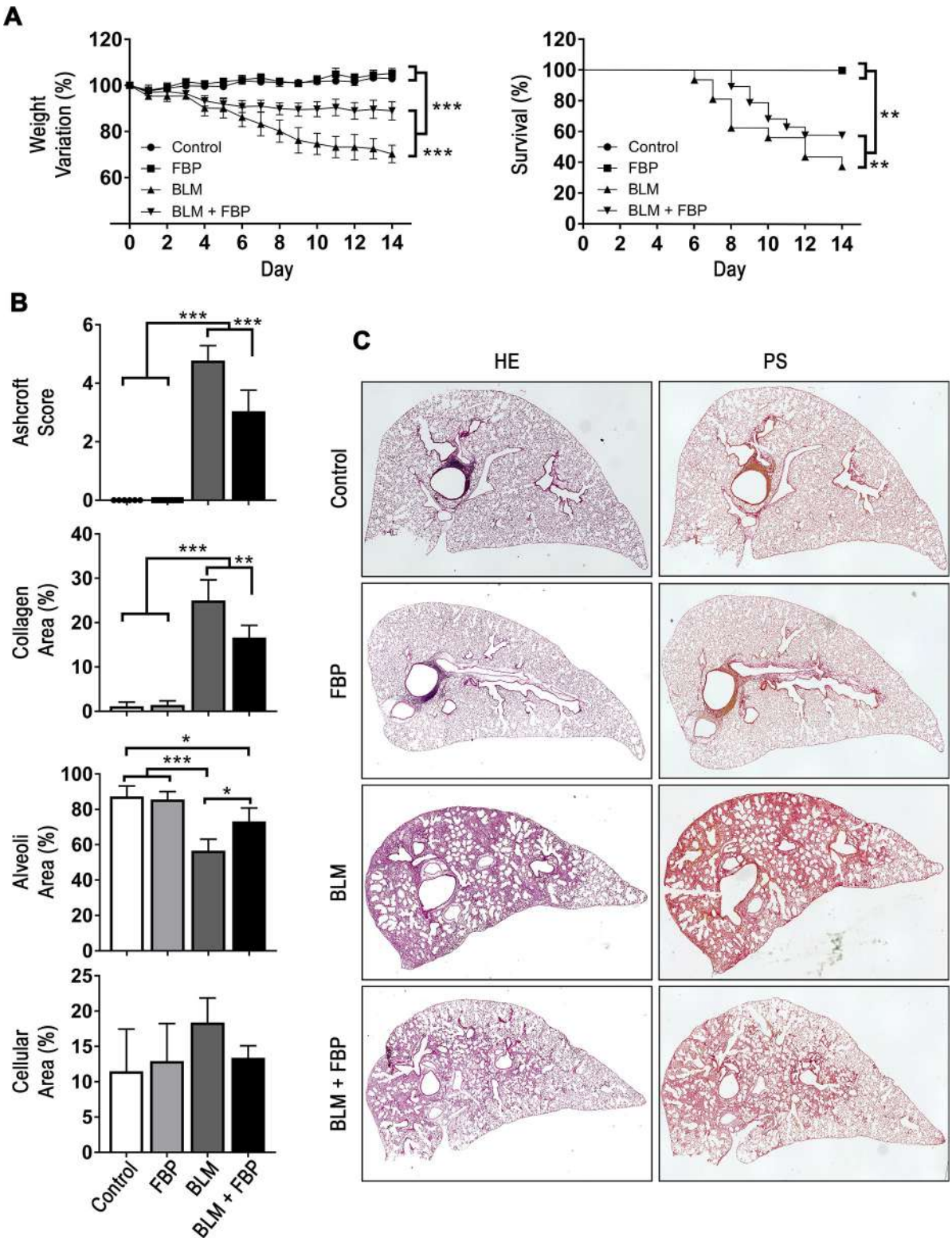


**Fig 1. Fructose-1,6-bisphosphate prevents pulmonary fibrosis development and collagen deposition in the lungs.** (A) Body weight variation (%) and survival rate (%) are shown during 14 days post-BLM treatment. (B) Ashcroft modified score was used to quantify fibrosis and architecture distortion degree while morphometric analysis was performed to assess area of collagen deposition in the lungs after BLM intratracheal administration and FBP treatment. (C) Representative images of lung sections stained with hematoxylin and eosin (HE) or Picro Sirius Red (PS) showing a high parenchyma distortion and collagen content in the lung after BLM administration. Treatment with FBP

shows a lower degree of fibrosis and collagen. Groups' description given for the whole panel B is on the bottom of the graph showing Cellular Area (%). Weight variation (%) was analyzed by Two-way ANOVA followed by Tukey's multiple comparison test. Values are expressed as mean ± SD. Survival rate (%) was analyzed by Kaplan-Meier followed by log-rank (Mantel-Cox) test. Ashcroft and morphometric analysis were analyzed by One-way ANOVA followed by Tukey's multiple comparison test (B). Values are expressed as mean ± SD; For weight variation and survival analysis, n = 6–20/group. For Ashcroft and morphometric analysis, n = 6–12/group; $^{*}p<0.05$; $^{**}p<0.01$; $^{***}p<0.001$.

https://doi.org/10.1371/journal.pone.0222202.g001

Fibrosis also increase tissue stiffness, which leads to lung function loss. Accordingly, intratracheal BLM administration caused a decrease in overall lung function, as illustrated by increased on tissue elastance (H), tissue damping (G), resistance (R) and elastance (E), while lowered compliance (C). For Newtonian resistance (Rn) parameter, BLM group was lower only when compared to Control group (Fig 2B). BLM+FBP group had lung function range similar to Control and FBP groups in all tested criterions.

## Fructose-1,6-bisphosphate regulates extracellular matrix-related genes *in vivo*

The fibrotic process leads to the upregulation of many ECM genes. Thus, *Col1a1*, *Col2a1*, *Col5a1* and *Col6a1* mRNAs were measured. All mRNAs were increased 14 days after BLM intratracheal administration when compared to the control, FBP, and BLM + FBP groups (Fig 3). The mRNAs encoding fibronectin (*Fn1*), another important ECM component, and C-X-C motif chemokine ligand 12 (*Cxcl12*), a fibrosis-associated chemokine, were also increased by BLM administration and FBP was able to downregulate the expression of these mRNAs. Further, BLM decreased *Cdh1* (E-cadherin) mRNA levels, which is inversely associated with the EMT process, and was not affected by treatment with FBP.

## Fructose-1,6-bisphosphate induces deactivation of fibroblasts *in vitro*

When activated, myofibroblasts acquire a high proliferative phenotype. In order to determine whether FBP interferes with the proliferation rate of primary fibroblasts, cells extracted from healthy (HLF) and fibrotic (FLF) mouse lungs were subjected to FBP treatment. FLF had a significantly higher proliferation rate than HLF and treatment with FBP slowed the proliferation rate of both FLF and HLF after three days of treatment with 0.6 and 1.25 mM FBP (Fig 4A). These two doses were chosen because the lower dose of 0.3 mM FBP did not show significantly different effects after three days, while the higher doses of 2.5 to 10 mM FBP were toxic to the cells (S1 Fig). To confirm the nature of HLF and FLF cells, their gene expression profiles were analyzed. The mRNAs encoding all three major ECM components, *α-SMA*, *Col1a1*, and *Fn1*, were higher in cells extracted from mice that were fibrotic (FLF) when compared to those from healthy non-fibrotic mice (HLF) (Fig 4B).

High contractility and EMT process are also important characteristics of myofibroblasts for wound closure and migration to the wound site. In the analysis of contraction on collagen gels, HLF treated with FBP were not different from control cells at any dose tested. However, FLF were more contractile than HLF and FBP-treatment decreased cell contractility at both doses tested (Fig 4C). For insert migration assay, cells were treated with FBP for 3 days. The migration rates of healthy and fibrotic cells were not altered after 24 hours. However, when FBP was maintained for another 24 hours (re-treatment), the migration rates of healthy and fibrotic cells decreased. This effect was more profound in fibrotic cells, and their levels were much lower than healthy re-treated cells (Fig 4D). Together, these results indicate that FBP can influence fibroblast behavior and lead to a deactivated, fibroblast-like phenotype.

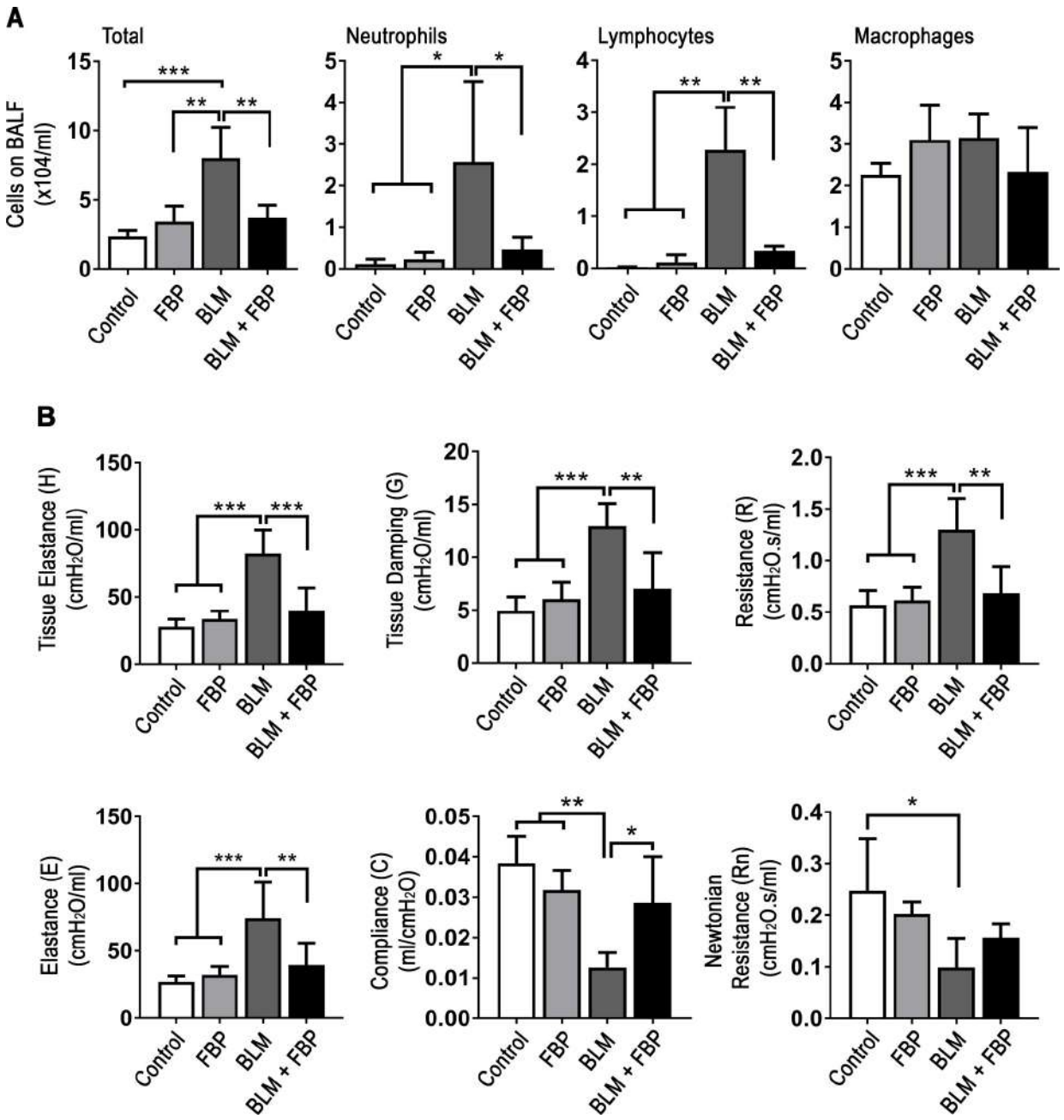


**Fig 2. Fructose-1,6-bisphosphate decreases inflammatory cell migration to the lungs and improves lung function.** (A) Total number of cells, neutrophils, lymphocytes, and macrophages in BALF assessed by direct counting in hemocytometer. (B) Lung function measurement for tissue elastance (H, parenchyma stiffness), tissue damping (G, tissue resistance that reflects the peripheral airways), resistance (R, level of constriction in the lungs), elastance (E, stiffness of respiratory system), compliance (C, easiness with which respiratory system can be extended), and Newtonian resistance (Rn, reflects the resistance of central and conducting airways). One-way ANOVA followed by Tukey's multiple comparison test was used. Values are expressed as mean ± SD; n = 6–12/group; $^{*}p<0.05$; $^{**}p<0.01$; $^{***}p<0.001$.

https://doi.org/10.1371/journal.pone.0222202.g002

## Fructose-1,6-bisphosphate down-regulates collagen-related gene expression *in vitro*

Since myofibroblasts are source of collagen production and deposition in fibrosis, the expression of collagen subtypes and lysil oxidase (LOX), a protein responsible for cross linking and

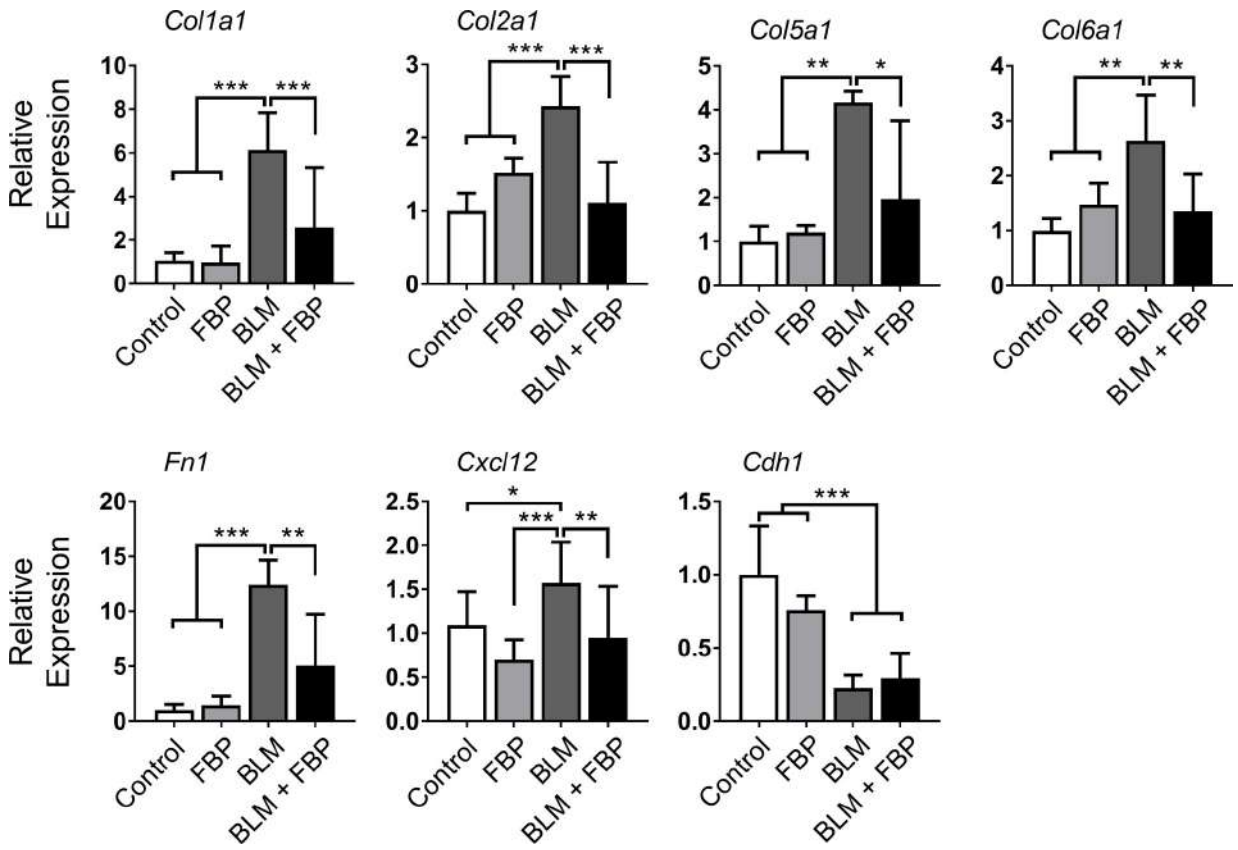


**Fig 3. Fructose-1,6-bisphosphate regulates extracellular matrix-related genes *in vivo*.** qRT-PCR analysis of mRNA encoding for collagen subtypes, collagen 1a1 (*Col1a1*), collagen 2a1 (*Col2a1*), collagen 5a1 (*Col5a1*), collagen 6a1 (*Col6a1*), and *Fn1*, *Cxcl12* and *Cdh1*. One-way ANOVA followed by Tukey's multiple comparison test was used. Relative expression is presented based on the expression level of control as 1. Values are expressed as mean ± SD; $n$ = 6–12/group; $^{*}p<0.05$; $^{**}p<0.01$; $^{***}p<0.001$.

https://doi.org/10.1371/journal.pone.0222202.g003

maturation of collagen fibers [20], was examined using HLF and FLF treated with FBP for 72 h (Fig 5). FBP significantly downregulated expression of *Lox* mRNA and many collagen subtypes, both in HLF and FLF, such as *Col1a1*, *Col4a6*, *Col5a1*, *Col5a2* mRNAs, and this effect was most noticeable with the dose of 1.25 mM FBP. For *Col2a1*, *Col6a1* and *Col6a2* mRNAs, the expression was significantly decreased by FBP treatment only in FLF cells, and not in normal fibroblasts, while the expression of *Col4a3* and *Col4a4* mRNAs was not altered.

## Fructose-1,6-bisphosphate regulates expression of ECM and ECM-degrading proteins *in vitro*

Expression of *Fn1* and *Cxcl12* mRNAs were decreased in cells that were treated with FBP while *Cdh1* mRNA expression was increased only in HLF at the higher FBP dose (Fig 6A). FBP was also able to increase superoxide dismutase 1 (*Sod1*) mRNA expression at the higher dose and in FLF cells. *Mmp2* mRNA was not different from control in any cells or FBP doses tested. Myofibroblasts are recognized to be one of the main sources of extracellular matrix in fibrosis and its degradation is compromised through inhibition of MMPs. Immunoblotting showed that, compared to HLF, FLF expressed higher levels of COL1A1, α-SMA, TIMP-1 and MMP2 (Fig 6B). Three days of FBP-treatment clearly decreased the expression levels of COL1A1, MMP2, and TIMP-1 in FLF. MMP1 and TIMP-4 levels were higher in HLF compared to FLF

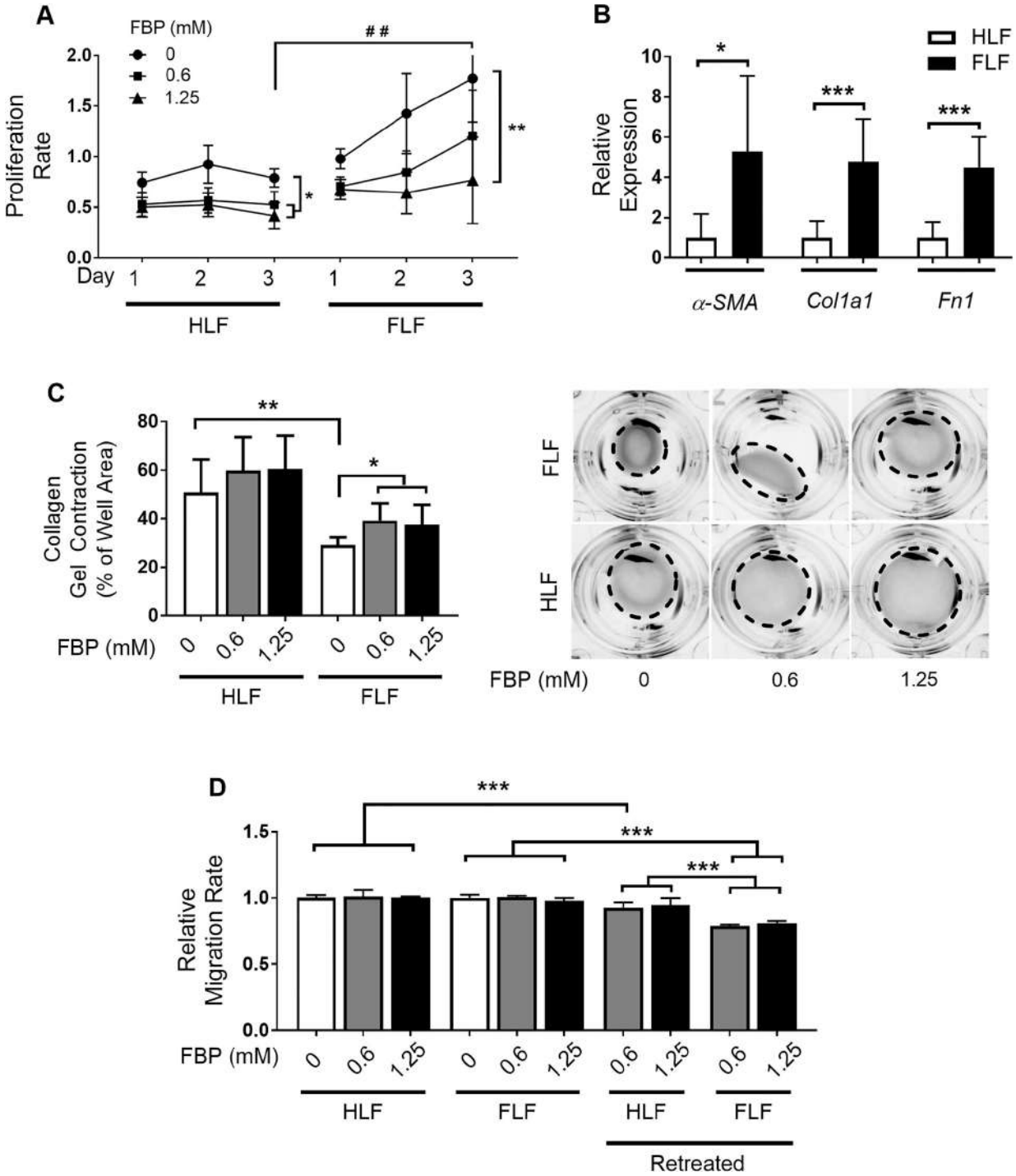


**Fig 4. Fructose-1,6-bisphosphate induces non-activated phenotype in fibroblasts.** (A) Cell growth. Cells were treated with 0, 0.6, and 1.25 mM FBP and proliferation rate of fibroblasts from healthy (HLF) and fibrotic (FLF) lungs was assessed in 1, 2, and 3 days after treatment. Y axis shows the absorbance of CCK8 assay. (B) Comparison of ECM components gene expression between cells extracted from healthy (HLF) and fibrotic (FLF) lung tissues. (C) Cell contraction analysis in collagen gel. Cells were embedded in a collagen solution and allowed to polymerize to form a gel. The gel was detached from the well and treated with different concentrations of FBP. Results are expressed as a percentage of well area occupied by the gel after a 24 h of incubation based on the size of empty well considered as 100%. Representative images used for the analysis are shown on the right. Dashed line shows the outline of the contracted gels after 24 h. (D) Cell migration assay. Cells were treated with FBP (0.6 or 1.25mM) for 3 days, detached and seeded inside an insert with 1% FBS RPMI-1640. The insert was placed inside a well of a 24-well plate with 20% FBS as chemoattractant and the invasion migration was assessed 24 h later. For retreatment, fresh FBP solution was added to the cells inside the insert (1% FBS RPMI-1640 + 0.6 or 1.25 mM FBP). The relative migration rate for all groups was calculated considering the migration values

of non-treated healthy fibroblasts (HLF 0 mM FBP) as 1. Two-way ANOVA followed by Tukey's multiple comparison test was used in A, unpaired two-tailed student's t-test was used in B, and One-way ANOVA followed by Tukey's multiple comparison test was used in C and D. Values are expressed as mean ± SD; n = 4–6/group; ## $p<0.01$ Healthy (HLF) vs. Fibrotic (FLF) without FBP (Control group) on Day 3; $^{*}p<0.05$; $^{**}p<0.01$; $^{***}p<0.001$.

https://doi.org/10.1371/journal.pone.0222202.g004

and the treatment with 1.25 mM FBP slightly reduced TIMP-4 expression while FBP had no effect on MMP1.

## Discussion

FBP is a metabolite from glycolysis produced by phosphofructokinase-1, that has many protective properties [13, 16]. In this study, the effects of FBP were evaluated in an experimental model of BLM-induced PF and in *in vitro* studies using lung fibroblasts derived from healthy and fibrotic mice. The results showed that FBP prevents the progression of PF, as revealed by improved lung function in mice, and altered ECM production, deposition and degradation. The *in vitro* results further demonstrated a phenotypical reversion-like phenomenon in lung fibroblasts by FBP treatment.

A previous study [16] showed that a single dose of FBP given at the time of BLM administration can prevent PF, with improvement of lung function. In the current study, mice were administered FBP once a day for 14 consecutive days. This was based on the hypotheses that this treatment schedule could exhibit a stronger protective effect. However, this did not seem to be the case since the mice still presented with considerable fibrosis, as seen by the Ashcroft score, mortality and weight loss. This suggests that the protective effect may be limited. Another possible reason could be the variable ranges of bleomycin activity (10 mg of bleomycin can range through 15 to 20 units) depending on the source of manufacturer. Alternatively, it is known that the fibrotic response to bleomycin is strain-dependent and C57BL/6 mice are more susceptible than BALB/c mice because of different expression of bleomycin hydrolase, cytokines and proteases [21, 22]. Since the genetic background is very important, even different mouse substrains could lead to different experimental observations even under similar conditions [23].

In the earlier studies, a human cell lineage of lung fetal fibroblasts were used [16]. Fetal and adult fibroblasts behave in different ways. Notably, human lung fetal fibroblasts have higher expression of TGF-β1 receptor interacting protein 1, and are less able to contract collagen gels than adult lung fibroblasts [24]. In heart, fetal fibroblasts have more plasma membrane and higher expression of proteins that promote the development and proliferation of cardiomyocytes, whereas adult fibroblasts are more enriched with ECM components [25]. Fetal lung fibroblasts, when confluence is reached *in vitro*, undergo cell cycle arrest even under the stimulation of growth factors, while adult fibroblasts will continue to proliferate [26]. Thus, adult fibroblasts may better reflect the response under pathological conditions, differentiating the characteristics of normal from fibrotic lungs. In the current study, in order to better demonstrate the effect of FBP, we extracted lung fibroblasts from healthy and fibrotic adult mice and treated these cells *in vitro* with FBP for 3 days.

It was thought that FBP loses its phosphates and crosses the membrane as fructose [27]. Another study demonstrated that cells and tissues treated with labelled [$C^{13}$]FBP produce [$C^{13}$]lactate, which indicates that exogenously given FBP can participate in the glycolytic pathway to reestablish ATP pool inside the cells [28]. One hypothesis is that FBP could briefly interact with calcium that stabilizes bilayer lipid membrane, leading to an increase in membrane fluidity that would allow FBP to cross it through passive diffusion [29]. Further, the permeability of FBP through a dicarboxylate transporter was reported, although only the linear

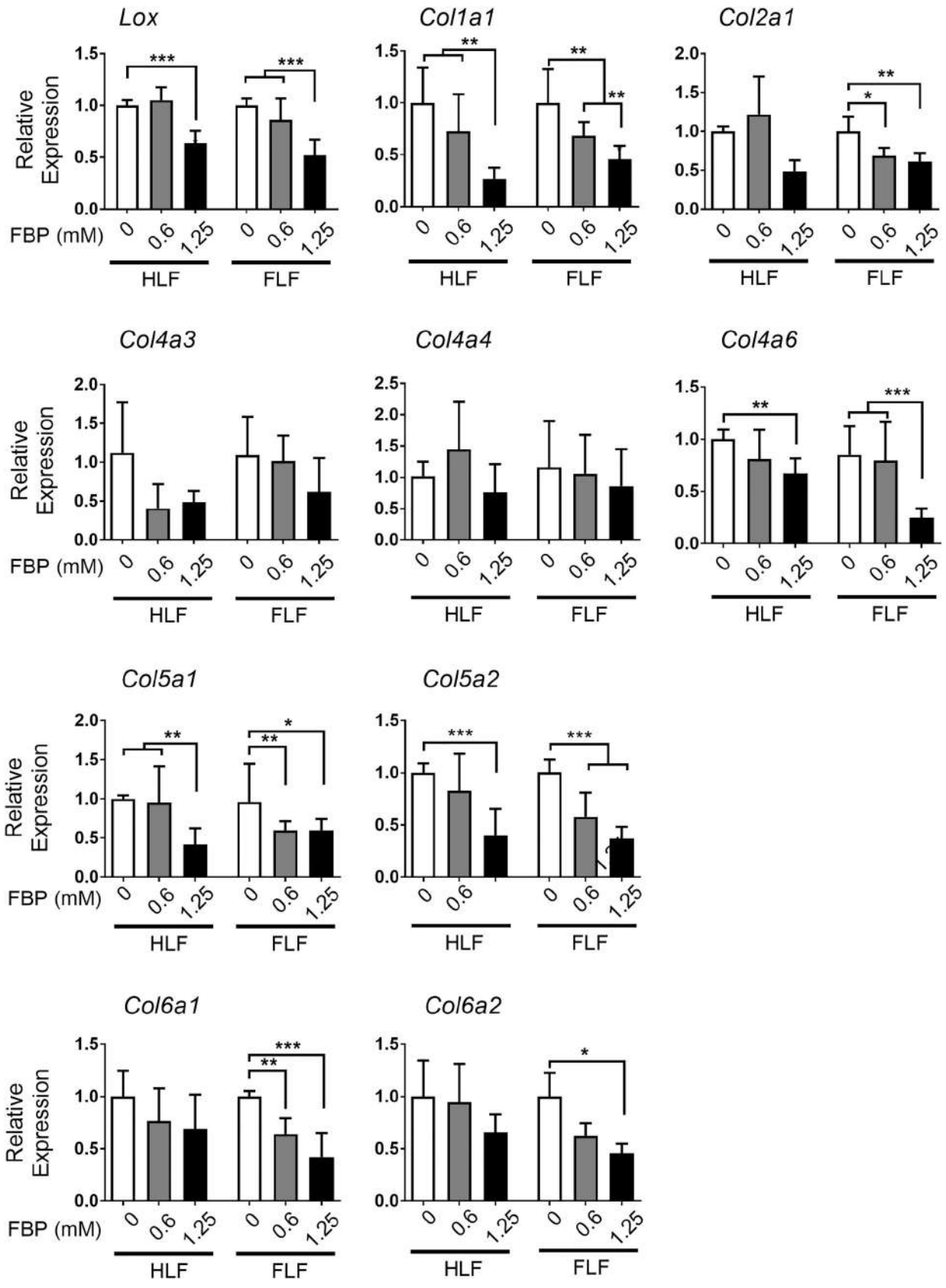
Lox
Col1a1
Col2a1
Col4a3
Col4a4
Col4a6
Col5a1
Col5a2
Col6a1
Col6a2
Relative Expression
FBP (mM)
0
0.6
1.25
HLF
FLF

**Fig 5. Fructose-1,6-bisphosphate regulates collagen-related gene expression in HLF and FLF *in vitro*.** Results show qRT-PCR analysis of mRNAs encoding for lysil oxidase (*Lox*), collagen 1a1 (*Col1a1*), collagen 2a1 (*Col1a2*), collagen 4a3 (*Col4a3*), collagen 4a4 (*Col4a4*), collagen 4a6 (*Col4a6*), collagen 5a1 (*Col5a1*), collagen 5a2 (*Col5a2*), collagen 6a1 (*Col6a1*), and collagen 6a2 (*Col6a2*). Relative expression is presented based on the expression level of control denoted as 1. One-way ANOVA followed by Tukey's multiple comparison test were used. Values are expressed as mean ± SD; $n$ = 4–6/group; $^{*}p<0.05$; $^{**}p<0.01$; $^{***}p<0.001$.

https://doi.org/10.1371/journal.pone.0222202.g005

form of FBP, a small fraction of total FBP, can use this system [30]. Despite of many authors have confirmed the effect of FBP in a variety of tissues, such as liver [31, 32], kidney [33], brain [34] and lung [9, 16], the exact mechanism of how FBP can enter the cells remains unknown.

The ranges of FBP doses used in our studies were between 12.5 and 15 mg per animal *in vivo* (animals with 25 and 30 g receiving 500 mg/kg, respectively), and 0.212 mg/ml (0.625 mM) or 0.425 mg/ml (1.25 mM) for *in vitro* treatment. A study that analyzed FBP concentration in blood of rats after a single dose of 500 mg/kg injected via IP demonstrated that the peak was reached 2 h after administration, going from control level of 15 to 35 μg/ml, which then came down to 20 μg/ml after 6 h and remained there for at least 72h [35]. This effect was also observed in the brain; the FBP levels peaked at 2 hours after administration (from 0.4 at

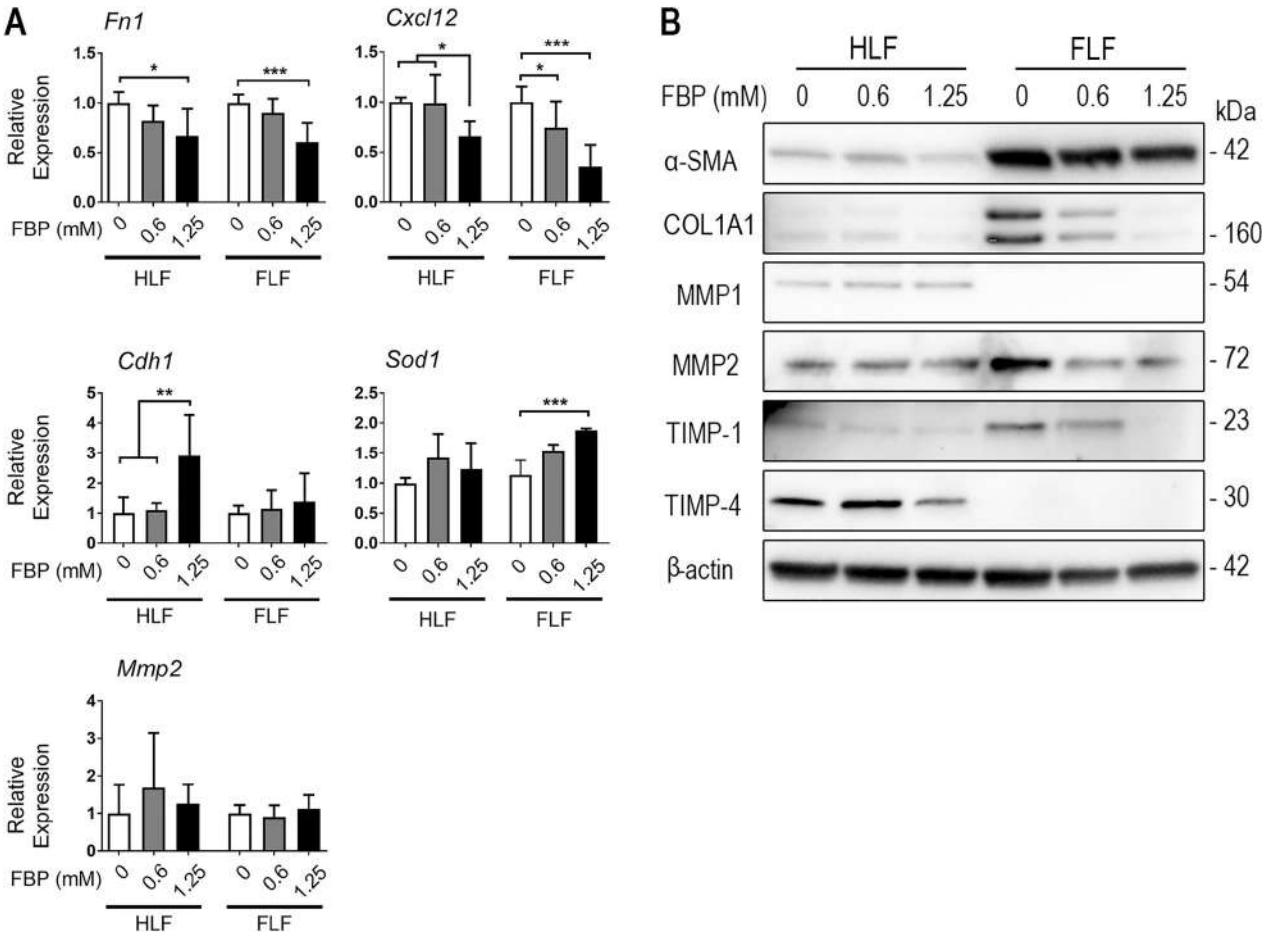


**Fig 6. Fructose-1,6-bisphosphate regulates expression of ECM and ECM-degrading proteins *in vitro*.** (A) qRT-PCR analysis for the levels of Fn1, Cxcl12, Cdh1, superoxide dismutase 1 (Sod1), and metalloproteinase 2 (Mmp2) mRNAs. Relative expression is presented based on the expression level of control as 1. One-way ANOVA followed by Tukey's multiple comparison test was used. Values are expressed as mean ± SD; n = 4–6/group; $^{*}p<0.05$; $^{**}p<0.01$; $^{***}p<0.001$. (B) Protein expression of α-SMA, COL1A1, MMP1, MMP2, TIMP-1, and TIMP-4 in HLF and FLF treated with FBP for 3 days.

https://doi.org/10.1371/journal.pone.0222202.g006

control level to 0.6 mg of FBP/g of brain tissue), followed by slow decrease during the follow 48 h (to 0.5 mg FBP/g brain tissue). The level stayed above the base line concentration up to 72h. For rats receiving 180 mg/kg FBP orally every 8 h for 7 consecutive days, FBP levels in plasma peaked at 182 μg/ml after 45 min [36]. To our knowledge, there is no report on the amount of FBP captured by lung after IP administration in mice, although reports can be found that it can prevent ischemic lung injury in rats [37]. Based on these, we believe that the amount of FBP we used in *in vitro* experiments is close to *in vivo* physiological range.

Lung function is a hallmark of PF and an important clinical indicator in humans [1, 38]. It reflects the changes in quality and an increase in the quantity of ECM components accumulated during the fibrogenic process, leading to tissue stiffening [39]. Degradation of ECM by MMPs is highly dysregulated in PF and, paradoxically, some MMPs can be overexpressed and linked to a more severe and advanced pathology stage in the lung. This is well known for MMP2, which can disrupt the basement membrane, leading to increased fibroblast invasion of the alveolar spaces. MMP1, an interstitial collagenase, is not as widely distributed in PF lungs as its inhibitor, TIMP-1. TIMPs, that inhibit MMP lytic activity, are present in great amounts in lung parenchyma of IPF patients and animals with induced PF, which contributes to an environment where collagen and other ECM components are not properly degraded [5, 40]. In mice, invasive pulmonary function, used in this study, can exhibit the same functional parameters that are measured in humans and it is the one that better reflects the diseased state of the lung [41]. The present results showed an improvement in lung function by FBP both *in vivo* and in *in vitro* experiments, which is due to FBP regulating the deposition and degradation of many ECM components. Several studies linked levels of production and deposition of collagen and other ECM components with the severity of fibrosis [42]. Cross-linking of collagen fiber is an essential step for collagen maturation and to acquire its mechanical and physical properties. This process is carried out mainly by the LOX enzyme, which is highly increased in PF [39, 42, 43] but decreased in both HLF and FLF treated with FBP. This leads us to believe that FBP may influence collagen maturation and prevent from its uncontrolled deposition.

The aspect of inflammation on human idiopathic pulmonary fibrosis (IPF) is very controversial since no treatment with immunosuppressant was able to improve the clinical course or increase survival rate of patients in clinical trials. However, some authors believe that inflammation is still crucial for IPF development, because inflammatory cells can be seen in lung biopsies and many cytokine levels are higher in BALF from IPF patients [44]. CXCL12 is a cytokine that stimulates leucocyte migration to inflammation site [45] and fibroblast activation [46]. Our data show that FBP-treatment 1) decreases bleomycin-induced pulmonary fibrosis in mice, 2) inhibits inflammatory cell migration to the lungs of mice, and 3) decreases CXCL12 expression levels in healthy and fibrotic mouse lung fibroblasts *in vitro*. These suggest that an inflammatory activity may be involved in pulmonary fibrosis development and FBP plays a role in this process. Based on the expression of ECM components, MMPs, and TIMPs, however, we believe that there may be other mechanisms behind FBP actions than anti-inflammatory activity. Further studies are required to address these questions.

Recently, Zhao and coworkers showed that skin ECM production, including collagen, is related to an upregulation of glycolysis and downregulation of gluconeogenesis, PPARγ expression and fatty acid oxidation, as observed both *in vitro* in dermal primary human fibroblasts and *in vivo* in patients that presented skin fibrosis [47]. On skin equivalents, FBP increased the amount of collagen fibrils on dermis, with increased phosphorylation of p38 MAPK and decreased desmosomal components [48]. Similarly, another study showed that idiopathic pulmonary fibrosis and fibroblast activation are related to an upregulated glycolysis with higher activity of glycolytic enzymes and lactate production [49]. However, a metabolomic analysis on IPF patients showed the contrary; downregulated glycolysis with lower rate of

phosphofructokinase (PFK) and lower level of FBP with increased lactate production, reduced mitochondrial beta-oxidation, and downregulated tricarboxylic acid (TCA) cycle in IPF lungs [50]. To proliferate, cells can deviate metabolism from oxidative phosphorylation to aerobic glycolysis, generating lactate, in a phenomenon that is known as Warburg effect. Although less efficient in producing ATP from glucose, it allows cells to divert glucose to produce macromolecular precursors to sustain growth [51]. Even if increased glycolysis is a key element for fibrosis development, it is difficult to know whether glycolysis is the inducer of fibroblast activation, as postulated in some of the studies [47–50]. In this way, it is plausible that Warburg effect happens to sustain the growth and metabolic changes needed after a growth factor signaling, i.e. TGF-β1, and the upregulation of glycolysis would be a consequence, not the trigger, of fibrotic changes in tissues and cells.

Exogenously administered FBP can also act as an activator of glycolysis, increasing lactate production rate [28] and serum ATP [52], but not preserving intracellular pH as shown in cerebral ischemia [53]. As PFK activity is inhibited by high levels of ATP and low pH [54], FBP administration could even result in a halt on PFK activity, leading to an inhibition of glycolytic pathway and consequent downregulation of fibrosis. Others report that FBP could upregulate the expression of PPARγ in hepatic stellate cells, which could increase fatty acid oxidation and decrease glycolysis [15]. Further studies are necessary to determine the exact role of FBP in cell metabolism, which are currently underway.

There are studies supporting that a fully differentiated myofibroblast phenotype is necessary to increase collagen production [55], and the present results showed that cells extracted from the fibrotic lung indeed presents increased proliferation, contraction, invasion and ECM components gene expression. Three days after FBP exposure, both healthy and fibrotic cells were significantly affected by FBP *in vitro*, showing signs of going to a quiescent state that is characteristic of normal fibroblasts. In agreement with these results, previous studies showed that FBP treatment *in vitro* promotes the deactivation of liver fibroblasts [14] even in the presence of free iron that activates fibroblasts to become myofibroblasts [15]. These results mirror some of the *in vivo* experiments, showing that FBP can have protective effects in a more complex system such as intact tissues. While most mechanisms are shared between different organs and tissues, each one represents its own challenge regarding therapeutic approach. Further, it is likely that the *in vitro* experiments presented herein may not be totally extrapolated to the much more complex *in vivo* system. However, it's interesting to note how FBP can robustly reproduce its effects in different cell lines (lung vs liver) *in vitro* and animals.

Cellular senescence is an irreversible cell-cycle arrest, where the cell maintains a metabolic and secretory profile, and can be induced by many stimuli, including oxidative stress DNA damage [56]. Others showed that FBP induced oxidative stress in hepatic carcinoma cells, which caused an inhibition in proliferation, and this effect was suppressed when these cells were treated with anti-oxidants, such as N-acetyl-l-cysteine or catalase [12]. In contrast, using the same cell line, HepG2, FBP-treatment led to cell senescence, an increase in catalase activity [10] and a decrease in thiobarbituric acid reactive substances, which is a lipid peroxidation product and an indirect measure of radical oxygen species (ROS) [57]. Regardless of this discrepancy, there is a strong body of evidence suggesting that FBP has anti-oxidant properties [13] and, in the present study, FBP was able to increase expression of an antioxidant enzyme, SOD1, in FLF. A study also showed that FBP treatment induced senescence in human lung fetal fibroblasts, which resulted in a lower proliferation rate [16]. This is in good agreement with the present study showing a lower proliferation rate and many other aspects of phenotypical reversion of lung fibroblasts after FBP treatment. Myofibroblasts are initially activated from fibroblasts by various causes including tissue/cell damage. After prolonged damage, myofibroblasts can become senescent, which results in reduced ECM deposition and increased

production of ECM degrading enzymes. This phenomena will limit the accumulation of fibrotic tissue and help fibrosis to resolve [58]. In cancer, senescent myofibroblasts express α-SMA and possess a high contractile phenotype. However, their ability to generate organized collagenous matrix is greatly reduced, suggesting that senescent myofibroblasts are α-SMA positive but non-fibrogenic cells [59].

In conclusion, the present results show that FBP prevents BLM-induced PF development in mice. *In vitro* and *in vivo* results demonstrate that this may be due to reduced expression of collagens and other ECM components, which may partly be the consequence of a reduced TIMP-1 and MMP2 expression. However, understanding the exact mechanism for the anti-fibrotic activity of FBP awaits further studies. To our knowledge, this is the first study that demonstrates a regulatory mechanism of FBP in terms of expression of genes and proteins that are responsible for ECM production and degradation. This may open the possibility of evaluating the activity of FBP on patients undergoing cancer treatment as a preventive tool against the harmfull effects of BLM in the lung.

## Supporting information

**S1 Fig. Fructose-1,6-bisphosphate inhibits healthy lung fibroblasts (HLF).** Cells were treated with 0 to 10 mM of FBP and proliferation rate of fibroblasts from healthy (HLF) lungs was assessed through 1 to 7 days after treatment. Y axis shows the proliferation rate as determined by MTT assay. Two-way ANOVA followed by Tukey's multiple comparison test was used. Values are expressed as mean ± SD; n = 4–6/group; * $p<0.05$ determined on Day 3.
(TIF)

**S1 Table. Primer sequences used for qRT-PCR analysis.**
(DOCX)

## Acknowledgments

We would like to thank Dr. Danielle Springer, Ms. Michele Allen, and Ms. Audrey Noguchi at the NHLBI Mouse Phenotyping Core for the advice and use of FlexiVent.

## Author Contributions

**Conceptualization:** Henrique Bregolin Dias, Jarbas Rodrigues de Oliveira, Márcio Vinícius Fagundes Donadio.

**Data curation:** Henrique Bregolin Dias.

**Formal analysis:** Henrique Bregolin Dias.

**Funding acquisition:** Henrique Bregolin Dias, Shioko Kimura.

**Investigation:** Henrique Bregolin Dias.

**Methodology:** Henrique Bregolin Dias.

**Resources:** Shioko Kimura.

**Supervision:** Jarbas Rodrigues de Oliveira, Márcio Vinícius Fagundes Donadio, Shioko Kimura.

**Validation:** Shioko Kimura.

**Writing – original draft:** Henrique Bregolin Dias.

**Writing – review & editing:** Henrique Bregolin Dias, Jarbas Rodrigues de Oliveira, Márcio Vinícius Fagundes Donadio, Shioko Kimura.

## References


1. Raghu G, Collard HR, Egan JJ, Martinez FJ, Behr J, Brown KK, et al. An official ATS/ERS/JRS/ALAT statement: idiopathic pulmonary fibrosis: evidence-based guidelines for diagnosis and management. Am J Respir Crit Care Med. 2011; 183(6):788–824. https://doi.org/10.1164/rccm.2009-040GL PMID: 21471066
2. Provencher DM, Jauregui AR. Recommendations for evaluating and managing idiopathic pulmonary fibrosis. JAAPA. 2018; 31(9):21–6. https://doi.org/10.1097/01.JAA.0000544299.00459.a4 PMID: 30095512
3. Tomos IP, Tzouvelekis A, Aidinis V, Manali ED, Bouros E, Bouros D, et al. Extracellular matrix remodeling in idiopathic pulmonary fibrosis. It is the 'bed' that counts and not 'the sleepers'. Expert Rev Respir Med. 2017; 11(4):299–309. https://doi.org/10.1080/17476348.2017.1300533 PMID: 28274188
4. Murtha LA, Schuliga MJ, Mabotuwana NS, Hardy SA, Waters DW, Burgess JK, et al. The processes and mechanisms of cardiac and pulmonary fibrosis. Front Physiol. 2017; 8:777. https://doi.org/10.3389/fphys.2017.00777 PMID: 29075197
5. Selman M, Ruiz V, Cabrera S, Segura L, Ramirez R, Barrios R, et al. TIMP-1, -2, -3, and -4 in idiopathic pulmonary fibrosis. A prevailing nondegradative lung microenvironment? Am J Physiol Lung Cell Mol Physiol. 2000; 279(3):L562–74. https://doi.org/10.1152/ajplung.2000.279.3.L562 PMID: 10956632
6. Misharin AV, Budinger GRS. Targeting the myofibroblast in pulmonary fibrosis. Am J Respir Crit Care Med. 2018; 198(7):834–5. https://doi.org/10.1164/rccm.201806-1037ED PMID: 29966099
7. Hinz B, Phan SH, Thannickal VJ, Galli A, Bochaton-Piallat ML, Gabbiani G. The myofibroblast: one function, multiple origins. Am J Pathol. 2007; 170(6):1807–16. https://doi.org/10.2353/ajpath.2007.070112 PMID: 17525249
8. Catarina AV, Luft C, Greggio S, Venturin GT, Ferreira F, Marques EP, et al. Fructose-1,6-bisphosphate preserves glucose metabolism integrity and reduces reactive oxygen species in the brain during experimental sepsis. Brain Res. 2018; 1698:54–61 https://doi.org/10.1016/j.brainres.2018.06.024 PMID: 29932894
9. Santos RC, Moresco RN, Pena Rico MA, Susperregui AR, Rosa JL, Bartrons R, et al. Fructose-1,6-bisphosphate protects against Zymosan-induced acute lung injury in mice. Inflammation. 2012; 35(3):1198–203. https://doi.org/10.1007/s10753-012-9429-6 PMID: 22327861
10. Krause GC, Lima KG, Haute GV, Schuster AD, Dias HB, Mesquita FC, et al. Fructose-1,6-bisphosphate decreases IL-8 levels and increases the activity of pro-apoptotic proteins in HepG2 cells. Biomed Pharmacother. 2017; 89:358–65. https://doi.org/10.1016/j.biopha.2017.01.178 PMID: 28242545
11. Li Y, Wei W, Shen HW, Hu WQ. The study of inducing apoptosis effect of fructose 1,6-bisphosphate on the papillary thyroid carcinoma cell and its related mechanism. Tumour Biol. 2014; 35(5):4539–44. https://doi.org/10.1007/s13277-013-1597-y PMID: 24414485
12. Lu YX, Yu XC, Zhu MY. Antitumor effect of fructose 1,6-bisphosphate and its mechanism in hepatocellular carcinoma cells. Tumour Biol. 2014; 35(2):1679–85. https://doi.org/10.1007/s13277-013-1231-z PMID: 24081674
13. Alva N, Alva R, Carbonell T. Fructose 1,6-Bisphosphate: A summary of its cytoprotective mechanism. Curr Med Chem. 2016; 23(39):4396–417. https://doi.org/10.2174/0929867323666161014144250 PMID: 27758716
14. de Mesquita FC, Bitencourt S, Caberlon E, da Silva GV, Basso BS, Schmid J, et al. Fructose-1,6-bisphosphate induces phenotypic reversion of activated hepatic stellate cell. Eur J Pharmacol. 2013; 720(1–3):320–5. https://doi.org/10.1016/j.ejphar.2013.09.067 PMID: 24144957
15. Dias HB, Krause GC, Squizani ED, Lima KG, Schuster AD, Pedrazza L, et al. Fructose-1,6-bisphosphate reverts iron-induced phenotype of hepatic stellate cells by chelating ferrous ions. Biometals. 2017; 30(4):549–58. https://doi.org/10.1007/s10534-017-0025-y PMID: 28639108
16. Jost RT, Dias HB, Krause GC, de Souza RG, de Souza TR, Nunez NK, et al. Fructose-1,6-bisphosphate prevents bleomycin-induced pulmonary fibrosis in mice and inhibits the proliferation of lung fibroblasts. Inflammation. 2018; 41(5):1987–2001. https://doi.org/10.1007/s10753-018-0842-3 PMID: 29995294
17. Cai Y, Kimura S. Noninvasive intratracheal intubation to study the pathology and physiology of mouse lung. J Vis Exp. 2013;(81):e50601. https://doi.org/10.3791/50601 PMID: 24300823
18. Santos RC, Moresco RN, Pena Rico MA, Susperregui AR, Rosa JL, Bartrons R, et al. Fructose-1,6-bisphosphate reduces the mortality in Candida albicans bloodstream infection and prevents the septic-

induced platelet decrease. Inflammation. 2012; 35(4):1256–61. E https://doi.org/10.1007/s10753-012-9436-7 PMID: 22367598

19. Hubner RH, Gitter W, El Mokhtari NE, Mathiak M, Both M, Bolte H, et al. Standardized quantification of pulmonary fibrosis in histological samples. Biotechniques. 2008; 44(4):507–11, 14–7. https://doi.org/10.2144/000112729 PMID: 18476815
20. Shoulders MD, Raines RT. Collagen structure and stability. Annu Rev Biochem. 2009; 78:929–58. https://doi.org/10.1146/annurev.biochem.77.032207.120833 PMID: 19344236
21. Moore BB, Hogaboam CM. Murine models of pulmonary fibrosis. Am J Physiol Lung Cell Mol Physiol. 2008; 294(2):L152–60. https://doi.org/10.1152/ajplung.00313.2007 PMID: 17993587
22. Phan SH, Kunkel SL. Lung cytokine production in bleomycin-induced pulmonary fibrosis. Exp Lung Res. 1992; 18(1):29–43. https://doi.org/10.3109/01902149209020649 PMID: 1374023
23. Simon MM, Greenaway S, White JK, Fuchs H, Gailus-Durner V, Wells S, et al. A comparative phenotypic and genomic analysis of C57BL/6J and C57BL/6N mouse strains. Genome Biol. 2013; 14(7):R82. https://doi.org/10.1186/gb-2013-14-7-r82 PMID: 23902802
24. Navarro A, Rezaiekhaligh M, Keightley JA, Mabry SM, Perez RE, Ekekezie, II. Higher TRIP-1 level explains diminished collagen contraction ability of fetal versus adult fibroblasts. Am J Physiol Lung Cell Mol Physiol. 2009; 296(6):L928–35. https://doi.org/10.1152/ajplung.00012.2009 PMID: 19329541
25. Jonsson MKB, Hartman RJG, Ackers-Johnson M, Tan WLW, Lim B, van Veen TAB, et al. A transcriptomic and epigenomic comparison of fetal and adult human cardiac fibroblasts reveals novel key transcription factors in adult cardiac fibroblasts. JACC Basic Transl Sci. 2016; 1(7):590–602. https://doi.org/10.1016/j.jacbts.2016.07.007 PMID: 30167544
26. Pratsinis H, Kletsas D, Stathakos D. Autocrine growth regulation in fetal and adult human fibroblasts. Biochem Biophys Res Commun. 1997; 237(2):348–53. https://doi.org/10.1006/bbrc.1997.7136 PMID: 9268714
27. Sano W, Watanabe F, Tamai H, Furuya E, Mino M. Beneficial effect of fructose-1,6-bisphosphate on mitochondrial function during ischemia-reperfusion of rat liver. Gastroenterology. 1995; 108(6):1785–92. https://doi.org/10.1016/0016-5085(95)90141-8 PMID: 7768384
28. Hardin CD, Roberts TM. Metabolism of exogenously applied fructose 1,6-bisphosphate in hypoxic vascular smooth muscle. Am J Physiol. 1994; 267(6 Pt 2):H2325–32.
29. Ehringer WD, Su S, Chiangb B, Stillwell W, Chien S. Destabilizing effects of fructose-1,6-bisphosphate on membrane bilayers. Lipids. 2002; 37(9):885–92. https://doi.org/10.1007/s11745-002-0975-2 PMID: 12458624
30. Hardin CD, Lazzarino G, Tavazzi B, Di Pierro D, Roberts TM, Giardina B, et al. Myocardial metabolism of exogenous FDP is consistent with transport by a dicarboxylate transporter. Am J Physiol Heart Circ Physiol. 2001; 281(6):H2654–60. https://doi.org/10.1152/ajpheart.2001.281.6.H2654 PMID: 11709435
31. Hirokawa F, Nakai T, Yamaue H. Storage solution containing fructose-1,6-bisphosphate inhibits the excess activation of Kupffer cells in cold liver preservation. Transplantation. 2002; 74(6):779–83. https://doi.org/10.1097/00007890-200209270-00008 PMID: 12364855
32. Moresco RN, Santos RC, Alves Filho JC, Cunha AA, Dos Reis C, Reichel CL, et al. Protective effect of fructose-1,6-bisphosphate in the cold storage solution for liver preservation in rat hepatic transplantation. Transplant Proc. 2004; 36(5):1261–4. https://doi.org/10.1016/j.transproceed.2004.05.040 PMID: 15251307
33. Didlake R, Kirchner KA, Lewin J, Bower JD, Markov A. Protection from ischemic renal injury by fructose-1,6-diphosphate infusion in the rat. Circ Shock. 1985; 16(2):205–12. PMID: 4053295
34. Kaakinen T, Heikkinen J, Dahlbacka S, Alaoja H, Laurila P, Kiviluoma K, et al. Fructose-1,6-bisphosphate supports cerebral energy metabolism in pigs after ischemic brain injury caused by experimental particle embolization. Heart Surg Forum. 2006; 9(6):E828–35. https://doi.org/10.1532/HSF98.20061079 PMID: 16893758
35. Xu K, Stringer JL. Pharmacokinetics of fructose-1,6-diphosphate after intraperitoneal and oral administration to adult rats. Pharmacol Res. 2008; 57(3):234–8. https://doi.org/10.1016/j.phrs.2008.01.008 PMID: 18325780
36. Li TT, Xie JZ, Wang L, Gao YY, Jiang XH. Rational application of fructose-1,6-diphosphate: From the perspective of pharmacokinetics. Acta Pharm. 2015; 65(2):147–57. https://doi.org/10.1515/acph-2015-0020 PMID: 26011931
37. Chu SJ, Chang DM, Wang D, Chen YH, Hsu CW, Hsu K. Fructose-1,6-diphosphate attenuates acute lung injury induced by ischemia-reperfusion in rats. Crit Care Med. 2002; 30(7):1605–9. https://doi.org/10.1097/00003246-200207000-00034 PMID: 12130986
38. Nava S, Rubini F. Lung and chest wall mechanics in ventilated patients with end stage idiopathic pulmonary fibrosis. Thorax. 1999; 54(5):390–5. https://doi.org/10.1136/thx.54.5.390 PMID: 10212101

39. Kristensen JH, Karsdal MA, Genovese F, Johnson S, Svensson B, Jacobsen S, et al. The role of extracellular matrix quality in pulmonary fibrosis. Respiration. 2014; 88(6):487–99. https://doi.org/10.1159/000368163 PMID: 25359084

40. Houghton AM. Matrix metalloproteinases in destructive lung disease. Matrix Biol. 2015; 44–46:167–74. https://doi.org/10.1016/j.matbio.2015.02.002 PMID: 25686691

41. Vanoirbeek JA, Rinaldi M, De Vooght V, Haenen S, Bobic S, Gayan-Ramirez G, et al. Noninvasive and invasive pulmonary function in mouse models of obstructive and restrictive respiratory diseases. Am J Respir Cell Mol Biol. 2010; 42(1):96–104. https://doi.org/10.1165/rcmb.2008-0487OC PMID: 19346316

42. Barry-Hamilton V, Spangler R, Marshall D, McCauley S, Rodriguez HM, Oyasu M, et al. Allosteric inhibition of lysyl oxidase-like-2 impedes the development of a pathologic microenvironment. Nat Med. 2010; 16(9):1009–17. https://doi.org/10.1038/nm.2208 PMID: 20818376

43. Oggionni T, Morbini P, Inghilleri S, Palladini G, Tozzi R, Vitulo P, et al. Time course of matrix metalloproteases and tissue inhibitors in bleomycin-induced pulmonary fibrosis. Eur J Histochem. 2006; 50 (4):317–25. PMID: 17213041

44. Bringardner BD, Baran CP, Eubank TD, Marsh CB. The role of inflammation in the pathogenesis of idiopathic pulmonary fibrosis. Antioxid Redox Signal. 2008; 10(2):287–301. https://doi.org/10.1089/ars.2007.1897 PMID: 17961066

45. Domanska UM, Kruizinga RC, Nagengast WB, Timmer-Bosscha H, Huls G, de Vries EG, et al. A review on CXCR4/CXCL12 axis in oncology: no place to hide. Eur J Cancer. 2013; 49(1):219–30. https://doi.org/10.1016/j.ejca.2012.05.005 PMID: 22683307

46. Lin CH, Shih CH, Tseng CC, Yu CC, Tsai YJ, Bien MY, et al. CXCL12 induces connective tissue growth factor expression in human lung fibroblasts through the Rac1/ERK, JNK, and AP-1 pathways. PLoS One. 2014; 9(8):e104746. https://doi.org/10.1371/journal.pone.0104746 PMID: 25121739

47. Zhao X, Psarianos P, Ghoraie LS, Yip K, Goldstein D, Gilbert R, et al. Metabolic regulation of dermal fibroblasts contributes to skin extracellular matrix homeostasis and fibrosis. Nature Metabolism. 2019; 1 (1):147–57.

48. Choi H, Yang SH, Bae IH, Park JY, Kim HJ, Noh M, et al. Fructose 1, 6-diphosphate regulates desmosomal proteins and collagen fibres in human skin equivalents. Exp Dermatol. 2013; 22(12):847–9. https://doi.org/10.1111/exd.12279 PMID: 24171778

49. Xie N, Tan Z, Banerjee S, Cui H, Ge J, Liu RM, et al. Glycolytic reprogramming in myofibroblast differentiation and lung fibrosis. Am J Respir Crit Care Med. 2015; 192(12):1462–74. https://doi.org/10.1164/rccm.201504-0780OC PMID: 26284610

50. Zhao YD, Yin L, Archer S, Lu C, Zhao G, Yao Y, et al. Metabolic heterogeneity of idiopathic pulmonary fibrosis: a metabolomic study. BMJ Open Respir Res. 2017; 4(1):e000183. https://doi.org/10.1136/bmjresp-2017-000183 PMID: 28883924

51. Vander Heiden MG, Cantley LC, Thompson CB. Understanding the Warburg effect: the metabolic requirements of cell proliferation. Science. 2009; 324(5930):1029–33. https://doi.org/10.1126/science.1160809 PMID: 19460998

52. Veras FP, Peres RS, Saraiva AL, Pinto LG, Louzada-Junior P, Cunha TM, et al. Fructose 1,6-bisphosphate, a high-energy intermediate of glycolysis, attenuates experimental arthritis by activating anti-inflammatory adenosinergic pathway. Sci Rep. 2015; 5:15171. https://doi.org/10.1038/srep15171 PMID: 26478088

53. Espanol MT, Litt L, Hasegawa K, Chang LH, Macdonald JM, Gregory G, et al. Fructose-1,6-bisphosphate preserves adenosine triphosphate but not intracellular pH during hypoxia in respiring neonatal rat brain slices. Anesthesiology. 1998; 88(2):461–72. https://doi.org/10.1097/00000542-199802000-00025 PMID: 9477067

54. Underwood AH, Newsholme EA. Properties of phosphofructokinase from rat liver and their relation to the control of glycolysis and gluconeogenesis. Biochem J. 1965; 95:868–75. https://doi.org/10.1042/bj0950868 PMID: 14342527

55. Phan SH. Biology of fibroblasts and myofibroblasts. Proc Am Thorac Soc. 2008; 5(3):334–7. https://doi.org/10.1513/pats.200708-146DR PMID: 18403329

56. Waters DW, Blokland KEC, Pathinayake PS, Burgess JK, Mutsaers SE, Prele CM, et al. Fibroblast senescence in the pathology of idiopathic pulmonary fibrosis. Am J Physiol Lung Cell Mol Physiol. 2018; 315(2):L162–L72. https://doi.org/10.1152/ajplung.00037.2018 PMID: 29696986

57. da Silva EF, Krause GC, Lima KG, Haute GV, Pedrazza L, Mesquita FC, et al. Rapamycin and fructose-1,6-bisphosphate reduce the HEPG2 cell proliferation via increase of free radicals and apoptosis. Oncol Rep. 2016; 36(5):2647–52. https://doi.org/10.3892/or.2016.5111 PMID: 27665945

58. Krizhanovsky V, Yon M, Dickins RA, Hearn S, Simon J, Miething C, et al. Senescence of activated stellate cells limits liver fibrosis. Cell. 2008; 134(4):657–67. https://doi.org/10.1016/j.cell.2008.06.049 PMID: 18724938

59. Mellone M, Hanley CJ, Thirdborough S, Mellows T, Garcia E, Woo J, et al. Induction of fibroblast senescence generates a non-fibrogenic myofibroblast phenotype that differentially impacts on cancer prognosis. Aging (Albany NY). 2016; 9(1):114–32.

# CAPÍTULO III

CONSIDERAÇÕES FINAIS

## CONSIDERAÇÕES FINAIS

Devido ao número crescente de novos casos de FPI sendo diagnosticados a cada ano e à sua alta mortalidade, médicos e cientistas tem buscado terapias que possam reverter o quadro fibrótico, porém ainda sem sucesso. A FBP, quando administrada de forma exógena, tem a capacidade de exercer inúmeras propriedades benéficas e proteger contra o dano celular em diferentes tecidos. A FBP vem sendo estudada, pelo menos, desde os anos 1950, mas seu potencial total ainda não foi elucidado e muitos dos efeitos que a FBP exerce ainda não possuem seus mecanismos detalhados.

Considerando estudos anteriores que mostravam que a FBP poderia ter um efeito protetor no pulmão (72) e sobre fibroblastos (106, 107), nós iniciamos testes que, primeiramente, demonstraram que esse açúcar poderia proteger contra a fibrose pulmonar desenvolvida pela administração de bleomicina intratraqueal em camundongos (108). Assim, o objetivo desse trabalho foi investigar quais mecanismos e efeitos da FBP poderiam estar relacionados a essa ação preventiva no pulmão.

A indução de fibrose pulmonar por bleomicina ocorre dentro de 14 a 21 dias. Imediatamente após a administração da droga, ocorre um extenso processo inflamatório e destruição do parênquima pulmonar, que no processo da cicatrização, resulta em fibrose. Embora o consenso geral seja de que a fibrose irá se resolver a partir do 21° dia, existem evidências que mostram que as alterações são estáveis por, no mínimo, 6 meses. Ainda, considerando a severidade do dano, existe uma alta mortalidade associada à técnica e uma significativa perda de peso durante o período de indução. Assim, as primeiras características que pudemos avaliar foram o peso e a sobrevida desses animais, o que nos deu o primeiro indício de que o tratamento foi eficaz, pois a FBP foi capaz de aumentar a sobrevida dos animais e reduzir a perda de peso inerente à indução da fibrose.

Nosso próximo passo foi realizar a análise histológica dos pulmões coletados no 15° dia após a indução para avaliarmos o grau de fibrose presente no tecido, de acordo com o método de Ashcroft modificado (109). Vimos que, em relação ao controle e àqueles animais que receberam FBP durante 15 dias, mas sem a administração da BLM (escore de zero - sem fibrose), o grupo que recebeu somente BLM teve um escore de aproximadamente 5. Isto, de acordo com o método, corresponde a uma massa fibrótica confluente, com estrutura

severamente lesada, mas ainda preservada em algumas áreas do campo visual ao microscópio. Quando os animais receberam BLM, mas foram tratados com FBP, esse escore caiu para 3, o que significa que o tecido apresentava paredes fibróticas contíguas, com espessamento de septo não maior que 3 vezes do normal, alvéolos parcialmente alargados, mas sem a presença de massa fibrótica. Ainda, visto a importância da ECM na fibrose, utilizamos a coloração com *PicroSirius Red* para visualizar e quantificar a área do tecido com produção de fibras de colágeno que foram depositadas ao longo do período de indução. Nossos resultados mostraram que a administração de BLM aumentou significativamente a área de deposição colágeno, diminuindo a área alveolar, e a FBP foi capaz de prevenir o acúmulo de colágeno, preservando a estrutura do tecido e aumentando a área alveolar.

A piora progressiva da função pulmonar é outra característica importante encontrada em pacientes com FPI, onde o colágeno leva à rigidez do tecido e dificulta uma troca gasosa eficiente. Assim, considerando os resultados obtidos pela análise do *PicroSirius*, analisamos vários parâmetros da função pulmonar dos camundongos, como elastância tecidual, *damping*, resistência, elastância, complacência e resistência *newtoniana*. Como esperado e de acordo com os resultados anteriores (108), a BLM alterou significativamente todos esses parâmetros e, com exceção da resistência *newtoniana*, nosso tratamento foi capaz de impedir o declínio da função pulmonar dos animais.

Um aspecto ainda muito controverso em relação à FPI é o papel que a inflamação exerce nessa doença. Ainda assim, a inflamação sempre foi considerada um fator extremamente importante no processo fibrótico e, mesmo considerando que a terapêutica com anti-inflamatórios não é eficaz no tratamento da FPI, há um consenso de que existe uma subinflamação, ou seja, uma inflamação mais branda que não causa uma destruição severa do tecido e ocorre ao longo dos anos de desenvolvimento da fibrose. Pacientes podem apresentar declínios agudos do quadro clínico, o que é chamado de exacerbação, e se caracterizam pelo influxo de células inflamatórias para o pulmão, podendo ser identificadas no lavado broncoalveolar (LBA) e nas biópsias. Assim, visto que existem estudos que mostram que a FBP é capaz de diminuir a migração de células inflamatórias (64), nós extraímos e quantificamos células presentes no LBA dos animais após a indução da fibrose e, de fato, a FBP foi capaz de diminuir a migração celular induzida pela BLM.

O próximo passo do nosso estudo foi tentar investigar possíveis mecanismos para os resultados encontrados. Para isso, analisamos a expressão gênica de genes relacionados à produção de ECM, EMT e à migração de leucócitos. Nossos dados indicam que o tratamento com FBP foi capaz de regular a expressão de diferentes subtipos de colágeno, o que vai de encontro à análise histológica, e Fn1, que é outro importante componente da ECM e responsável por aumentar a rigidez tecidual. A expressão de E-caderina, que está relacionada à EMT, como esperado, diminuiu nos animais que receberam apenas BLM e a FBP não foi capaz de reverter esse efeito. Ainda, a FBP regulou a expressão de CXCL12, que é uma citocina que estimula migração de leucócitos (110) e que está associada à FPI.

Esses resultados nos mostraram que a FBP pode, *in vivo*, prevenir o desenvolvimento da fibrose pulmonar e diminuir o depósito de ECM no pulmão, o que resulta na manutenção da elasticidade normal do pulmão e impede a alteração da função pulmonar. Esse efeito pareceu, em princípio, ser ocasionado pela regulação da migração de leucócitos, visto que a FBP reduz o número de células no LBA e diminui a expressão de CXCL12. Considerando que estudos do nosso laboratório mostram que a FBP reverte o fenótipo de fibroblastos ativados (106, 107) *in vitro* e que o papel da inflamação não é considerado o principal aspecto da FPI, nós decidimos avaliar o efeito da exposição de FBP em uma cultura primária de fibroblastos e miofibroblastos de camundongos. Para isso, realizamos a extração dessas células de animais saudáveis (fibroblastos) ou fibróticos (miofibroblastos). Em relação aos fibroblastos, vimos que miofibroblastos apresentam uma maior taxa de proliferação, contração e migração. Ainda, a expressão de *α-SMA, Fn1 e Col-1* foi aumentada nessas células. Com esses resultados confirmamos que as células extraídas de animais fibróticos eram miofibroblastos de fato.

Após essa confirmação, iniciamos os experimentos que buscavam analisar se a exposição *in vitro* dessas células reproduziriam alguns resultados encontrados em estudos anteriores e, mais importante, do nosso estudo *in vivo*. Testamos diferentes concentrações de FBP (0.3mM – 10mM) e escolhemos 0.6mM e 1.2mM para prosseguir com o restante dos experimentos, pois foram as concentrações que reduziram a proliferação de ambas células significativamente após 3 dias de tratamento, sem demonstrar sinais de toxicidade. Nosso laboratório mostrou que a FBP pode induzir um processo de senescência celular, que é uma parada irreversível no ciclo celular (108), e esse poderia ser um dos motivos que explicariam essa redução na proliferação. Ainda, nosso tratamento com FBP reduziu a contração de miofibroblastos, enquanto não teve efeito significativo na contração de fibroblastos, e foi capaz

de reduzir a migração celular somente quando ainda presente no cultivo celular. Esse efeito foi observado em maior grau também em miofibroblastos. Considerando a diferença de comportamento de ambas as células, cogitou-se que a FBP poderia estar exercendo uma reversão fenotípica e que esse efeito seria maior em miofibroblastos.

Assim, avaliamos genes e proteínas que pudessem estar envolvidas nesses processos. Embora alguns estudos tenham reportado que a expressão de colágeno é relativamente constante durante alguns processos de lesão celular, nossos resultados mostraram que a FBP é capaz de diminuir a expressão de diferentes subtipos dessa proteína tanto *in vivo* quanto *in vitro*. Ainda, a FBP foi capaz de diminuir a expressão de *Lox*, que é importantíssima na maturação das fibras de colágeno. Além disso, a FBP também diminuiu a expressão de *Fn1*. Visto que a composição e quantidade de ECM produzida e depositada é fundamental na fibrose, esses resultados demonstram que a FBP é capaz de regulá-la.

A citocina CXCL12 também foi analisada. Estudos mostram que essa citocina derivada de fibroblastos associados à câncer aumenta a habilidade de invasão de certos tumores (111). Isso nos levou a cogitar que fibroblastos e miofibroblastos que possuem uma expressão aumentada desse gene, além de alterar a estrutura e rigidez do tecido, podem estimular a migração de diferentes células e a liberação de mais fatores fibróticos no local da lesão. Nosso tratamento com FBP reduziu a expressão de CXCL12, o que está de acordo com nossos resultados *in vivo,* e nos leva a crer que a FBP pode inibir a migração de outras células além de leucócitos. Surpreendentemente, assim como a FBP não foi capaz de reestabelecer a expressão de e-caderina *in vivo*, em miofibroblastos também não houve diferença com nosso tratamento. Ao contrário, a FBP foi capaz de aumentar a expressão desse gene em fibroblastos saudáveis. Isso sugere que a FBP não é capaz de regular o processo de EMT. Além disso, alguns estudos demonstram que a FBP possui um papel antioxidante e vimos que nosso tratamento foi capaz de aumentar a expressão de *SOD* somente em miofibroblastos e na concentração de 1.2mM. Isso sugere que a FBP pode ter um efeito protetor contra radicais livres nessas células. Por fim, analisamos a expressão de *Mmp2*, que hidroliza diferentes subtipos de colágeno, elastina e Fn1, e está altamente desregulada na fibrose pulmonar (48). Ainda, alguns estudos mostram que a MMP2 pode causar uma ruptura na membrana basal e facilitar a invasão do espaço alveolar. Nossos dados mostram que a expressão dessa enzima não foi afetada pelo tratamento com FBP.

Por fim, considerando os resultados que obtivemos pela expressão gênica, analisamos a expressão de proteínas relacionadas a degradação da ECM. Primeiramente, vimos que miofibroblastos, quando comparados a fibroblastos, produzem grandes quantidades de α-SMA e colágeno e que o tratamento com 0,6mM e 1,2mM foi capaz de diminuir essa produção tanto em fibroblastos quanto em miofibroblastos. Ainda, vimos que miofibroblastos não produzem, ou produzem em níveis indetectáveis, MMP1, que é uma colagenase importante para o reestabelecimento do tecido saudável durante a resolução da fibrose. Isso ocorre por que inibidores de metaloproteinase tecidual 1 (TIMP-1), presente em miofibroblastos, inibe a produção de MMP1, impedindo a degradação eficiente do colágeno. A FBP foi capaz de diminuir a produção de TIMP-1 em miofibroblastos enquanto não teve efeito visível em fibroblastos. Ao mesmo tempo, o tratamento não teve efeito sobre a produção de MMP1. Isso sugere que a FBP é capaz de regular a produção, além da expressão, de importantes componentes de ECM, mas esse efeito não parece ser resultado da degradação por MMP1, visto que, mesmo diminuindo a produção de TIMP-1, a FBP não foi capaz levar à produção de MMP1 em miofibroblastos. A MMP2 está desregulada na FPI e a inibição dessa proteína melhora o desenvolvimento de fibrose pulmonar em modelos experimentais. Fibroblastos apresentaram níveis menores de MMP2 quando comparados com miofibroblastos, o que vai de encontro com a literatura, e a FBP diminui esses níveis em miofibroblastos. Inibidores de metaloproteinase tecidual 4 (TIMP-4), através de uma ligação no C-terminal, interage com a MMP2 para exercer seu papel inibidor. Nossos dados mostraram a ausência da produção de TIMP-4 em miofibroblastos e, em fibroblastos, uma diminuição com tratamento de 1.2mM.

Em resumo, essa tese fornece evidências de que a FBP previne o desenvolvimento de fibrose pulmonar em camundongos. Nossos resultados, tanto *in vivo* quanto *in vitro*, sugerem que esse efeito pode ser consequência da regulação da composição e degradação da ECM no tecido pulmonar, como expressão reduzida de colágeno e outros componentes de ECM, e da diminuição da TIMP-1 em miofibroblastos tratados com FBP. É sabido que se necessita de cautela para extrapolar resultados encontrados *in vitro* diretamente para modelos *in vivo*, porém é interessante o fato de que a FBP é capaz de, sistematicamente, reproduzir seus efeitos em diferentes tipos celulares e nos mais variados modelos experimentais. Por isso, o estudo detalhado desse açúcar bifosforilado deve continuar para que possamos identificar em detalhes todo o seu potencial.

## REFERÊNCIAS


1. Wynn TA, Ramalingam TR. Mechanisms of fibrosis: therapeutic translation for fibrotic disease. Nat Med. 2012;18(7):1028-40.

2. Kim KK, Kugler MC, Wolters PJ, Robillard L, Galvez MG, Brumwell AN, et al. Alveolar epithelial cell mesenchymal transition develops in vivo during pulmonary fibrosis and is regulated by the extracellular matrix. Proc Natl Acad Sci U S A. 2006;103(35):13180-5.

3. Hinz B, Phan SH, Thannickal VJ, Galli A, Bochaton-Piallat ML, Gabbiani G. The myofibroblast: one function, multiple origins. The American journal of pathology. 2007;170(6):1807-16.

4. King TE, Jr., Pardo A, Selman M. Idiopathic pulmonary fibrosis. Lancet. 2011;378(9807):1949-61.

5. Adamson IYR, Young L, Bowden DH. Relationship of Alveolar Epithelial Injury and Repair to the Induction of Pulmonary Fibrosis. American Journal of Pathology. 1988;130(2):377-83.

6. Sime PJ, O'Reilly KMA. Fibrosis of the lung and other tissues: New concepts in pathogenesis and treatment. Clinical immunology. 2001;99(3):308-19.

7. Lama VN, Flaherty KR, Toews GB, Colby TV, Travis WD, Long Q, et al. Prognostic value of desaturation during a 6-minute walk test in idiopathic interstitial pneumonia. Am J Respir Crit Care Med. 2003;168(9):1084-90.

8. Schwartz DA, Van Fossen DS, Davis CS, Helmers RA, Dayton CS, Burmeister LF, et al. Determinants of progression in idiopathic pulmonary fibrosis. Am J Respir Crit Care Med. 1994;149(2 Pt 1):444-9.

9. Schwartz DA, Helmers RA, Galvin JR, Van Fossen DS, Frees KL, Dayton CS, et al. Determinants of survival in idiopathic pulmonary fibrosis. Am J Respir Crit Care Med. 1994;149(2 Pt 1):450-4.

10. Martinez FJ, Safrin S, Weycker D, Starko KM, Bradford WZ, King TE, et al. The clinical course of patients with idiopathic pulmonary fibrosis. Ann Intern Med. 2005;142(12):963-7.

11. Oldham JM, Noth I. Idiopathic pulmonary fibrosis: early detection and referral. Respiratory medicine. 2014;108(6):819-29.

12. Fernandez IE, Eickelberg O. New cellular and molecular mechanisms of lung injury and fibrosis in idiopathic pulmonary fibrosis. Lancet. 2012;380(9842):680-8.

13. Lederer DJ, Martinez FJ. Idiopathic Pulmonary Fibrosis. N Engl J Med. 2018;378(19):1811-23.

14. Sauleda J, Nunez B, Sala E, Soriano JB. Idiopathic Pulmonary Fibrosis: Epidemiology, Natural History, Phenotypes. Med Sci (Basel). 2018;6(4).

15. American Thoracic Society. Idiopathic pulmonary fibrosis: diagnosis and treatment. International consensus statement. American Thoracic Society (ATS), and the European Respiratory Society (ERS). Am J Respir Crit Care Med. 2000;161(2 Pt 1):646-64.

16. American Thoracic S, European Respiratory S. American Thoracic Society/European Respiratory Society International Multidisciplinary Consensus Classification of the Idiopathic Interstitial Pneumonias. This joint statement of the American Thoracic Society (ATS), and the European Respiratory Society (ERS) was adopted by the ATS board of directors, June 2001 and by the ERS Executive Committee, June 2001. Am J Respir Crit Care Med. 2002;165(2):277-304.

17. Michaelson JE, Aguayo SM, Roman J. Idiopathic pulmonary fibrosis: a practical approach for diagnosis and management. Chest. 2000;118(3):788-94.

18. Collard HR, Chen SY, Yeh WS, Li Q, Lee YC, Wang A, et al. Health care utilization and costs of idiopathic pulmonary fibrosis in U.S. Medicare beneficiaries aged 65 years and older. Ann Am Thorac Soc. 2015;12(7):981-7.

19. Raghu G, Weycker D, Edelsberg J, Bradford WZ, Oster G. Incidence and prevalence of idiopathic pulmonary fibrosis. Am J Respir Crit Care Med. 2006;174(7):810-6.

20. Navaratnam V, Fleming KM, West J, Smith CJ, Jenkins RG, Fogarty A, et al. The rising incidence of idiopathic pulmonary fibrosis in the U.K. Thorax. 2011;66(6):462-7.

21. Baddini-Martinez J, Pereira CA. How many patients with idiopathic pulmonary fibrosis are there in Brazil? J Bras Pneumol. 2015;41(6):560-1.

22. Algranti E, Saito CA, Silva D, Carneiro APS, Bussacos MA. Mortality from idiopathic pulmonary fibrosis: a temporal trend analysis in Brazil, 1979-2014. J Bras Pneumol. 2017;43(6):445-50.

23. Purokivi M, Hodgson U, Myllarniemi M, Salomaa ER, Kaarteenaho R. Are physicians in primary health care able to recognize pulmonary fibrosis? Eur Clin Respir J. 2017;4(1):1290339.

24. Raghu G, Remy-Jardin M, Myers JL, Richeldi L, Ryerson CJ, Lederer DJ, et al. Diagnosis of Idiopathic Pulmonary Fibrosis. An Official ATS/ERS/JRS/ALAT Clinical Practice Guideline. Am J Respir Crit Care Med. 2018;198(5):e44-e68.

25. Hansell DM, Bankier AA, MacMahon H, McLoud TC, Muller NL, Remy J. Fleischner Society: glossary of terms for thoracic imaging. Radiology. 2008;246(3):697-722.

26. Lynch DA, Godwin JD, Safrin S, Starko KM, Hormel P, Brown KK, et al. High-resolution computed tomography in idiopathic pulmonary fibrosis: diagnosis and prognosis. Am J Respir Crit Care Med. 2005;172(4):488-93.

27. Silva CI, Marchiori E, Souza Junior AS, Muller NL, Comissao de Imagem da Sociedade Brasileira de Pneumologia e T. Illustrated Brazilian consensus of terms and fundamental patterns in chest CT scans. J Bras Pneumol. 2010;36(1):99-123.

28. Raghu G, Collard HR, Egan JJ, Martinez FJ, Behr J, Brown KK, et al. An official ATS/ERS/JRS/ALAT statement: idiopathic pulmonary fibrosis: evidence-based guidelines for diagnosis and management. Am J Respir Crit Care Med. 2011;183(6):788-824.

29. Nava S, Rubini F. Lung and chest wall mechanics in ventilated patients with end stage idiopathic pulmonary fibrosis. Thorax. 1999;54(5):390-5.

30. Kristensen JH, Karsdal MA, Genovese F, Johnson S, Svensson B, Jacobsen S, et al. The role of extracellular matrix quality in pulmonary fibrosis. Respiration. 2014;88(6):487-99.

31. Thannickal VJ, Henke CA, Horowitz JC, Noble PW, Roman J, Sime PJ, et al. Matrix biology of idiopathic pulmonary fibrosis: a workshop report of the national heart, lung, and blood institute. Am J Pathol. 2014;184(6):1643-51.

32. Finnson KW, Arany PR, Philip A. Transforming Growth Factor Beta Signaling in Cutaneous Wound Healing: Lessons Learned from Animal Studies. Advances in wound care. 2013;2(5):225-37.

33. Liu RM, Gaston Pravia KA. Oxidative stress and glutathione in TGF-beta-mediated fibrogenesis. Free radical biology & medicine. 2010;48(1):1-15.

34. Bocchino M, Agnese S, Fagone E, Svegliati S, Grieco D, Vancheri C, et al. Reactive oxygen species are required for maintenance and differentiation of primary lung fibroblasts in idiopathic pulmonary fibrosis. PloS one. 2010;5(11):e14003.

35. Shi M, Zhu J, Wang R, Chen X, Mi L, Walz T, et al. Latent TGF-beta structure and activation. Nature. 2011;474(7351):343-9.

36. Leask A, Abraham DJ. TGF-beta signaling and the fibrotic response. FASEB journal : official publication of the Federation of American Societies for Experimental Biology. 2004;18(7):816-27.

37. Nakao A, Imamura T, Souchelnytskyi S, Kawabata M, Ishisaki A, Oeda E, et al. TGF-beta receptor-mediated signalling through Smad2, Smad3 and Smad4. The EMBO journal. 1997;16(17):5353-62.

38. Nakao A, Afrakhte M, Moren A, Nakayama T, Christian JL, Heuchel R, et al. Identification of Smad7, a TGFbeta-inducible antagonist of TGF-beta signalling. Nature. 1997;389(6651):631-5.

39. Barry-Hamilton V, Spangler R, Marshall D, McCauley S, Rodriguez HM, Oyasu M, et al. Allosteric inhibition of lysyl oxidase-like-2 impedes the development of a pathologic microenvironment. Nat Med. 2010;16(9):1009-17.

40. Shoulders MD, Raines RT. Collagen structure and stability. Annu Rev Biochem. 2009;78:929-58.

41. Oggionni T, Morbini P, Inghilleri S, Palladini G, Tozzi R, Vitulo P, et al. Time course of matrix metalloproteases and tissue inhibitors in bleomycin-induced pulmonary fibrosis. Eur J Histochem. 2006;50(4):317-25.

42. Georges PC, Hui JJ, Gombos Z, McCormick ME, Wang AY, Uemura M, et al. Increased stiffness of the rat liver precedes matrix deposition: implications for fibrosis. Am J Physiol Gastrointest Liver Physiol. 2007;293(6):G1147-54.

43. Hernnas J, Nettelbladt O, Bjermer L, Sarnstrand B, Malmstrom A, Hallgren R. Alveolar accumulation of fibronectin and hyaluronan precedes bleomycin-induced pulmonary fibrosis in the rat. Eur Respir J. 1992;5(4):404-10.

44. Torr EE, Ngam CR, Bernau K, Tomasini-Johansson B, Acton B, Sandbo N. Myofibroblasts exhibit enhanced fibronectin assembly that is intrinsic to their contractile phenotype. J Biol Chem. 2015;290(11):6951-61.

45. Kessenbrock K, Plaks V, Werb Z. Matrix metalloproteinases: regulators of the tumor microenvironment. Cell. 2010;141(1):52-67.

46. Herrera I, Cisneros J, Maldonado M, Ramirez R, Ortiz-Quintero B, Anso E, et al. Matrix metalloproteinase (MMP)-1 induces lung alveolar epithelial cell migration and proliferation, protects from apoptosis, and represses mitochondrial oxygen consumption. The Journal of biological chemistry. 2013;288(36):25964-75.

47. Craig VJ, Zhang L, Hagood JS, Owen CA. Matrix Metalloproteinases As Therapeutic Targets For Idiopathic Pulmonary Fibrosis. American journal of respiratory cell and molecular biology. 2015.

48. Cai Y, Zhu L, Zhang F, Niu G, Lee S, Kimura S, et al. Noninvasive monitoring of pulmonary fibrosis by targeting matrix metalloproteinases (MMPs). Mol Pharm. 2013;10(6):2237-47.

49. King TE, Jr., Bradford WZ, Castro-Bernardini S, Fagan EA, Glaspole I, Glassberg MK, et al. A phase 3 trial of pirfenidone in patients with idiopathic pulmonary fibrosis. N Engl J Med. 2014;370(22):2083-92.

50. Kono M, Nakamura Y, Enomoto N, Saito G, Koyanagi Y, Miyashita K, et al. Prognostic impact of an early marginal decline in forced vital capacity in idiopathic pulmonary fibrosis patients treated with pirfenidone. Respir Investig. 2019.

51. Perelas A, Glennie J, van Kerkhove K, Li M, Scheraga RG, Olman MA, et al. Choice of antifibrotic medication and disease severity predict weight loss in idiopathic pulmonary fibrosis. Pulm Pharmacol Ther. 2019;59:101839.

52. Sakamoto S, Itoh T, Muramatsu Y, Satoh K, Ishida F, Sugino K, et al. Efficacy of pirfenidone in patients with advanced-stage idiopathic pulmonary fibrosis. Intern Med. 2013;52(22):2495-501.

53. Ogura T, Taniguchi H, Azuma A, Inoue Y, Kondoh Y, Hasegawa Y, et al. Safety and pharmacokinetics of nintedanib and pirfenidone in idiopathic pulmonary fibrosis. Eur Respir J. 2015;45(5):1382-92.

54. Idiopathic Pulmonary Fibrosis Clinical Research N, Raghu G, Anstrom KJ, King TE, Jr., Lasky JA, Martinez FJ. Prednisone, azathioprine, and N-acetylcysteine for pulmonary fibrosis. The New England journal of medicine. 2012;366(21):1968-77.

55. Della Latta V, Cecchettini A, Del Ry S, Morales MA. Bleomycin in the setting of lung fibrosis induction: From biological mechanisms to counteractions. Pharmacol Res. 2015;97:122-30.

56. Molina-Molina M, Pereda J, Xaubet A. [Experimental models for the study of pulmonary fibrosis: current usefulness and future promise]. Archivos de bronconeumologia. 2007;43(9):501-7.

57. Moore BB, Hogaboam CM. Murine models of pulmonary fibrosis. Am J Physiol Lung Cell Mol Physiol. 2008;294(2):L152-60.

58. Usuki J, Fukuda Y. Evolution of three patterns of intra-alveolar fibrosis produced by bleomycin in rats. Pathol Int. 1995;45(8):552-64.

59. Limjunyawong N, Mitzner W, Horton MR. A mouse model of chronic idiopathic pulmonary fibrosis. Physiological reports. 2014;2(2):e00249.

60. Santos-Silva MA, Pires KM, Trajano ET, Martins V, Nesi RT, Benjamin CF, et al. Redox imbalance and pulmonary function in bleomycin-induced fibrosis in C57BL/6, DBA/2, and BALB/c mice. Toxicol Pathol. 2012;40(5):731-41.

61. Safaeian L, Jafarian-Dehkordi A, Rabbani M, Sadeghi HM, Afshar-Moghaddam N, Sarahroodi S. Comparison of bleomycin-induced pulmonary apoptosis between NMRI mice and C57BL/6 mice. Research in pharmaceutical sciences. 2013;8(1):43-50.

62. Chen LJ, Ye H, Zhang Q, Li FZ, Song LJ, Yang J, et al. Bleomycin induced epithelial-mesenchymal transition (EMT) in pleural mesothelial cells. Toxicology and applied pharmacology. 2015;283(2):75-82.

63. de Mello RO, Lunardelli A, Caberlon E, de Moraes CM, Christ Vianna Santos R, da Costa VL, et al. Effect of N-acetylcysteine and fructose-1,6-bisphosphate in the treatment of experimental sepsis. Inflammation. 2011;34(6):539-50.

64. Bordignon Nunes F, Meier Graziottin C, Alves Filho JC, Lunardelli A, Caberlon E, Peres A, et al. Immunomodulatory effect of fructose-1,6-bisphosphate on T-lymphocytes. Int Immunopharmacol. 2003;3(2):267-72.

65. Alva N, Alva R, Carbonell T. Fructose 1,6-Bisphosphate: A Summary of Its Cytoprotective Mechanism. Curr Med Chem. 2016;23(39):4396-417.

66. Hirokawa F, Nakai T, Yamaue H. Storage solution containing fructose-1,6-bisphosphate inhibits the excess activation of Kupffer cells in cold liver preservation. Transplantation. 2002;74(6):779-83.

67. Cuesta E, Boada J, Calafell R, Perales JC, Roig T, Bermudez J. Fructose 1,6-bisphosphate prevented endotoxemia, macrophage activation, and liver injury induced by D-galactosamine in rats. Crit Care Med. 2006;34(3):807-14.

68. Moresco RN, Santos RC, Alves Filho JC, Cunha AA, Dos Reis C, Reichel CL, et al. Protective effect of fructose-1,6-bisphosphate in the cold storage solution for liver preservation in rat hepatic transplantation. Transplant Proc. 2004;36(5):1261-4.

69. Didlake R, Kirchner KA, Lewin J, Bower JD, Markov A. Protection from ischemic renal injury by fructose-1,6-diphosphate infusion in the rat. Circ Shock. 1985;16(2):205-12.

70. Bickler PE, Buck LT. Effects of fructose-1,6-bisphosphate on glutamate release and ATP loss from rat brain slices during hypoxia. J Neurochem. 1996;67(4):1463-8.

71. Kaakinen T, Heikkinen J, Dahlbacka S, Alaoja H, Laurila P, Kiviluoma K, et al. Fructose-1,6-bisphosphate supports cerebral energy metabolism in pigs after ischemic brain injury caused by experimental particle embolization. Heart Surg Forum. 2006;9(6):E828-35.

72. Santos RC, Moresco RN, Pena Rico MA, Susperregui AR, Rosa JL, Bartrons R, et al. Fructose-1,6-bisphosphate protects against Zymosan-induced acute lung injury in mice. Inflammation. 2012;35(3):1198-203.

73. Markov AK, Warren ET, Cohly HH, Sauls DJ, Skelton TN. Influence of fructose-1,6-diphosphate on endotoxin-induced lung injuries in sheep. J Surg Res. 2007;138(1):45-50.

74. Chu SJ, Chang DM, Wang D, Chen YH, Hsu CW, Hsu K. Fructose-1,6-diphosphate attenuates acute lung injury induced by ischemia-reperfusion in rats. Crit Care Med. 2002;30(7):1605-9.

75. Hardin CD, Roberts TM. Metabolism of exogenously applied fructose 1,6-bisphosphate in hypoxic vascular smooth muscle. Am J Physiol. 1994;267(6 Pt 2):H2325-32.

76. Sun JX, Farias LA, Markov AK. Fructose 1-6 diphosphate prevents intestinal ischemic reperfusion injury and death in rats. Gastroenterology. 1990;98(1):117-26.

77. Rigobello MP, Galzigna L. Pharmacokinetics of fructose-1, 6-diphosphate in the rat. Farmaco Sci. 1982;37(7):459-62.

78. Sano W, Watanabe F, Tamai H, Furuya E, Mino M. Beneficial effect of fructose-1,6-bisphosphate on mitochondrial function during ischemia-reperfusion of rat liver. Gastroenterology. 1995;108(6):1785-92.

79. Hardin CD, Lazzarino G, Tavazzi B, Di Pierro D, Roberts TM, Giardina B, et al. Myocardial metabolism of exogenous FDP is consistent with transport by a dicarboxylate transporter. Am J Physiol Heart Circ Physiol. 2001;281(6):H2654-60.

80. Ehringer WD, Su S, Chiangb B, Stillwell W, Chien S. Destabilizing effects of fructose-1,6-bisphosphate on membrane bilayers. Lipids. 2002;37(9):885-92.

81. Gregory GA, Yu AC, Chan PH. Fructose-1,6-bisphosphate protects astrocytes from hypoxic damage. J Cereb Blood Flow Metab. 1989;9(1):29-34.

82. Nunes FB, Gaspareto PB, Santos RC, de Assis M, Graziottin CM, Biolchi V, et al. Intravenous toxicity of fructose-1,6-bisphosphate in rats. Toxicology letters. 2003;143(1):73-81.

83. Vexler Z, Berrios M, Ursell PC, Sola A, Ferriero DM, Gregory GA. Toxicity of fructose-1,6-bisphosphate in developing normoxic rats. Pharmacology & toxicology. 1999;84(3):115-21.

84. Valerio DA, Ferreira FI, Cunha TM, Alves-Filho JC, Lima FO, De Oliveira JR, et al. Fructose-1,6-bisphosphate reduces inflammatory pain-like behaviour in mice: role of adenosine acting on A1 receptors. British journal of pharmacology. 2009;158(2):558-68.

85. Xu K, Stringer JL. Pharmacokinetics of fructose-1,6-diphosphate after intraperitoneal and oral administration to adult rats. Pharmacol Res. 2008;57(3):234-8.

86. Spasojevic I, Mojovic M, Blagojevic D, Spasic SD, Jones DR, Nikolic-Kokic A, et al. Relevance of the capacity of phosphorylated fructose to scavenge the hydroxyl radical. Carbohydrate research. 2009;344(1):80-4.

87. Spasojevic I, Bajic A, Jovanovic K, Spasic M, Andjus P. Protective role of fructose in the metabolism of astroglial C6 cells exposed to hydrogen peroxide. Carbohydrate research. 2009;344(13):1676-81.

88. Bochi GV, Torbitz VD, Cargnin LP, Sangoi MB, Santos RC, Gomes P, et al. Fructose-1,6-bisphosphate and N-acetylcysteine attenuate the formation of advanced oxidation protein products, a new class of inflammatory mediators, in vitro. Inflammation. 2012;35(6):1786-92.

89. Calafell R, Boada J, Santidrian AF, Gil J, Roig T, Perales JC, et al. Fructose 1,6-bisphosphate reduced TNF-alpha-induced apoptosis in galactosamine sensitized rat hepatocytes through activation of nitric oxide and cGMP production. European journal of pharmacology. 2009;610(1-3):128-33.

90. Gilg K, Mayer T, Ghaschghaie N, Klufers P. The metal-binding sites of glycose phosphates. Dalton Trans. 2009(38):7934-45.

91. Bajic A, Zakrzewska J, Godjevac D, Andjus P, Jones DR, Spasic M, et al. Relevance of the ability of fructose 1,6-bis(phosphate) to sequester ferrous but not ferric ions. Carbohydrate research. 2011;346(3):416-20.

92. Hassinen IE, Nuutinen EM, Ito K, Nioka S, Lazzarino G, Giardina B, et al. Mechanism of the effect of exogenous fructose 1,6-bisphosphate on myocardial energy metabolism. Circulation. 1991;83(2):584-93.

93. Kelleher JA, Chan TY, Chan PH, Gregory GA. Protection of astrocytes by fructose 1,6-bisphosphate and citrate ameliorates neuronal injury under hypoxic conditions. Brain Res. 1996;726(1-2):167-73.

94. Sola A, Panes J, Xaus C, Hotter G. Fructose-1,6-biphosphate and nucleoside pool modifications prevent neutrophil accumulation in the reperfused intestine. J Leukoc Biol. 2003;73(1):74-81.

95. Nunes FB, Alves-Filho JC, Alves Bastos CM, Tessele PM, Caberlon E, Moreira KB, et al. Effect of the chlorpropamide and fructose-1,6-bisphosphate of soluble TNF receptor II levels. Pharmacological research : the official journal of the Italian Pharmacological Society. 2004;49(5):449-53.

96. Kim YC, Park TY, Baik E, Lee SH. Fructose-1,6-bisphosphate attenuates induction of nitric oxide synthase in microglia stimulated with lipopolysaccharide. Life sciences. 2012;90(9-10):365-72.

97. Alves Filho JC, Santos RC, Castaman TA, de Oliveira JR. Anti-inflammatory effects of fructose-1,6-bisphosphate on carrageenan-induced pleurisy in rat. Pharmacological research : the official journal of the Italian Pharmacological Society. 2004;49(3):245-8.

98. Catarina AV, Luft C, Greggio S, Venturin GT, Ferreira F, Marques EP, et al. Fructose-1,6-bisphosphate preserves glucose metabolism integrity and reduces reactive oxygen species in the brain during experimental sepsis. Brain Res. 2018;1698:54-61.

99. Veras FP, Peres RS, Saraiva AL, Pinto LG, Louzada-Junior P, Cunha TM, et al. Fructose 1,6-bisphosphate, a high-energy intermediate of glycolysis, attenuates experimental arthritis by activating anti-inflammatory adenosinergic pathway. Sci Rep. 2015;5:15171.

100. Liu J, Li L, Wang Y, Chang Y. [Clinical study of fructose 1,6-diphosphate on myocardial ischemia/reperfusion injuries]. Hunan Yi Ke Da Xue Xue Bao. 1998;23(5):476-8.

101. Pasotti C, Nicrosini S, Fiori G. [Effects of fructose-1,6-diphosphate in patients with chronic ischemic heart disease. Echocardiographic study]. Riv Eur Sci Med Farmacol. 1989;11(4):315-20.

102. Karaca M, Kilic E, Yazici B, Demir S, de la Torre JC. Ischemic stroke in elderly patients treated with a free radical scavenger-glycolytic intermediate solution: a preliminary pilot trial. Neurol Res. 2002;24(1):73-80.

103. Markov AK, Neely WA, Didlake RH, Terry J, 3rd, Causey A, Lehan PH. Metabolic responses to fructose-1,6-diphosphate in healthy subjects. Metabolism. 2000;49(6):698-703.

104. Marchesani F, Valerio G, Dardes N, Viglianti B, Sanguinetti CM. Effect of intravenous fructose 1,6-diphosphate administration in malnourished chronic obstructive pulmonary disease patients with chronic respiratory failure. Respiration. 2000;67(2):177-82.

105. Munger MA, Botti RE, Grinblatt MA, Kasmer RJ. Effect of intravenous fructose-1,6-diphosphate on myocardial contractility in patients with left ventricular dysfunction. Pharmacotherapy. 1994;14(5):522-8.

106. de Mesquita FC, Bitencourt S, Caberlon E, da Silva GV, Basso BS, Schmid J, et al. Fructose-1,6-bisphosphate induces phenotypic reversion of activated hepatic stellate cell. Eur J Pharmacol. 2013;720(1-3):320-5.

107. Dias HB, Krause GC, Squizani ED, Lima KG, Schuster AD, Pedrazza L, et al. Fructose-1,6-bisphosphate reverts iron-induced phenotype of hepatic stellate cells by chelating ferrous ions. Biometals. 2017;30(4):549-58.

108. Jost RT, Dias HB, Krause GC, de Souza RG, de Souza TR, Nunez NK, et al. Fructose-1,6-Bisphosphate Prevents Bleomycin-Induced Pulmonary Fibrosis in Mice and Inhibits the Proliferation of Lung Fibroblasts. Inflammation. 2018;41(5):1987-2001.

109. Hubner RH, Gitter W, El Mokhtari NE, Mathiak M, Both M, Bolte H, et al. Standardized quantification of pulmonary fibrosis in histological samples. Biotechniques. 2008;44(4):507-11, 14-7.

110. Janssens R, Struyf S, Proost P. The unique structural and functional features of CXCL12. Cell Mol Immunol. 2018;15(4):299-311.

111. Sugihara H, Ishimoto T, Yasuda T, Izumi D, Eto K, Sawayama H, et al. Cancer-associated fibroblast-derived CXCL12 causes tumor progression in adenocarcinoma of the esophagogastric junction. Med Oncol. 2015;32(6):618.

## ANEXO I – CARTA DE APROVAÇÃO DO COMITÊ DE ÉTICA PARA O USO DE ANIMAIS

SIPESQ

Sistema de Pesquisas da PUCRS

Código SIPESQ: 7085 Porto Alegre, 22 de abril de 2016.

Prezado(a) Pesquisador(a),

A Comissão de Ética no Uso de Animais da PUCRS apreciou e aprovou o Projeto de Pesquisa "Avaliação da atividade da frutose-1,6-bisfosfato sobre fibrose pulmonar e remodelamento de vias aéreas em asma experimental" coordenado por MARCIO VINICIUS F DONADIO.

Sua investigação, respeitando com detalhe as descrições contidas no projeto e formulários avaliados pela CEUA, está autorizada a partir da presente data, conforme recomendações abaixo:

| |
|---|
| APROVADO |

Informamos que é necessário o encaminhamento de relatório final quando finalizar esta investigação. Adicionalmente, ressaltamos que conforme previsto na Lei no. 11.794, de 08 de outubro de 2008 (Lei Arouca), que regulamenta os procedimentos para o uso científico de animais, é função da CEUA zelar pelo cumprimento dos procedimentos informados, realizando inspeções periódicas nos locais de pesquisa.

| Nº de Animais | Espécie | Duração do Projeto |
|---|---|---|
| 322 | Camundongos | 22/04/2016 - 22/04/2020 |

Atenciosamente,

Comissão de Ética no Uso de Animais (CEUA)

## ANEXO II – CARTADE APROVAÇÃO DO COMITÊ DE ÉTICA DO NCI

**Department of Health & Human Services** — **Public Health Service**

**National Institutes of Health**
**National Cancer Institute**
**Bethesda, Maryland 20892**

iRIS Reference Number ***371230***

IACUC Number: **LM-063-2-F**

***TO:*** **Shioko Kimura**
Principal Investigator

***FROM:*** NCI-Bethesda Animal Care and Use Committee

***SUBJECT:*** Animal Study Proposal Modification - **APPROVAL**

Your NCI-Bethesda Animal Study Proposal Modification **LM-063-2-F** entitled "Role of SCGB3A2 in lung damage" was given **APPROVAL** by the NCI-Bethesda Animal Care and Use Committee (ACUC) by full board review on .

APPROVAL DATE: **08/04/2017**
EXPIRATION DATE: **Same as original protocol**

Please obtain the study documents from https://iris.nci.nih.gov/iMedris/Login.jsp, if needed. Any additional change to the proposal requires the submission of a modification for ACUC review and approval in advance. Please refer to the *ACUC Guidelines for modifying an Animal Study Proposals* at http://web.ncifcrf.gov/rtp/lasp/intra/acuc/beth/GuidelinesforMod.asp
For additional information on NCI-Bethesda ACUC procedures, policies, guidelines, forms, training, etc., please visit our website at https://ncifrederick.cancer.gov/lasp/acuc/bethesda/Guidelines.aspx

The modification was electronically signed by the following ACUC members:
Dr. Jonathan Ashwell (ACUC Chair)
Dr. Bob Hoyt (Attending Veterinarian)
Mr. Glenn Rameres (Safety)

**Please note the following safety requirements & comments:**

No additional comments.

**Modification Review Submission Form (Animal Studies Only) - (Version 5.2)**

## 1.0 Modification Review Submission Form
(version 1.3 10-19-2015)

**1.1 Protocol Number:**

LM-063-2-F

**1.2 Protocol Title:**

Role of SCGB3A2 in lung damage

**1.3 * Provide a brief title for this modification (50 char limit):**

Effect of fructose-1,6-bisphosphate on fibrosis

**1.4 * Principal Investigator Information**

**Principal Investigator:**

Shioko Kimura

**Principal Investigator E-Mail Address:**

kimuras@mail.nih.gov

**Principal Investigator Building/Room/MSC:**

37/3112B

**Principal Investigator Primary Phone Number:**

240.760.6877

**Principal Investigator Fax:**

301-496-8419

**1.5 Instructions:**

All changes must relate to a previously approved proposal.

**ANEXO III**

Artigo original realizado durante o doutorado-sanduiche em Bethesda/USA, em parceria com o Laboratório de Metabolismo, National Cancer Institute. Publicado na revista *The Journal of Pharmacology and Experimental Therapeutics*.

JPET Fast Forward. Published on August 16, 2019 as DOI: 10.1124/jpet.119.256792
This article has not been copyedited and formatted. The final version may differ from this version.

JPET # 256792

# Withaferin A improves non-alcoholic steatohepatitis in mice

Daxesh P. Patel[1†], Tingting Yan[1†], Donghwan Kim[1], Henrique B. Dias[1,2], Kristopher W. Krausz[1], Shioko Kimura[1] and Frank J. Gonzalez[1*]

[1]Laboratory of Metabolism, Center for Cancer Research, National Cancer Institute, National Institutes of Health, Bethesda, Maryland, USA

[2]Laboratory of Cellular Biophysics and Inflammation, Pontifical Catholic University of Rio Grande do Sul, Brazil

**[†]DPP and TY contributed equally to this study**

JPET # 256792

**Running Head:** Withaferin A therapeutically improves NASH

***Corresponding author:** Frank J. Gonzalez, Laboratory of Metabolism, Center for Cancer Research, National Cancer Institute, National Institutes of Health, Bethesda, Maryland 20892, USA. Email: gonzalef@mail.nih.gov

Number of text pages: 31

Number of tables: 1

Number of figures: 13

Number of supplemental figures: 3

Number of references: 39

Words in Abstract: 222

Words in Introduction: 761

Words in Discussion: 1337

**Section assignment for table of contents:** Drug Discovery and Translational Medicine

**ABBREVIATIONS:** ALT, alanine aminotransferase; AST, aspartate aminotransferase; Cer, ceramide; H & E, hematoxylin and eosin; HFD, high-fat-diet; LFD, low-fat-diet; MCD, methionine-choline-deficient; MCS, methionine-choline-sufficient; NAFLD, non-alcoholic fatty liver disease; NASH, non-alcoholic steatohepatitis; NEFAs, non-esterified fatty acids; NRF2, nuclear factor erythroid 2-related factor 2; WA, withaferin A; TC, total cholesterol; TG, triglycerides. *Tnfa*, tumor necrosis factor alpha; *Il1b*, interleukin 1b; *Il6*, interleukin 6; *Hspa5*, heat shock protein family A (*Hsp70*) member 5; *Didt3,* DNA damage-inducible transcript 3*;*

*Srebp1c*, sterol regulatory element-binding protein 1c; *Fas*, fatty acid synthase; *Scd1*, stearoyl-CoA desaturase-1. *Timp2*, tissue inhibitor of metalloproteinase 2; *Col1a1*, collagen type I alpha 1; *Mmp2*, matrix metalloproteinase 2; *Acta2*, alpha smooth muscle actin; *Sptlc*, serine palmitoyltransferase, long-chain base subunit; *Smpd*, sphingomyelin phosphodiesterase; *Acer*, alkaline ceramidase; *Sgms*, sphingomyelin synthase; *Cers*, ceramide synthase; *NLRP3,* NLR family pyrin domain containing 3; *Gapdh,* glyceraldehyde 3-phosphate dehydrogenase; *Actb,* β-actin.

**Abstract**

Non-alcoholic steatohepatitis (NASH) is the progressive stage of non-alcoholic fatty liver disease (NAFLD) that highly increases the risk of cirrhosis and liver cancer, and there are few therapeutic options available in the clinic. Withaferin A (WA), extracted from the ayurvedic medicine *Withania Somnifera,* has a wide range of pharmacological activities, however, little is known about its effects on NASH. To explore the role of WA in treating NASH, two well-defined NASH models were employed, the methionine-choline-deficient (MCD) diet and the 40 kcal% high-fat diet (HFD). In both NASH models, WA treatment or control vehicle was administered to evaluate its hepatoprotective effects. As assessed by biochemical and histological analyses, WA prevented and therapeutically improved liver injury in both models, as revealed by lower serum aminotransaminases, hepatic steatosis, liver inflammation and fibrosis. In the HFD-induced NASH model, both elevated serum ceramides and increased hepatic oxidative stress were decreased in the WA-treated group compared to the control vehicle-treated group. To further explore whether WA has an anti-NASH effect independent of its known action in leptin signaling during combating obesity, leptin signaling-deficient ob/ob mice maintained on a HFD were employed to induce NASH. WA was also found to therapeutically reduce NASH in HFD-treated leptin-deficient ob/ob mice, thus demonstrating a leptin-independent hepatoprotective effect. This study revealed that WA treatment could be a therapeutic option for NASH treatment.

**Keywords:** Withania Somnifera; herb; hepatic steatosis; NASH; anti-oxidant

## Introduction

Nonalcoholic steatohepatitis (NASH) is the progressive stage of nonalcoholic fatty liver disease (NAFLD) that results in a high risk of the end-stage liver diseases, cirrhosis and hepatocellular cancer (Farrell and Larter, 2006; Michelotti et al., 2013). While virus-induced hepatitis has been sharply reduced with vaccine application and curative drugs (Scott et al., 2015; Flemming et al., 2017), there continues to be an increase in NAFLD incidence due to the rapid rise of obesity and diabetes (Wong et al., 2014; Estes et al., 2018). NASH is currently listed as the second leading cause of liver disease among adults awaiting liver transplantation in the United States (Wong et al., 2015) and is estimated to overtake hepatitis C virus infection as the leading cause of liver transplantation in the US in the coming decades (Oseini and Sanyal, 2017). Although some conventional therapies such as vitamin E and pioglitazone could improve steatosis and inflammation, few treatments that could significantly decrease fibrosis, one of the strongest indicators of liver damage caused by NASH, have been found (Cassidy and Syed, 2016; Oseini and Sanyal, 2017), indicating that while market-available drugs are mostly effective in treating hepatic steatosis, they have minimal effects on fibrosis associated with NASH. There are no current FDA-approved therapies for treating NASH, and the development of novel medical treatments is urgently needed.

Withaferin A (WA), is a steroidal lactone derived from the plant *Withania Somnifera* used in traditional ayurvedic medicine (Vanden Berghe et al., 2012). WA was originally used as an anti-tumor agent (Lee and Choi, 2016) and has other pharmacological properties including cardioprotective, anti-inflammation and anti-oxidant activities (Vanden Berghe et al., 2012). Recently, WA was demonstrated to be a leptin sensitizer with strong antidiabetic properties in mice that could decrease obesity-associated metabolic abnormalities including hepatic steatosis

(Lee et al., 2016). Several other studies demonstrate that WA has hepatoprotective activity as revealed by its ability to mitigate acetaminophen-induced acute liver injury (Jadeja et al., 2015; Palliyaguru et al., 2016) and alleviate bromobenzene-induced liver injury (Vedi and Sabina, 2016). Since obesity is usually associated with insulin resistance and fatty liver, the pharmacological potential of WA in treating NASH needs to be evaluated.

NAFLD/NASH is known to be caused by a hepatic overload of fatty acids, leading to the production of toxic lipids that could cause hepatic oxidative stress, inflammation, endoplasmic reticulum (ER) stress and cell death (Friedman et al., 2018). Among the toxic lipids, ceramides are signaling molecules that accumulate in the blood and tissues in animal models of metabolic diseases. High cellular levels of ceramides are correlated with inflammation, cell death, oxidative stress, ER stress and insulin resistance (Pagadala et al., 2012; Chaurasia and Summers, 2015). Thus, strategies that decrease ceramides could efficiently improve NAFLD and NASH (Kurek et al., 2014; Jiang et al., 2015; Xie et al., 2017). On the other hand, WA is known to suppress oxidative stress, evidenced by its nuclear factor erythroid 2-related factor 2 (NRF2)-dependent effect in alleviating acetaminophen-induced liver injury and its effect in inducing heme oxygenase (HO-1) expression in endothelial cells via activating NRF2 pathway (Vanden Berghe et al., 2012; Jadeja et al., 2015; Heyninck et al., 2016; Palliyaguru et al., 2016). Besides, WA is a known leptin sensitizer that could both leptin signaling-dependently and leptin signaling-independently reduce diet-induced obesity as reported previously (Lee et al., 2016). Although there is no conclusive evidence that leptin is of value for the treatment of NAFLD patients, leptin was suggested to have a potential role in benefiting NASH treatment, as revealed by that recombinant leptin administration showed a beneficial effect in hepatic steatosis in NAFLD patients with hyperleptinemia (Polyzos et al.,

2015) or lipodystrophy patients (Javor et al., 2005). However, whether WA modulates ceramides homeostasis and alleviates oxidative stress during treating NASH, and whether WA affects NASH dependent on its effect on leptin signaling are still not known.

In the present study, two widely-used NASH models, the methionine- and choline-deficient (MCD) diet and the high-fat diet (HFD) were firstly employed to evaluate the efficacy of WA in treating NASH. WA had both preventive and therapeutic effects in improving NASH, as revealed by significant decreases of serum aminotransferases, hepatic steatosis, inflammation, ER stress and fibrosis. In the HFD-induced NASH model, WA alleviated NASH-associated oxidative stress and lowered serum ceramide levels. By using leptin-deficient ob/ob mice maintained on a NASH-promoting HFD, we further demonstrated that WA had a therapeutic effect in improving HFD-induced NASH in ob/ob mice, suggesting an leptin-independent anti-NASH effect of WA. All the present results indicate that WA could be repurposed as a novel therapy in treating NASH patients.

## Materials and Methods

**Chemicals and Reagents.** WA was purchased from ChromaDex (Irvine, CA). PeroxiDetect kit, superoxide dismutase kit, glutathione assay kit and dimethyl sulfoxide were purchased from Sigma Aldrich (MO, USA). Alanine aminotransferase (ALT) kits and aspartate aminotransferase (AST) kits were purchased from Catachem (CT, USA). Total cholesterol (TC), triglyceride (TG), and non-esterified fatty acids (NEFAs) kits were purchased from Wako Pure Chemical Industries (Osaka, Japan). Ceramides standards C16, C18, C20, C22, C24, C18:1, C24:1 were purchased from Avanti polar Lipids (Alabaster, AL). Rodent diets with 40 kcal% high-fat, 20 kcal% fructose and 2% cholesterol (HFD, Cat# D09100301 for C57BL/6N mice and Cat# D09100310 for ob/ob mice) and 10 kcal% fat control diet (LFD, Cat# D09100304) were purchased

JPET Fast Forward. Published on August 16, 2019 as DOI: 10.1124/jpet.119.256792
This article has not been copyedited and formatted. The final version may differ from this version.



from Research Diets (NJ, USA). Methionine and choline sufficient (MCS) diet and MCD diet were purchased from Dyets Inc (Bethlehem, PA, USA).

**Drugs Preparation and Dosing.** The WA stock solution was dissolved in dimethyl sulfoxide and frozen, and before use diluted with saline to generate the treatment doses (the final dimethyl sulfoxide percentage was the same for all final injection solutions). WA was injected intraperitoneally (0.1 ml/20 g mouse) at the doses indicated once per day before the dark cycle of the day.

**Animal Studies.** Age-matched 6- to 8-week-old C57BL/6N males were housed in a specific pathogen-free environment controlled for temperature and light (25°C, 12-h light/dark cycle) and humidity (45-65%). The National Cancer Institute Animal Care and Use Committee approved all animal experiments conducted in this study. The mice were administered WA at a dose of 1 mg/kg, 2.5 mg/kg and 5 mg/kg for the MCD model and at the dose of 5 mg/kg for the HFD models. To test the preventative effect of WA in treating MCD-induced NASH, the mice were randomly divided into six groups: (1), MCS: mice fed the MCS diet and treated with control vehicle; (2), MCS+WA5: mice fed the MCS diet and treated with 5 mg/kg of WA; (3), MCD: mice fed the MCD diet and treated with control vehicle; (4), MCD+WA1: mice fed the MCD diet and treated with 1 mg/kg of WA; (5) MCD+WA2.5: mice fed the MCD diet and treated with 2.5 mg/kg of WA; (6) MCD+WA5: mice fed the MCD diet and treated with 5 mg/kg of WA. All mice were fed the MCS or MCD diets for four weeks, and WA or control vehicle was injected once per day from the first day of diet feeding. To test the therapeutic effect of WA in treating MCD diet-induced NASH, the mice were fed with the MCD diet for 6 weeks and then injected with WA once a day at the dose of 5 mg/kg during the last two weeks of MCD feeding. To test the preventive and therapeutic effect of WA in HFD-induced NASH model, mice were fed a HFD or LFD for 20

JPET Fast Forward. Published on August 16, 2019 as DOI: 10.1124/jpet.119.256792
This article has not been copyedited and formatted. The final version may differ from this version.



weeks. Mice were fed a HFD or LFD for 8 weeks and then divided into 4 groups; (1) mice treated with vehicle for 12 weeks; (2) mice treated with WA for 12 consecutive weeks; (3) mice treated with vehicle for 4 weeks from week 9 to week 12, and then treated with WA for the last 8 weeks; (4) mice treated with vehicle for 8 weeks from week 9 to week 16 and then treated with WA for 4 weeks. To test the therapeutic effect of WA in leptin-deficient NASH, the leptin-deficient ob/ob NASH mouse model was employed. Eight-week-old age-matched ob/ob mice, obtained from Jackson Laboratories, were fed a HFD for 8 weeks and then divided into two groups: (1) mice maintained on a HFD and treated with WA or control vehicle for 4 weeks; (2) mice maintained on a HFD and treated with WA for 4 weeks. The mice were injected with vehicle or WA before the dark cycle of the day and not fasted during the study. One hour after the last injection of WA or control vehicle, the mice were killed with $CO_2$ and serum and tissues collected for further analysis.

**Histology Analysis.** Formalin-fixed liver tissues were embedded in paraffin. A portion of fresh livers were embedded in Tissue-Tek Optimal Cutting Temperature compound (Sakura Finetek, Torrance, USA) and then flash frozen for Oil Red O staining. Five μm thick sections were cut for both H&E and picrosirius red staining. Further sample processing, and analysis for H&E staining, and Oil red O staining were performed at Histoserv Inc (Germantown, MD, USA) or VitroVivo Biotech (Rockville, MD, USA). For picrosirius staining in Figure 8, paraffin-embedded livers were sectioned at Histoserv Inc and stained with picrosirius based on its manual, while picrosirius staining for Figure 12 were performed in VitroVivo Biotech (Rockville, MD, USA). Digital images from picrosirius red-stained liver sections were analyzed with ImagePro plus software (Media Cybernetics, Inc., Rockville, MD, USA), and the collagen positive area was assessed. Large blood vessels and corner sections were excluded from analysis and at least five different fields of each slide were measured to allow a realistic picture of the entire organ's fibrotic

state. Results were expressed as collagen percentage of all images related to the total area of the tissue.

**Biochemical Analysis of Liver and Serum.** Biochemical parameters including levels of ALT, AST, TC, TG and NEFAs, as well as levels of superoxide dismutase, hydroxide peroxide and glutathione in serum or liver were tested with commercial kits based on the manuals. Serum ceramides were quantified as described previously (Xie et al., 2017).

**Quantitative Polymerase Chain Reaction.** The livers were flash frozen in liquid nitrogen and stored at -80°C. Total RNA from frozen livers was extracted with TRIzol reagent (Invitrogen, Carlsbad, CA). cDNA was synthesized from 1 μg of total RNA using qScript cDNA SuperMix (Gaithersburg, MD). Analysis was performed by using the ABI PRISM 7900 Sequence Detection System (Applied Biosystems, Bedford, MA). Values were normalized to *Actb* or *Gapdh* mRNAs and the results expressed as fold change relative to the control group. Primer sequences are listed in Supplementary table 1.

**Pharmacokinetic Analysis.** Age and body weight-matched 8-week-old C57BL/6N mice were randomly-grouped and dosed with 5 mg/kg of WA via intraperitoneal administration. Blood was collected at 0 min (pre-dose), 10 min, 20 min, 40 min, 1 h, 2 h, 4 h, 8 h, 24 h and 48 h for isolation of plasma. Samples were diluted with acetonitrile and protein removed by centrifugation, and then analyzed using UPLC-MS/MS under reverse phase chromatography after optimizing chromatographic conditions for WA. MassLynx software version 4.1 was used to analyze the data of drug concentration. The pharmacokinetic parameters of WA were calculated by non-compartmental model using WinNonlin software version 5.2.1 (Pharsight Corporation, Sunnyvale, CA, USA). The $C_{max}$ values and the time to reach maximum plasma concentration ($T_{max}$) were calculated directly from the observed plasma concentration vs time data. The area under the plasma

drug concentration–time curve from time 0-48h ($AUC_{0-48h}$) was calculated using the linear trapezoidal rule. The $AUC_{0-infinity}$ was calculated as: $AUC_{0-infinity}=AUC_{0-48h}+ C_t/K_{el}$ , where $C_t$ is the last plasma concentration measured and $K_{el}$ is the elimination rate constant; $K_{el}$ was determined using linear regression analysis of the logarithm linear part of the plasma concentration–time curve. The $t_{1/2}$ of WA was calculated as $t_{1/2}=ln2/K_{el}$.

**Statistical Analysis.** Experimental values were presented as mean ± SD. Statistical analyses were determined by two-tail t test between two groups or by one-way ANOVA followed by Dunnett's multiple comparisons test among multiple groups using Prism version 7.0 (GraphPad Software, San Diego, CA). P values less than 0.05 were considered statistically significant.

## Results

**WA Dose-dependently Attenuates MCD Diet-induced Liver Injury.** To explore the effect and effective dose of WA in the MCD diet-induced liver injury model, WA at 1, 2.5, and 5 mg/kg were administered. From the first day of MCD diet feeding, WA was injected once a day for four consecutive weeks (Fig. 1A). The MCD diet induced body weight loss, which was significantly attenuated by WA at 5 mg/kg (Fig. 1B). WA dose-dependently increased the liver weight and liver index in mice on the MCD diet (Fig. 1, C and D). WA treatment alone caused no significant histologic changes indicating liver damage (Fig. 1E) and did not significantly affect serum ALT and AST levels (Fig. 2, A and B) in the control MCS diet feeding group, indicating that WA at 5 mg/kg was not hepatotoxic. Further biochemical assays showed that WA dose-dependently inhibited the MCD diet-induced increase of serum ALT and AST levels (Fig. 2, A and B) as well as hepatic levels of TC and TG (Fig. 2, C and D). The MCD diet induced a marked

decrease of serum TC and TG, which was significantly attenuated by 5 mg/kg WA (Fig. 2, E and F). Given that WA at 5 mg/kg, among the tested doses, showed a consistent effect in reversing body weight changes, serum ALT and AST levels, TC and TG levels in livers and serum, the effect of 5 mg/kg of WA in hepatic inflammation and histology were measured at this dose. WA alleviated MCD diet-induced liver inflammation (Fig. 2G), and histological analyses by H & E and Oil Red O staining showed that 5 mg/kg of WA improved MCD diet-induced hepatic steatosis (Fig. 2, H and I). These data demonstrate that WA dose-dependently prevents MCD diet-induced fatty liver, and that the 5 mg/kg dose of WA ameliorates NASH.

With a dose of 5 mg/kg WA chosen for further extensive study, a pharmacokinetic analysis was performed to investigate the exposure and clearance behavior of WA in blood after intraperitoneal injection. The chemical structure of WA and drug concentration-time curve of WA are shown (Supplemental Fig. 1, A and B). The pharmacokinetic parameters including $C_{max,}$ $T_{1/2}$, $AUC_{0–48h}$, $AUC_{0-\infty}$ and elimination rates ($K_{eli,}$ 1/h) were calculated (Supplemental Fig.1C). Following a single intraperitoneal injection dose of 5 mg/kg WA, a $C_{max}$ level of 14.3 ± 1.8 nM was observed at 20 min. The plasma $T_{1/2}$ value of WA was 2.0 ± 0.6 h. These data and a previous study (Thaiparambil et al., 2011) that found intraperitoneally-injected WA had a half-life of 1.36 h, suggest that WA has a rapid clearance from blood after intraperitoneal dosing. However, WA was readily detected across the time-course of 48 h and was maintained at 2-4 nM (14%-29% percent of WA peak concentration) at the later phase after a single dose of 5 mg/kg WA (Supplemental Fig. 1B). These data suggest that WA could be maintained at a relatively low level for 48 h, while having a short half-life of 2 h in mice. However, its pharmacokinetics my differ in humans.

**WA Prevents MCD Diet-induced Liver Injury Independent of Body Weight Change.** To examine whether WA could prevent MCD diet-induced NASH independent of its effect in changing MCD diet-induced body weight loss, a short-term MCD diet feeding study was performed. Mice were fed an MCD diet for 10 days, during which 5 mg/kg of WA or control vehicle was injected once a day for 10 consecutive days (Fig. 3A). In this short-term study, 5 mg/kg of WA did not change the body mass of MCD diet-fed mice (Fig. 3B). However, WA markedly increased the liver weight and the liver index when compared with control vehicle-treated controls (Fig. 3, C and D). Five mg/kg of WA significantly decreased the MCD diet-induced serum ALT and AST levels (Fig. 3, E and F). These data demonstrate that 5 mg/kg WA is sufficient to alleviate MCD diet-induced liver injury at the early stage in the absence of significant body weight changes.

**WA Therapeutically Improves MCD Diet-induced Liver Injury.** To further explore whether WA could therapeutically treat MCD diet-induced NASH, 5 mg/kg WA was administered for two weeks after the onset of liver damage induced by 6 weeks of MCD diet feeding (Fig. 4A). WA did not affect the body weight, liver weight and liver index (Fig. 4, B-D), while it significantly decreased the MCD diet-induced increases of serum ALT and AST levels (Fig. 4, E and F). WA also improved hepatic steatosis as revealed by histological analyses (Fig. 4, G and H). These data suggest that 5 mg/kg WA therapeutically improves MCD diet-induced liver injury.

**WA Improves HFD-induced Liver Injury.** In contrast to the MCD diet-induced NASH model that results in body weight loss and does not cause insulin resistance coincident with inducing steatohepatitis, the 40 kcal% HFD-induced obese NASH model is thought to better mimic the typical human NASH pathologies of insulin resistance, high serum lipids accumulation and obesity (Hebbard and George, 2011; Griffett et al., 2015; Honda et al., 2016; Ding et al., 2018).

JPET Fast Forward. Published on August 16, 2019 as DOI: 10.1124/jpet.119.256792
This article has not been copyedited and formatted. The final version may differ from this version.



To further confirm the effect of WA in treating NASH, the HFD regimen and its matched LFD were used to test the effect of WA both in preventing and therapeutically improving NASH. Mice were fed a HFD for 20 weeks and injected with 5 mg/kg of WA or control vehicle for the last 12, 8, or 4 weeks before killing (Fig. 5A). WA significantly decreased body weights in both the HFD-fed and LFD-fed mice (Fig. 5, B and C). WA also decreased liver weights and liver indexes (Fig. 5, D and E) and attenuated the HFD-induced increase of serum ALT and AST (Fig. 5, F and G) in a time-dependent manner. Similarly, WA treatment decreased the HFD-induced accumulation of hepatic TG and TC levels (Fig. 6, A and B) and serum TG and TC levels (Fig. 6, C and D). WA treatment time-dependently decreased the HFD-induced accumulation of NEFAs in both livers and serum (Fig. 6, E and F). Further histological analyses showed that WA treatment time-dependently improved NASH-associated hepatic steatosis as revealed by histological analyses (Fig. 7, A and B). WA treatment also significantly reduced the levels of the HFD-induced *Tnfa, Il1b*, and *Il6* mRNAs involved in hepatic inflammation (Fig. 7, *C-E*) and heat shock protein family A member 5 (*Hspa5)* and DNA damage-inducible transcript 3 (*Ddit3)* mRNA levels involved in ER stress (Fig.7, *F* and *G*). WA treatment decreased the HFD-induced increase of *Srebp1c* mRNA encoding the transcription factor SREBP1C and its downstream target gene mRNAs, *Scd1* and *Fas* involved in the control of lipogenesis (Fig. 7, H-J). These data demonstrate that WA treatments both prevent and therapeutically improve HFD-induced hepatic steatosis, inflammation, and ER stress accompanied by dampening the hepatic lipogenesis signaling.

**WA Attenuates Hepatic Fibrosis.** Fibrosis is a major hallmark of NALFD progression to NASH. Twenty-week HFD feeding markedly induced picrosirius red staining in the NASH group, which was rescued by WA treatment in a time-dependent manner (Fig. 8A). Further statistical analysis showed that WA treatment decreased NASH-associated hepatic collagen accumulation

(Fig. 8B). In addition, WA treatment decreased *Timp2*, *Col1a1*, *Mmp2*, and *Acta2* mRNAs encoding enzymes and structural proteins involved in liver fibrogenesis (Fig. 8, *C*-*F*). These data demonstrate that WA improves NASH-associated fibrosis induced by HFD in a time-dependent manner.

**WA Rescues NASH-associated Ceramide Accumulation, ER Stress and Oxidative Stress.** Previous studies demonstrated that HFD-induced hepatic steatosis was correlated with increased ceramide levels (Longato et al., 2012; Chaurasia and Summers, 2015; Kasumov et al., 2015). Genetically or biochemically decreasing ceramides improved NAFLD and NASH (Kurek et al., 2014; Xie et al., 2017). Oxidative stress that occurs in NASH could induce ceramide accumulation (Bikman and Summers, 2011) and WA has exhibited anti-oxidant activity in earlier experimental models (Vanden Berghe et al., 2012). Thus, the anti-oxidant effects of WA could potentially influence ceramide levels and oxidative stress during treating NASH. To examine this hypothesis, levels of serum ceramides were first measured using authentic standards. HFD significantly induced the accumulation of ceramides, such as C16 (m/z 582.5098), C18 (m/z 610.5411), C20 (m/z 638.5724), C22 (m/z 666.6037), C24 (m/z 694.6350), C18:1 (m/z 608.5254), and C24:1 (m/z 692.6193), all of which were reduced by WA treatment (Fig. 9, *A*-*G*).

Next, that possibility that WA attenuated HFD-induced oxidative stress was examined. WA treatment time-dependently rescued the NASH-induced decrease of hepatic superoxide dismutase and glutathione levels, and significantly attenuated the NASH-induced increase of hepatic peroxide levels (Fig. 9, H-J). These data suggest that WA treatment reduces HFD-induced ceramides accumulation in serum and oxidative stress in liver.

To further examine why WA alleviated serum ceramides accumulation and hepatic oxidative stress, mRNA levels of ceramides signaling and NRF2 signaling were analyzed. WA

JPET Fast Forward. Published on August 16, 2019 as DOI: 10.1124/jpet.119.256792
This article has not been copyedited and formatted. The final version may differ from this version.



treatment markedly decreased mRNAs of genes involved in ceramide biosynthesis pathways, such as serine palmitoyltransferase, long-chain base subunit 1 (*Sptlc1)* and *Sptlc2*, sphingomyelin phosphodiesterase *1 (Smpd1)*, *Smpd2*, *Smpd3*, *and Smpd4*, angiotensin-converting enzyme-related *2 (Acer2)* and *Acer3*, sphingomyelin synthase (*Sgms1)* and *Sgms2*, ceramide synthase 2 (*Cers2)*, *Cers4* and *Cers6* in a time-dependent manner (Fig. 10, A-M). These data demonstrate that WA attenuates HFD-induced accumulation of serum ceramides and oxidative stress. Further analysis of NRF2 signaling revealed that WA decreased mRNA levels of genes involved in NRF2 pathway both in 20-week HFD-treated mice (Supplemental Fig. 2) and 4-week MCD diet-treated mice (Supplemental Fig. 3A). Given that earlier reports revealed that WA could activate NRF2 (Jadeja et al., 2015; Heyninck et al., 2016; Palliyaguru et al., 2016), the possibility exists that the decreases NASH diet-induced NRF2 signaling by WA in the current study is due to a secondary result of its hepatoprotective effects. The marked hepatoprotective effect may decrease NASH diet-promoted NRF2 signaling, which could overcome the effect of WA on NRF2 activation under that pathological conditions of NASH. To answer this question, the effect of WA in hepatic NRF2 signaling pathway at an early stage of NASH model induced by the MCD diet or HFD was examined. Mice were fed with an MCD diet for 10 days or a HFD for one week, during which mice were cotreated with control vehicle or 5 m/kg of WA once a day via intraperitoneal injection, and all mice were killed one hour after the last WA injection to collect livers for further mRNAs analysis. In 10-days MCD diet-fed mice, WA was found to induce hepatic mRNAs of NRF2 target genes including *Gclc, Nqo1*, *Keap1*, *Cat* and *Nrf2* (Supplemental Fig. 3B), while in one-week HFD-treated mice, this NRF2-activating effect of WA was not found. These data suggest that WA may affect the mRNAs expression of NRF2 target genes in a context-dependent manner.

JPET Fast Forward. Published on August 16, 2019 as DOI: 10.1124/jpet.119.256792
This article has not been copyedited and formatted. The final version may differ from this version.



**WA Improves NASH in HFD-induced Liver Injury in Leptin Signaling Defective (ob/ob) Mice.** To determine the effect of WA in a leptin-deficient NASH model, ob/ob mice were fed a HFD for 12 weeks and injected with 5 mg/kg of WA or control vehicle for the last 4 weeks before killing (Fig. 11A). WA significantly decreased body weight, the liver weight and liver index (Fig. 11, B, C and D), and attenuated the HFD-induced increase of serum ALT and AST (Fig. 11, E and F). Histological analyses revealed that WA treatment improved NASH-associated hepatic steatosis (Fig. 11, G and H). Consistent with this finding, WA treatment reduced the mRNA levels of proinflammatory cytokines including *Il1b*, *Il6* and *Tnfa* mRNAs, as well as the mRNA levels of lipogenesis genes including *Srebp1*c, *Scd1* and *Fas* (Fig. 11I). WA treatment decreased the HFD-induced accumulation of TG, TC and NEFAs in liver and serum (Fig. 12, *A-F*). Furthermore, WA also significantly reduced the mRNA levels of the fibrogenesis genes *Timp2*, *Col1a1*, *Mmp2* and *Acta2* (Fig. 12G) and attenuated HFD-induced hepatic fibrosis as revealed by picrosirius red staining data (Fig. 12H). Similar to its effect in HFD-treated C57BL/6N mice, WA also significantly decreased HFD-induced ER stress markers *Hspa5* and *Ddit3* mRNAs, as well as all the tested mRNAs involved in ceramide synthesis including *Sptlc1, Sptlc2*, *Smpd2*, *Smpd3*, *Acer2*, *Sgms1*, *Sgms2*, *Cers2*, *Cers4* and *Cers6* (Fig. 12, I and J). These results demonstrate that WA treatment decreases HFD-induced NASH in ob/ob mice, and this was in accompany by decreased hepatic ceramide synthesis.

## Discussion

The hepatoprotective roles of WA in treating liver diseases, especially the effects on NASH are largely unknown. The current study revealed that WA could both prevent and therapeutically improve NASH in two well-defined mouse NASH models, MCD-induced NASH model and HFD-

JPET Fast Forward. Published on August 16, 2019 as DOI: 10.1124/jpet.119.256792
This article has not been copyedited and formatted. The final version may differ from this version.



induced NASH model in C57BL/6N mice and could therapeutically alleviate a leptin-deficient HFD-induced NASH model in ob/ob mice. WA restored NASH-induced dysregulation of oxidative stress and lowered ceramides that may be involved in the mechanism of NASH (Fig. 13). However, detailed mechanistic analysis required further studies.

The MCD diet-induced NASH model has been a widely-used for evaluating the pharmacological effects of drugs on NASH (Hebbard and George, 2011) and provides convenience for its short-term experimental duration. By using this rapid short-term model, the efficient dose of WA on NASH was found to be 5 mg/kg that was efficient in both preventing and therapeutically treating MCD diet-induced NASH. Compared with the MCD diet-induced lean NASH model, the HFD-induced NASH model more accurately reflects the clinical NASH pathologies including obesity, insulin resistance and high serum triglycerides, in addition to the typical hepatic steatosis, inflammation and fibrosis (Hebbard and George, 2011), and thus this model was chosen for further determining the effects of WA on NASH. In the obese NASH model, WA treatment improved NASH-associated pathologies including hepatic steatosis, inflammation and fibrosis in a time-dependent manner. Since HFD diet feeding causes hepatic steatosis and minor fibrosis after a two-month diet feeding that gradually progresses to advanced NASH (Ding et al., 2018), the effect of WA treatments for twelve weeks during the full course of HFD feeding would be mainly regarded as a preventive effect, while WA treatment for eight weeks and four weeks after the onset of NASH would evaluate the therapeutic effects. In addition to WA's effect in improving NASH, WA also decreased HFD-induced body weight gain, in agreement with its known anti-obesity activity (Lee et al., 2016). Whether the effect of WA is the result of its anti-obesity effect or a direct effect on NASH in the present HFD-induced NASH model still requires further study. By using the NASH-promoting HFD, the current study extends the pharmacological known effects of WA to improving

JPET Fast Forward. Published on August 16, 2019 as DOI: 10.1124/jpet.119.256792
This article has not been copyedited and formatted. The final version may differ from this version.



NASH, beyond its known effects on obesity-accompanied hepatic steatosis associated with its anti-obesity effect (Lee et al., 2016). However, weight loss caused by WA treatment could potentially ameliorate the HFD-induced NASH. Given that the body weight was sharply decreased upon WA treatment in the current HFD-induced fat NASH model as well as in the previous study (Lee et al., 2016), it would be difficult to separate the anti-obesity effect as the cause of decreased NASH as opposed to a direct pharmacological effect of WA on NASH. However, the MCD-induced NASH mice show lean body weight instead of obesity, and the inhibitory effect of WA on MCD diet-induced NASH suggests that WA has a direct hepatoprotective effect in treating NASH independent of obesity at least in this non-obese NASH model. As noted earlier, the present study provides evidence that WA potently improves MCD diet-induced NASH, a lean NASH mouse model, in which some hepatoprotective effects, such as the therapeutic effect of WA at the dose of 5 mg/kg on MCD-induced NASH and the preventive effect on MCD-induced NASH at doses of 1 mg/kg and 2.5 mg/kg, are independent of body weight change. Furthermore, WA could also markedly decrease MCD diet-induced increase of serum ALT and AST and increased liver weights prior to body weight changes after MCD diet feeding for ten days. Similar with the present finding, it was reported that the hepatoprotective component glycyrrhizin also reduced MCD diet-induced NASH without significantly affecting the MCD diet-induced body weight loss (Yan et al., 2018). On the other hand, WA was reported to therapeutically improve acetaminophen-induced acute liver injury even when injected 1 hour after acetaminophen dosing (Jadeja et al., 2015), indicating that WA has a direct hepatoprotective effect. The current work, together with previous studies, suggests that WA could improve NASH, at least potentially due to its direct hepatoprotective activity, independent of its anti-obesity effect.

WA was previously reported to act as a leptin-sensitizer during obesity and was also shown to exert an anti-obesity effect independent of leptin signaling, as WA still had an anti-obesity effect in leptin-deficient mice (Lee et al., 2016). Thus, the question arose whether the anti-NASH effect of WA was dependent on leptin signaling. Consistent with this previous study, WA still elicited a potent therapeutic effect in HFD-induced NASH in leptin-deficient ob/ob mice. Thus, WA has leptin-independent pharmacological activity in obesity and obesity-associated NASH.

In the present study, WA was found to reduce the accumulation of ceramides in serum accompanied with attenuation of HFD-induced upregulation of ceramides. WA also decreased hepatic oxidative stress and hepatic ER stress, which were correlated with its anti-NASH effects. Although all these analyses provide potential hints for further mechanism exploration, the study does not determine how WA directly affects oxidative stress signaling, ER stress signaling, ceramides signaling or stress-treated ceramides signaling. *In vitro* studies are warranted to answer this question. Previous studies demonstrate that WA has antioxidant activity via activating NRF2 (Cassidy and Syed, 2016; Palliyaguru et al., 2016) and anti-inflammatory potential via directing inhibiting NLR family pyrin domain containing 3 (NLRP3) inflammasome activation (Kim et al., 2015; Dubey et al., 2018). Although in the present study, WA attenuated NASH-induced NRF2 signaling at the terminal stages of the NASH model, which may be a result of its hepatoprotective effects, WA could activate NRF2 signaling in the early stages of NASH within 10-days of commencing MCD diet treatment, although WA did not activate hepatic NRF2 signaling in after one-week of commencing HFD feeding. Thus, in the current study, WA was able to modulate NRF2 signaling in a context-dependent manner.

NRF2 activation could improve glucose tolerance, suppress NASH and liver fibrosis, and attenuate liver cirrhosis (Wu et al., 2014; Sharma et al., 2018). This suggest that NRF2 could be

JPET Fast Forward. Published on August 16, 2019 as DOI: 10.1124/jpet.119.256792
This article has not been copyedited and formatted. The final version may differ from this version.



an efficient target for anti-NASH therapy, consistent with the report that pharmacological activation of NRF2 by the potent NRF2 activator TBE-31 is able to ameliorate experimental NASH (Sharma et al., 2018). Multiple mechanisms are involved in the modulation of NRF2 signaling via interfering with kelch like ECH associated protein 1-NRF2 interaction or other posttranscriptionally and/or posttranslationally-modulated mechanisms, such as ERAD-associated E3 ubiquitin-protein ligase HRD1, glycogen synthase kinase 3 and β-transducin repeat-containing protein (Chowdhry et al., 2013; Wu et al., 2014; Hayes et al., 2015). Among these known NRF2-modulating mechanisms, WA was demonstrated to be an inducer of NRF2 signaling both *in vitro* and *in vivo*, and this effect is partially kelch like ECH associated protein 1-independent and in part dependent on the glycogen synthase kinase 3 -associated modulation pathway as in the acetaminophen-induced acute liver injury model in mice (Palliyaguru et al., 2016). In the present study, the mechanisms by which WA attenuates NASH may be dependent on its effect on NRF2 signaling or other pathways such as NLRP3. This requires further experimentation using NRF2 and NLRP3 knockout mice that are beyond the scope of the current study.

In summary, by evaluating various NASH pathological parameters in serum and livers in two well-defined NASH mouse models (MCD-induced NASH model and HFD-induced NASH model in wide-type mice), WA exhibits both the preventive and therapeutic effects in improving NASH. WA also therapeutically decreases HFD-induced NASH in leptin-deficient ob/ob mice. The anti-NASH effect of WA is accompanied by lower hepatic oxidative stress, ER stress, and ceramide accumulation in serum. These data suggest that WA has potent anti-NASH effects at least independent of its anti-obesity effect as revealed in the non-obese MCD-induced NASH model and is independent of its leptin-sensitizing effect as found in a HFD-fed leptin-deficient ob/ob mouse NASH model. While further studies to determine the exact mechanisms by which

WA decreases NASH are still needed, these findings suggest that the herbal medicine-derived compound WA may be a therapeutic option for treating NASH particularly that featured with ceramide accumulation and would help repurpose the ancient drug WA with its novel application in treating NASH.

**ACKNOWLEDGMENTS**

We thank Linda G. Byrd submission and approval of the animal protocols, John Buckley, Linda G. Byrd, Ping Wang, and Yangliu Xia for help with animal experiments, and Chad N. Brocker, Jie Zhao, Cen Xie for expert advice.

**AUTHOR CONTRIBUTIONS**

*Participated in research design*: Yan, Patel, Gonzalez

*Conducted experiments*: Patel, Yan, Kim, Dias, Krausz

*Performed data analysis*: Patel, Yan, Dias

*Wrote or contributed to the writing of the manuscript*: Yan, Patel, Gonzalez, Kimura

**GRANTS**

This research was supported by the National Cancer Institute Intramural Research Program, Center for Cancer Research, National Institutes of Health; H.B.D. was supported by a fellowship from the CAPES Foundation, Ministry of Education of Brazil, Brasilia.

**DISCLOSURES**

No conflicts of interest, financial or otherwise, are declared by the authors.

## REFERENCES

Bikman BT and Summers SA (2011) Ceramides as modulators of cellular and whole-body metabolism. *J Clin Invest* **121**:4222-4230.

Cassidy S and Syed BA (2016) Nonalcoholic steatohepatitis (NASH) drugs market. *Nat Rev Drug Discov* **15**:745-746.

Chaurasia B and Summers SA (2015) Ceramides - lipotoxic inducers of metabolic disorders. *Trends Endocrinol Metab* **26**:538-550.

Chowdhry S, Zhang Y, McMahon M, Sutherland C, Cuadrado A and Hayes JD (2013) Nrf2 is controlled by two distinct beta-TrCP recognition motifs in its Neh6 domain, one of which can be modulated by GSK-3 activity. *Oncogene* **32**:3765-3781.

Ding ZM, Xiao Y, Wu X, Zou H, Yang S, Shen Y, Xu J, Workman HC, Usborne AL and Hua H (2018) Progression and regression of hepatic lesions in a mouse model of NASH induced by dietary intervention and Its implications in pharmacotherapy. *Front Pharmacol* **9**:410.

Dubey S, Yoon H, Cohen MS, Nagarkatti P, Nagarkatti M and Karan D (2018) Withaferin A associated differential regulation of inflammatory cytokines. *Front Immunol* **9**:195.

Estes C, Razavi H, Loomba R, Younossi Z and Sanyal AJ (2018) Modeling the epidemic of nonalcoholic fatty liver disease demonstrates an exponential increase in burden of disease. *Hepatology* **67**:123-133.

Farrell GC and Larter CZ (2006) Nonalcoholic fatty liver disease: from steatosis to cirrhosis. *Hepatology* **43**:S99-S112.

Flemming JA, Kim WR, Brosgart CL and Terrault NA (2017) Reduction in liver transplant wait-listing in the era of direct-acting antiviral therapy. *Hepatology* **65**:804-812.

Friedman SL, Neuschwander-Tetri BA, Rinella M and Sanyal AJ (2018) Mechanisms of NAFLD development and therapeutic strategies. *Nat Med* **24**:908-922.

Griffett K, Welch RD, Flaveny CA, Kolar GR, Neuschwander-Tetri BA and Burris TP (2015) The LXR inverse agonist SR9238 suppresses fibrosis in a model of non-alcoholic steatohepatitis. *Mol Metab* **4**:353-357.

Hayes JD, Chowdhry S, Dinkova-Kostova AT and Sutherland C (2015) Dual regulation of transcription factor Nrf2 by Keap1 and by the combined actions of beta-TrCP and GSK-3. *Biochem Soc Trans* **43**:611-620.

Hebbard L and George J (2011) Animal models of nonalcoholic fatty liver disease. *Nat Rev Gastroenterol Hepatol* **8**:35-44.

Heyninck K, Sabbe L, Chirumamilla CS, Szarc Vel Szic K, Vander Veken P, Lemmens KJA, Lahtela-Kakkonen M, Naulaerts S, Op de Beeck K, Laukens K, Van Camp G, Weseler AR, Bast A, Haenen G, Haegeman G and Vanden Berghe W (2016) Withaferin A induces heme oxygenase (HO-1) expression in endothelial cells via activation of the Keap1/Nrf2 pathway. *Biochem Pharmacol* **109**:48-61.

Honda Y, Imajo K, Kato T, Kessoku T, Ogawa Y, Tomeno W, Kato S, Mawatari H, Fujita K, Yoneda M, Saito S and Nakajima A (2016) The selective SGLT2 inhibitor ipragliflozin has a therapeutic effect on nonalcoholic steatohepatitis in mice. *Plos One* **11**:e0146337.

Jadeja RN, Urrunaga NH, Dash S, Khurana S and Saxena NK (2015) Withaferin-A reduces acetaminophen-induced liver injury in mice. *Biochem Pharmacol* **97**:122-132.

Javor ED, Cochran EK, Musso C, Young JR, Depaoli AM and Gorden P (2005) Long-term efficacy of leptin replacement in patients with generalized lipodystrophy. *Diabetes* **54**:1994-2002.

Jiang C, Xie C, Li F, Zhang L, Nichols RG, Krausz KW, Cai J, Qi Y, Fang ZZ, Takahashi S, Tanaka N, Desai D, Amin SG, Albert I, Patterson AD and Gonzalez FJ (2015) Intestinal farnesoid X receptor signaling promotes nonalcoholic fatty liver disease. *J Clin Invest* **125**:386-402.

Kasumov T, Li L, Li M, Gulshan K, Kirwan JP, Liu XL, Previs S, Willard B, Smith JD and McCullough A (2015) Ceramide as a mediator of non-alcoholic fatty liver disease and associated atherosclerosis. *Plos One* **10**:e01269.

Kim JE, Lee JY, Kang MJ, Jeong YJ, Choi JA, Oh SM, Lee KB and Park JH (2015) Withaferin A Inhibits helicobacter pylori-induced production of IL-1beta in dendritic cells by regulating NF-kappaB and NLRP3 inflammasome activation. *Immune Netw* **15**:269-277.

Kurek K, Piotrowska DM, Wiesiolek-Kurek P, Lukaszuk B, Chabowski A, Gorski J and Zendzian-Piotrowska M (2014) Inhibition of ceramide de novo synthesis reduces liver lipid accumulation in rats with nonalcoholic fatty liver disease. *Liver Int* **34**:1074-1083.

Lee IC and Choi BY (2016) Withaferin-A-a natural anticancer agent with pleitropic mechanisms of action. *Int J Mol Sci* **17**.

Lee J, Liu JL, Feng XD, Hernandez MAS, Mucka P, Ibi D, Choi JW and Ozcan U (2016) Withaferin A is a leptin sensitizer with strong antidiabetic properties in mice. *Nat Med* **22**:1023-1032.

Longato L, Tong M, Wands JR and de la Monte SM (2012) High fat diet induced hepatic steatosis and insulin resistance: Role of dysregulated ceramide metabolism. *Hepatol Res* **42**:412-427.

Michelotti GA, Machado MV and Diehl AM (2013) NAFLD, NASH and liver cancer. *Nat Rev Gastroenterol Hepatol*. **10**:656-665.

Oseini AM and Sanyal AJ (2017) Therapies in non-alcoholic steatohepatitis (NASH). *Liver Int* **37 Suppl 1**:97-103.

Pagadala M, Kasumov T, McCullough AJ, Zein NN and Kirwan JP (2012) Role of ceramides in nonalcoholic fatty liver disease. *Trends Endocrinol Metab* **23**:365-371.

Palliyaguru DL, Chartoumpekis DV, Wakabayashi N, Skoko JJ, Yagishita Y, Singh SV and Kensler TW (2016) Withaferin A induces Nrf2-dependent protection against liver injury: Role of Keap1-independent mechanisms. *Free Radic Biol Med* **101**:116-128.

Polyzos SA, Kountouras J and Mantzoros CS (2015) Leptin in nonalcoholic fatty liver disease: a narrative review. *Metabolism* **64**:60-78.

Scott N, McBryde E, Vickerman P, Martin NK, Stone J, Drummer H and Hellard M (2015) The role of a hepatitis C virus vaccine: modelling the benefits alongside direct-acting antiviral treatments. *BMC Med* **13**:198.

Sharma RS, Harrison DJ, Kisielewski D, Cassidy DM, McNeilly AD, Gallagher JR, Walsh SV, Honda T, McCrimmon RJ, Dinkova-Kostova AT, Ashford MLJ, Dillon JF and Hayes JD (2018) Experimental Nonalcoholic Steatohepatitis and Liver Fibrosis Are Ameliorated by Pharmacologic Activation of Nrf2 (NF-E2 p45-Related Factor 2). *Cell Mol Gastroenter* **5**:367-398.

Thaiparambil JT, Bender L, Ganesh T, Kline E, Patel P, Liu Y, Tighiouart M, Vertino PM, Harvey RD, Garcia A and Marcus AI (2011) Withaferin A inhibits breast cancer invasion and metastasis at sub-cytotoxic doses by inducing vimentin disassembly and serine 56 phosphorylation. *Int J Cancer* **129**:2744-2755.

Vanden Berghe W, Sabbe L, Kaileh M, Haegeman G and Heyninck K (2012) Molecular insight in the multifunctional activities of Withaferin A. *Biochem Pharmacol* **84**:1282-1291.

Vedi M and Sabina EP (2016) Assessment of hepatoprotective and nephroprotective potential of withaferin A on bromobenzene-induced injury in Swiss albino mice: possible involvement of mitochondrial dysfunction and inflammation. *Cell Biol Toxicol* **32**:373-390.

Wong RJ, Aguilar M, Cheung R, Perumpail RB, Harrison SA, Younossi ZM and Ahmed A (2015) Nonalcoholic steatohepatitis Is the second leading etiology of liver disease among adults awaiting liver transplantation in the United States. *Gastroenterology* **148**:547-555.

Wong RJ, Cheung R and Ahmed A (2014) Nonalcoholic steatohepatitis is the most rapidly growing indication for liver transplantation in patients with hepatocellular carcinoma in the U. S. *Hepatology* **59**:2188-2195.

Wu T, Zhao F, Gao B, Tan C, Yagishita N, Nakajima T, Wong PK, Chapman E, Fang D and Zhang DD (2014) Hrd1 suppresses Nrf2-mediated cellular protection during liver cirrhosis. *Genes Dev* **28**:708-722.

Xie C, Yagai T, Luo Y, Liang X, Chen T, Wang Q, Sun D, Zhao J, Ramakrishnan SK, Sun L, Jiang C, Xue X, Tian Y, Krausz KW, Patterson AD, Shah YM, Wu Y, Jiang C and Gonzalez FJ (2017) Activation of intestinal hypoxia-inducible factor 2alpha during obesity contributes to hepatic steatosis. *Nat Med* **23**:1298-1308.

Yan TT, Wang H, Cao LJ, Wang Q, Takahashi S, Yagai T, Li GL, Krausz KW, Wang GJ, Gonzalez FJ and Hao HP (2018) Glycyrrhizin alleviates nonalcoholic steatohepatitis via modulating bile acids and meta-inflammation. *Drug Metab Dispos* **46**:1310-1319.

## Figure Legends

**Fig. 1: Effect of WA in body weight, liver weight, liver index and liver histology in MCS diet-fed mice. (A)** Experiment scheme for testing the preventive effects of WA in the MCD-induced liver injury model; **(B)** Effect of WA on body weight; **(C)** Effect of WA on liver weight; **(D)**, Effect of WA on liver index; **(E)**, Effect of WA on H&E staining of MCS diet-fed mouse livers. Scale bar size, 100 μm. Data were presented as means ± SD. MCS, mice fed the MCS diet and treated with vehicle; MCS+WA5, mice fed the MCS diet and treated with 5 mg/kg of WA only; MCD, mice fed the MCD diet and treated with vehicle; MCD+WA1, mice fed the MCD diet and treated with 1 mg/kg of WA; MCD+WA2.5, mice fed the MCD diet and treated with 2.5 mg/kg of WA; MCD+WA5, mice fed the MCD diet and treated with 5 mg/kg of WA. n=5 mice per group. Statistical differences were determined by the two-tailed t test between two groups or by one-way ANOVA among multiple MCD diet-fed groups. $^{###}P<0.005$ when compared with MCS group; * $P<0.05$ and ** $P<0.01$ when compared with the MCD group.

**Fig. 2: WA dose-dependently alleviated MCD diet-induced liver injury. (A and B)** Analysis of serum ALT (**A**) and AST levels (**B**). **(C and D)** Analysis of liver TC (**C**) and TG (**D**) levels. **(E and F)** Analysis of serum TC (**E**) and TG levels (**F**). **(G)** Analysis of hepatic pro-inflammatory cytokines mRNA levels. **(H)** H & E staining of livers from MCD diet-fed mice treated with vehicle or 5 mg/kg of WA. **(I)** Oil Red O staining of livers from MCD diet-fed mice treated with vehicle or 5 mg/kg of WA. Scale bar, 100 μm. Data were presented as means ± SD. Group descriptions for the MCS, MCS+WA5, MCD, MCD+WA1, MCD+WA2.5, MCD+WA5 groups were the same as described in the legend to Fig. 1. n=5 mice per group. $^{#}P<0.05$, $^{##}P<0.01$ and $^{###}P<0.005$ when compared with the MCS group; *$P<0.05$, **$P<0.01$, ***$P<0.005$ when compared with the MCD

group. Statistical differences were determined by the two-tailed t test or one-way ANOVA. *Tnfa*, tumor necrosis factor alpha; *Il1b*, interleukin 1b; *Il6*, interleukin 6.

**Fig. 3: WA alleviated MCD diet-induced liver injury independent of body weight change.** **(A)** Experiment scheme for testing the therapeutic effect of WA in MCD diet-induced NASH model; **(B)** Body weights; **(C)** liver weights; **(D)** Liver indexes calculated as the ratio of liver weight to body weight; **(E)** serum ALT levels; **(F)** serum AST levels. Data were presented as means ± SD. Group descriptions for MCS, MCD, and MCD+WA5 were same as described in the legend to Fig. 1. n=5 mice per group. Data were presented as means ± SD. Statistical differences were determined by the two-tailed t test between two groups. *P<0.05 and ***P<0.005 compared with MCD group.

**Fig. 4: WA therapeutically improved MCD diet-induced NASH.** **(A)** Experiment scheme for testing the therapeutic effect of WA in the MCD-induced NASH model. **(B)** Effect of 5 mg/kg WA on body weight. **(C)** Effect of 5 mg/kg WA on liver weight. **(D)** Effect of 5 mg/kg WA on liver indexes. **(E and F)** Analysis of serum ALT (**E**) and AST (**F**) levels in LFD-fed mice and HFD-fed mice treated with control vehicle or WA. **(G and H)** Histology analysis of hepatic steatosis by Oil Red O staining (**G**) and H & E staining (**H**). Scale bar, 100 μm. Data were presented as means ± SD. Descriptions for the MCS, MCS+WA5, MCD, MCD+WA5 groups were same as described in the legend to Fig. 1. n=5 mice per group. $^{\#}$P<0.05, $^{\#\#}$P<0.01 and $^{\#\#\#}$P<0.005 when compared with MCS group; *P<0.05 when compared with MCD group. Statistical differences were determined by the two-tailed t test or one-way ANOVA.

**Fig. 5: WA improved HFD-induced liver injury. (A)** Experiment scheme of the time-course dosing regimen. **(B and C)** Body weights of HFD-fed mice (**B**) and LFD-fed mice (**C**) treated with vehicle or WA. **(D and E)** Liver weights (**D**) and liver indexes calculated by liver weight/body weight ratio (E). **(F and G)** Analysis of serum ALT (**F**) and AST levels (**G**). Data were presented as means ± SD. LV, mice fed the LFD and treated with vehicle (V); L+4W WA, mice fed LFD and treated with WA for the last 4 weeks. L+8W WA, mice fed the LFD and treated with WA for the last 8 weeks; L+12W WA, mice fed the LFD and treated with WA for the last 12 weeks; NV, mice fed the HFD-induced NASH diet (N) and treated with vehicle (V); N+4W WA, mice fed the HFD-induced NASH diet (N) and treated with WA for the last four weeks; N+8W WA, mice fed the HFD-induced NASH diet (N) and treated with WA for the last 8 weeks; N+12W WA, mice fed the HFD-induced NASH diet (N) and treated with WA for the last 12 weeks. n=5 mice for the LFD-fed groups and n=7-10 for HFD-fed mice. $^{\#\#}P<0.01$ and $^{\#\#\#}P<0.005$ compared with the LFD group; $*P<0.05$ and $***P<0.005$ compared with HFD group. Statistical differences were determined by the two-tailed t test or one-way ANOVA.

**Fig. 6: WA improved serum and liver biochemical parameters in a time-dependent manner. (A and B)** Analysis of liver TG levels (**A**) and TC levels (**B**). **(C and D)** Analysis of serum TG (**C**) and TC (**D**) levels. **(E and F)** Analysis of liver NEFAs levels (E) and serum NEFAs levels (**F**). Data were presented as means ± SD. Groups for the LV, NV, N+4W WA, N+8W WA, and N+12W WA groups were same as described in the legend to Fig. 5. n=5 mice for the LFD group and n=7-10 for the other three HFD-fed groups. $^{\#\#}P<0.01$ and $^{\#\#\#}P<0.005$ compared with LFD group; $**P<0.01$ and $***P<0.005$ compared with the HFD group. Statistical differences were determined by the two-tailed t test or one-way ANOVA.

**Fig. 7: WA improved HFD-induced hepatic steatosis and inflammation. (A and B)** Representative histology pictures of H & E staining (**A**) and Oil Red O staining (**B**). Scale bar, 100 μm. **(C-E)** Effect of WA on HFD-induced liver *Tnfa*, *Il1b*, and *Il6* mRNA levels. **(F-G)** Effect of WA on HFD-induced hepatic ER stress signaling markers, *Hspa5* and *Didt3,* mRNAs levels. **(H-J)** Effect of WA on HFD-induced *Srebp1c*, *Fas*, and *Scd1* mRNAs levels. Data were presented as means ± SD. Descriptions for the LV, NV, N+4W WA, N+8W WA, and N+12W WA were same as described in the legend to Fig. 5. n=5 mice for the LFD group and n=7-10 for the other three HFD-fed groups. ###P<0.005 compared with LFD group; *P<0.05, **P<0.01 and ***P<0.005 compared with the HFD group. Statistical differences were determined by the two-tailed t test or one-way ANOVA.

**Fig. 8: WA improved HFD-induced hepatic fibrosis. (A)** Representative hepatic picrosirius red staining for both LFD-fed livers and HFD-fed livers. Scale bar, 100 μm. **(B)** Statistical quantitation analysis of picrosirius red staining for liver collagen. **(C-F)** Analysis of *Timp2*, *Col1a1*, *Mmp2*, and *Acta2* mRNAs. Data were presented as means ± SD. Descriptions for the LV, NV, N+4W WA, N+8W WA, and N+12W WA groups were same as described in the legend to Fig. 5. n=5 mice for LFD group and n=7-10 for the other three HFD-fed groups. ###P<0.005 when compared with the LFD group; *P<0.05, **P<0.01, while ***P<0.005 when compared with the HFD group. Statistical differences were determined by the two-tailed t test or one-way ANOVA.

**Fig. 9: WA rescued HFD-induced ceramides accumulation and oxidative stress. (A-G)** Quantitation of serum ceramide concentrations for C16 (**A**), C18 (**B**), C20 (**C**), C22 (**D**), C24 (E),

C18:1 (**F**) and C24:1 (**G**). **(H-J)** Analysis of hepatic superoxide dismutase levels (H), glutathione levels (**I**) and peroxide levels. (**J**) Data were presented as means ± SD. Descriptions for the LV, NV, N+4W WA, N+8W WA, and N+12W WA groups were same as described in the legend to Fig. 5. n=5 mice for the LFD-fed groups and n=7-10 for the HFD-fed groups. ###P<0.005 compared with the LFD group; *P<0.05, ** P<0.01 and *** P<0.005 compared with HFD group. Statistical differences were determined by the two-tailed t test or one-way ANOVA.

**Fig. 10: WA treatment reduced ceramides biosynthesis and catabolism in WA treated HFD-fed C57bl/6N mice and ER-stress markers in a time dependent manner. (A-M)** Ceramides biosynthesis and catabolism markers analysis of *Sptlc1* **(A)**, *Sptlc2* **(B)**, *Smpd1* **(C)**, *Smpd2* **(D)**, *Smpd3* **(E)**, *Smpd4* **(F)**, *Acer2* **(G)**, *Acer3* **(H)**, *Sgms1* **(I)**, *Sgms2* **(J)**, *Cers2* **(K)**, *Cers4* **(L)** and *Cers6* **(M)** mRNA levels. Descriptions for the LV, NV, N+4W WA, N+8W WA, and N+12W WA were same as described in the legend to Fig. 5. n=5 mice for the LFD group and n=7-10 for the other three HFD-fed groups. ###P<0.005 compared with LFD group; *P<0.05, **P<0.01, and *** P<0.005 compared with the HFD group. Statistical differences were determined by the two-tailed t test or one-way ANOVA.

**Fig. 11: WA improved HFD-induced liver injury in ob/ob mice and liver histology. (A)** Experimental scheme for testing the therapeutic effect of WA in the HFD diet-induced NASH model. **(B)** Body weights. **(C and D)** liver weights **(C)** and liver indexes calculated by liver weight/body weight ratios **(D)**. **(E and F)** Analysis of serum ALT (**E**) and AST levels (**F**). **(G and H)** Representative histology pictures of H & E staining (**G**) and Oil Red O staining (**H**) for HFD and WA treated HFD livers. Scale bar, 100 μm. (**I**) Effect of WA on HFD-induced liver *Il1b*, *Il6,*

*Tnfa*, *Srebp1c*, *Fas*, and *Scd1* mRNAs levels. Data were presented as means ± SD. NV, mice fed the HFD-induced NASH diet (N) and treated with vehicle (V) for 12 weeks; N+ WA5, mice fed the HFD diet and treated with 5 mg/kg of WA mice fed the HFD-induced NASH diet (N) and treated with WA for the last four weeks; n=5 mice for the HFD-fed vehicle groups and n=8 for WA treated HFD-fed ob/ob mice. *P<0.05, **P<0.01, and ***P<0.005 compared with HFD group. Statistical differences were determined by the two-tailed t test.

**Fig. 12: WA treatment improved serum and liver biochemical parameters, reduces HFD-induced hepatic fibrosis, and mRNAs associated with ER-stress and ceramides biosynthesis and catabolism in WA-treated HFD-fed ob/ob mice. (A-F)** Analysis of liver TG levels (**A**), TC levels (**B**); NEFAs levels **(C);** analysis of serum TG (**D**) serum TC (**D**) levels and serum NEFAs levels (**F**). **(G)** Hepatic fibrosis markers analysis of *Timp2*, *Col1a1*, *Mmp2*, and *Acta2* mRNAs levels. **(H)** Representative hepatic picrosirius red staining for HFD and WA treated HFD livers, Scale bar 100 μm. **(I)** Hepatic endoplasmic reticulum stress signaling markers analysis of *Hspa5* and *Didt3* mRNA levels **(J)** *Sptlc1*, *Sptlc2*, *Smpd2*, *Smpd3*, *Acer1*, *Acer2*, *Sgms1*, *Sgms2*, *Cers2*, *Cers4* and *Cers6* mRNA levels. Data were presented as means ± SD. NV, mice fed the HFD-induced NASH diet (N) and treated with vehicle (V) for 12 weeks; N+ WA5, mice fed the HFD diet and treated with 5 mg/kg of WA mice fed the HFD-induced NASH diet (N) and treated with WA for the last four weeks; n=5 mice for the HFD-fed vehicle groups and n=8 for WA treated HFD-fed ob/ob mice. *P<0.05, **P<0.01 and ***P<0.005 compared with HFD group. Statistical differences were determined by the two-tailed t test.

**Fig. 13: Summary of major findings and proposed mechanism.** In the current study, withaferin A (WA) was found to have both preventive and therapeutic effects in treating NASH as assessed by using two NASH models. MCD diet feeding, on the other hand, induced weight loss and thus was called the "Lean NASH" model, while the HFD-induced obesity was referred to as the "Obese NASH" model. HFD feeding induced oxidative stress and oxidative stress could contribute to the increase in serum ceramide accumulation that was known to promote the progression of NASH. In the HFD-induced obese NASH model, WA alleviated HFD-induced oxidative stress as revealed by the decreased $H_2O_2$ and increased glutathione and superoxide dismutase levels. WA also significantly alleviated HFD-induced ceramides accumulation in serum. However, other factors could also contribute to ceramide accumulation in the HFD-induced NASH model and how WA affects them still requires further study. Abbreviations used: MCD, methionine and choline deficient; HFD, high-fat diet; NASH, non-alcoholic steatohepatitis.

JPET Fast Forward. Published on August 16, 2019 as DOI: 10.1124/jpet.119.256792
This article has not been copyedited and formatted. The final version may differ from this version.

**Figure 1**

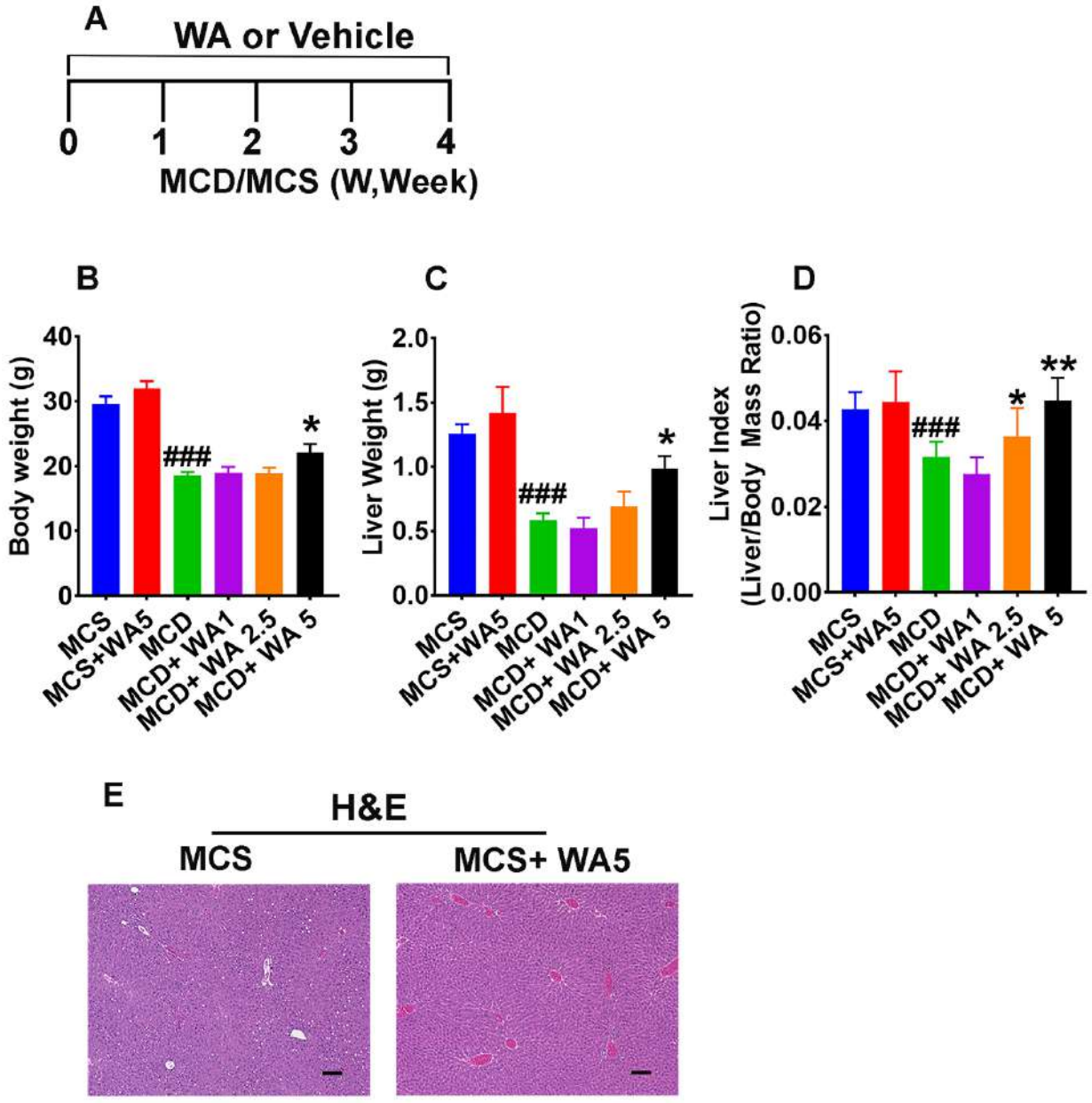

JPET Fast Forward. Published on August 16, 2019 as DOI: 10.1124/jpet.119.256792
This article has not been copyedited and formatted. The final version may differ from this version.

## Figure 2

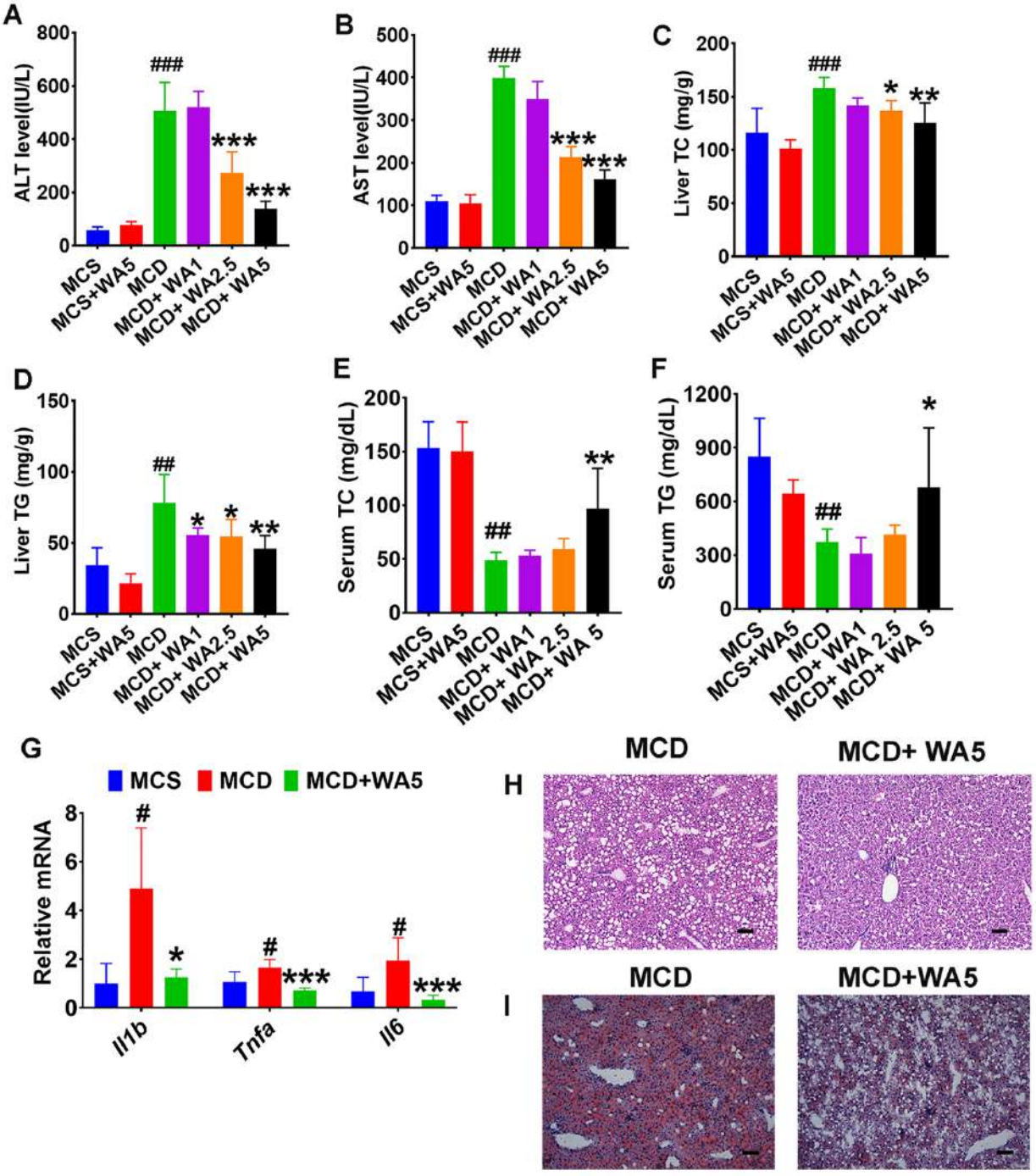

JPET Fast Forward. Published on August 16, 2019 as DOI: 10.1124/jpet.119.256792
This article has not been copyedited and formatted. The final version may differ from this version.

## Figure 3

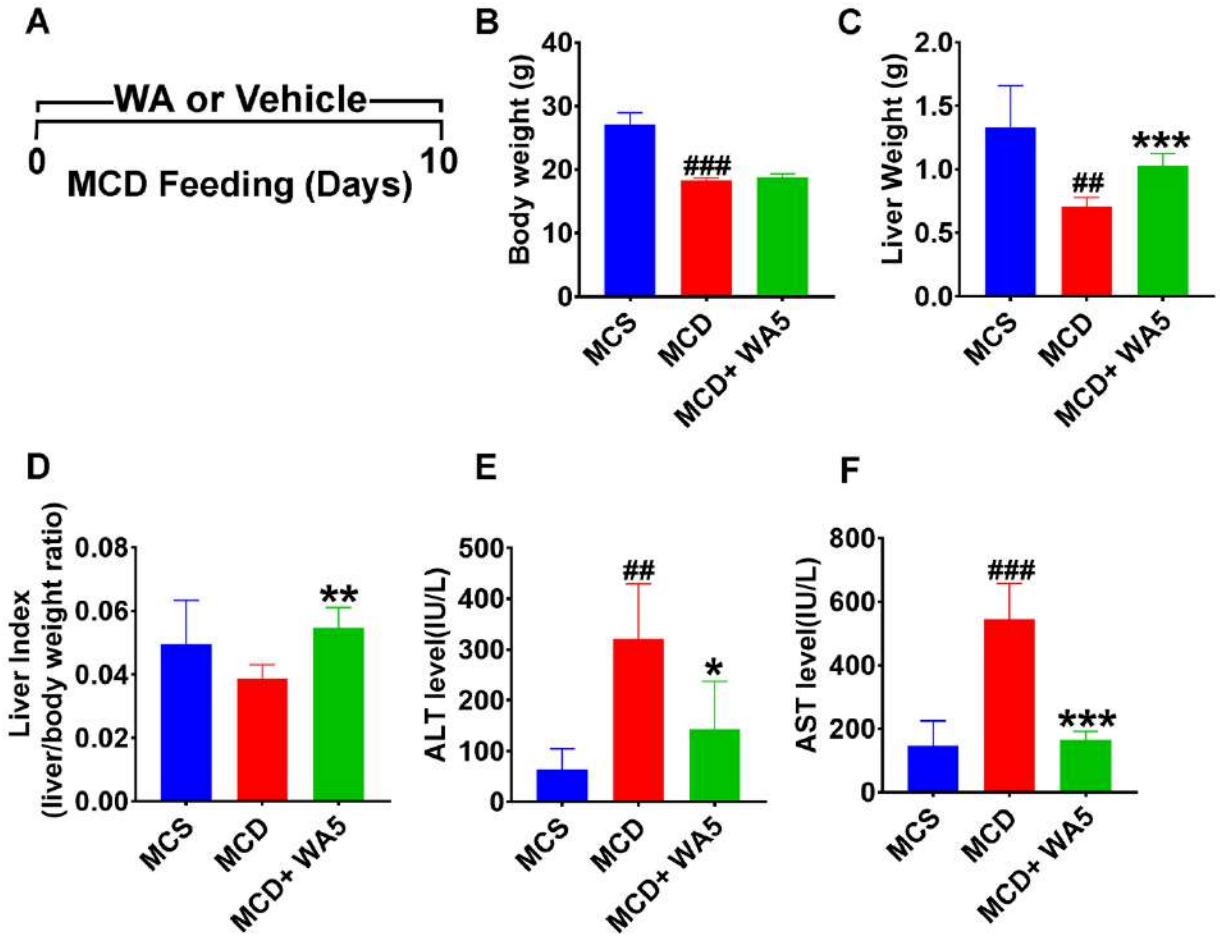

JPET Fast Forward. Published on August 16, 2019 as DOI: 10.1124/jpet.119.256792
This article has not been copyedited and formatted. The final version may differ from this version.

## Figure 4

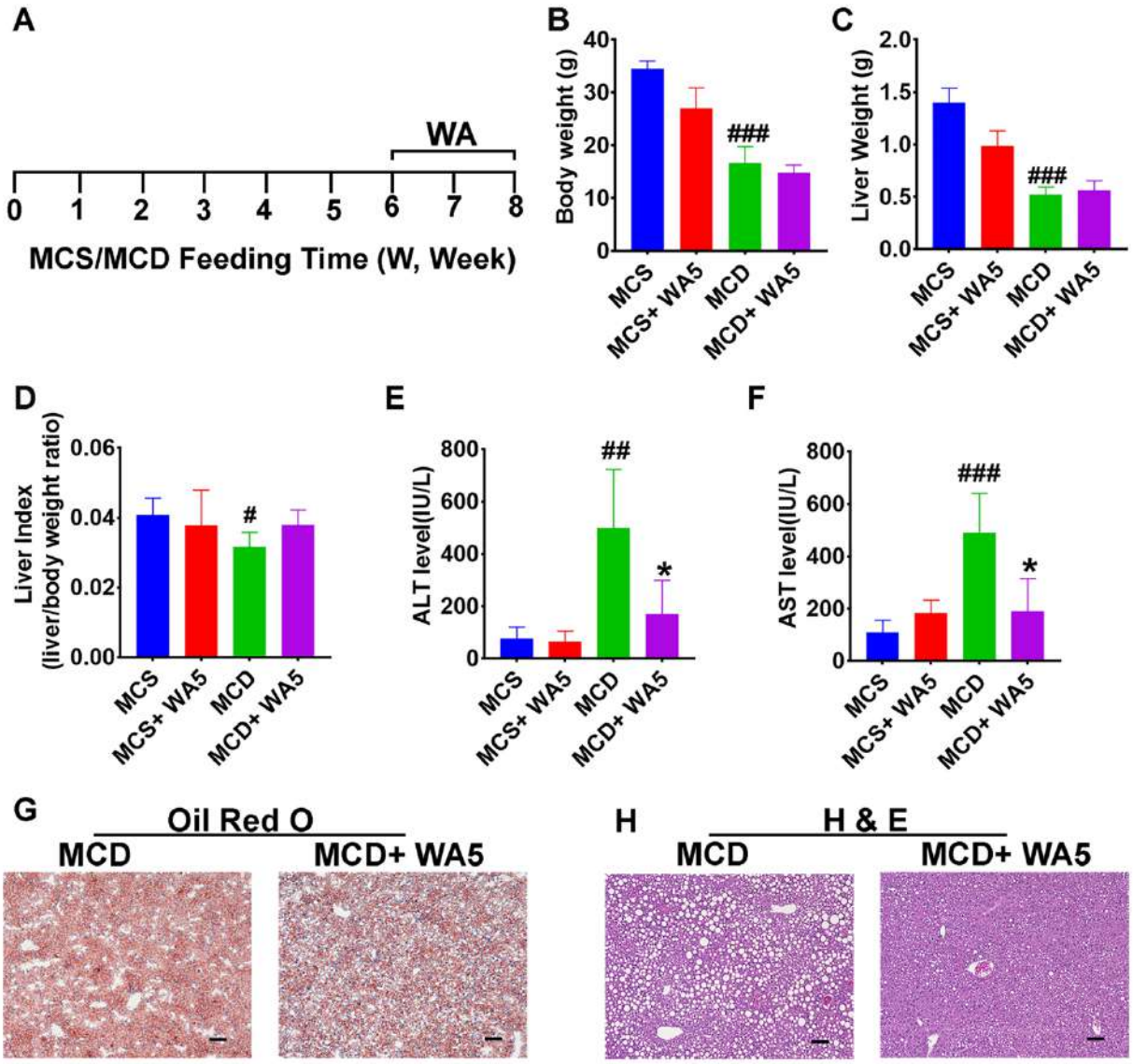

JPET Fast Forward. Published on August 16, 2019 as DOI: 10.1124/jpet.119.256792
This article has not been copyedited and formatted. The final version may differ from this version.

## Figure 5

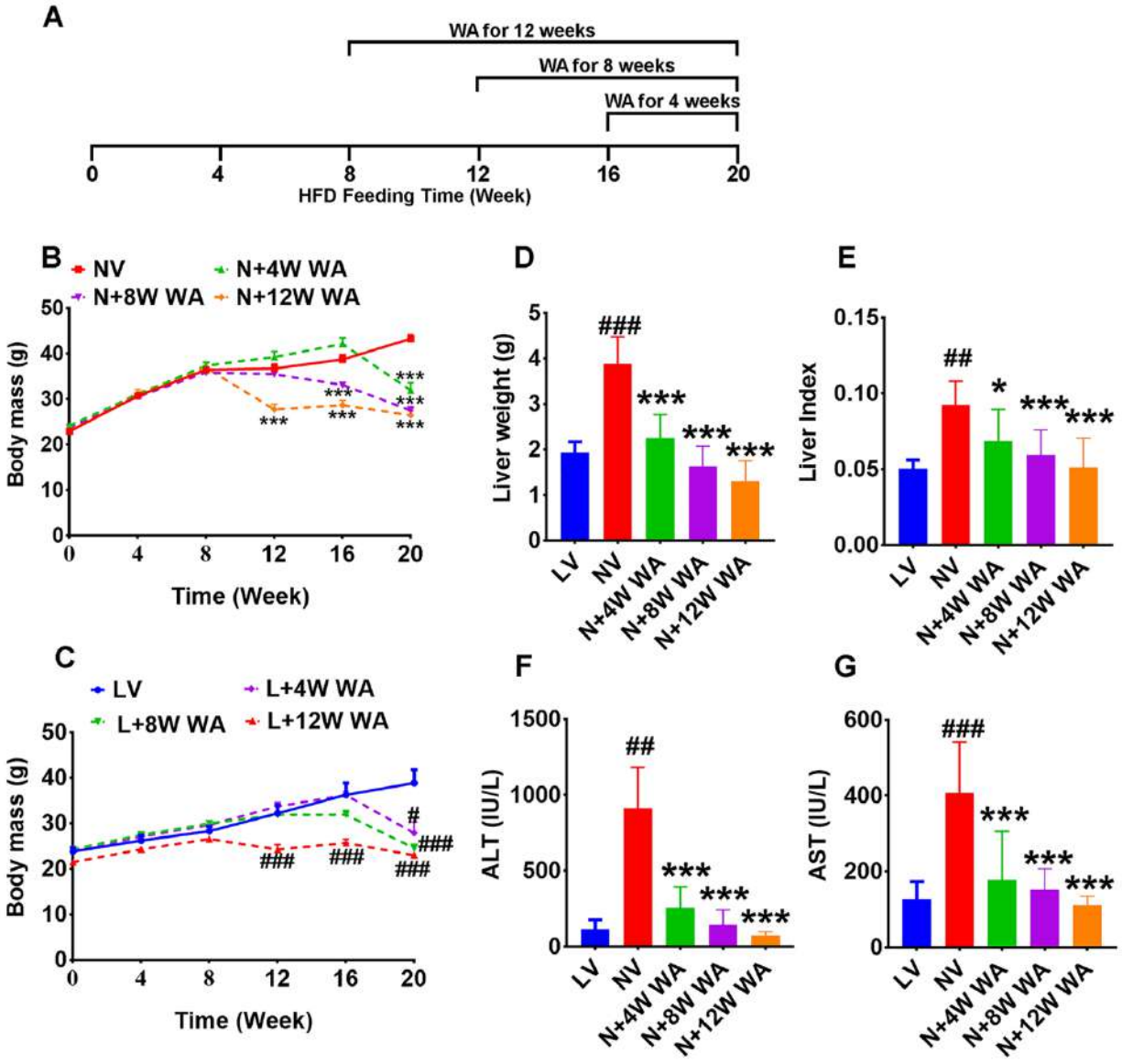

JPET Fast Forward. Published on August 16, 2019 as DOI: 10.1124/jpet.119.256792
This article has not been copyedited and formatted. The final version may differ from this version.

## Figure 6

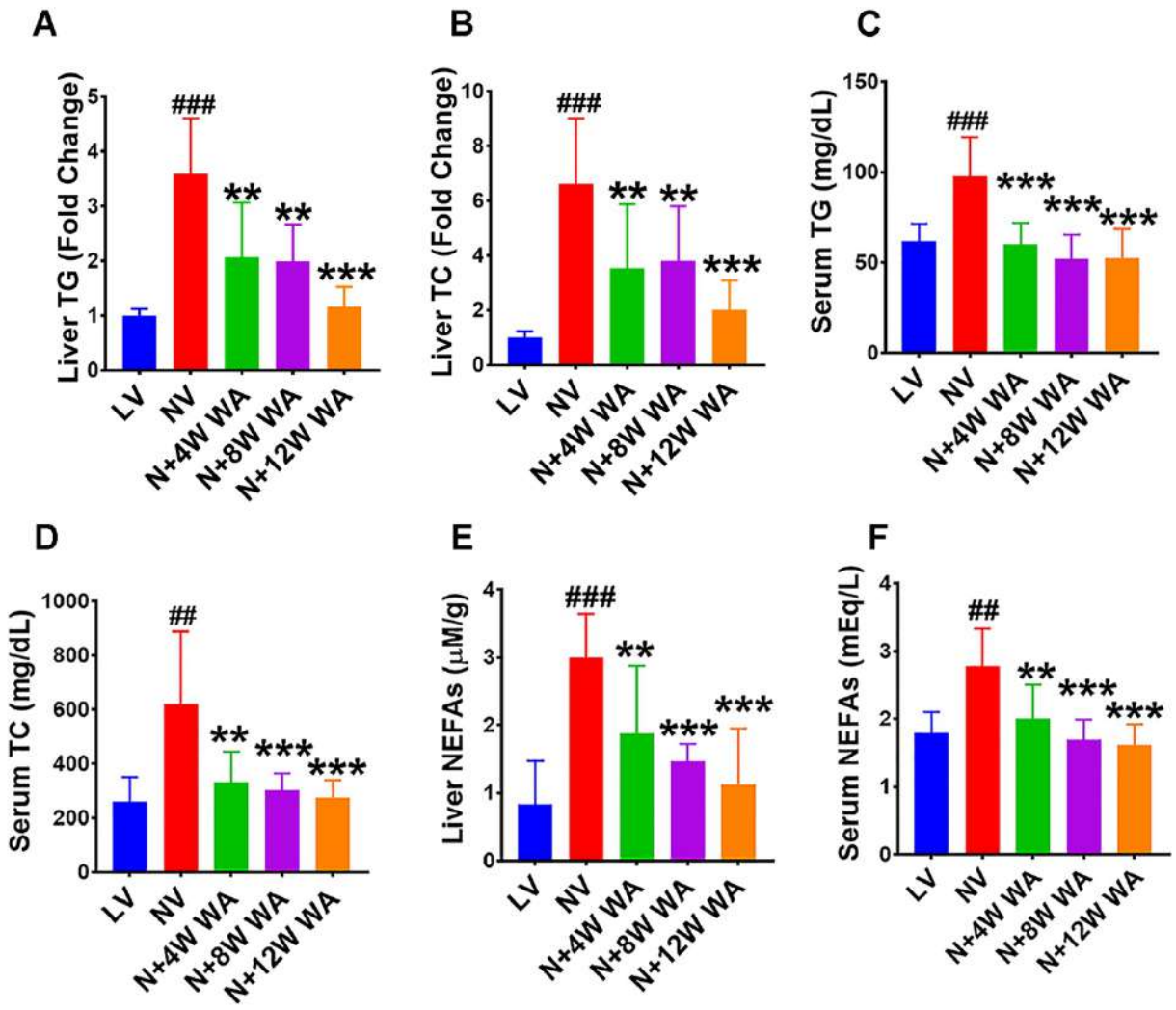

JPET Fast Forward. Published on August 16, 2019 as DOI: 10.1124/jpet.119.256792
This article has not been copyedited and formatted. The final version may differ from this version.

## Figure 7

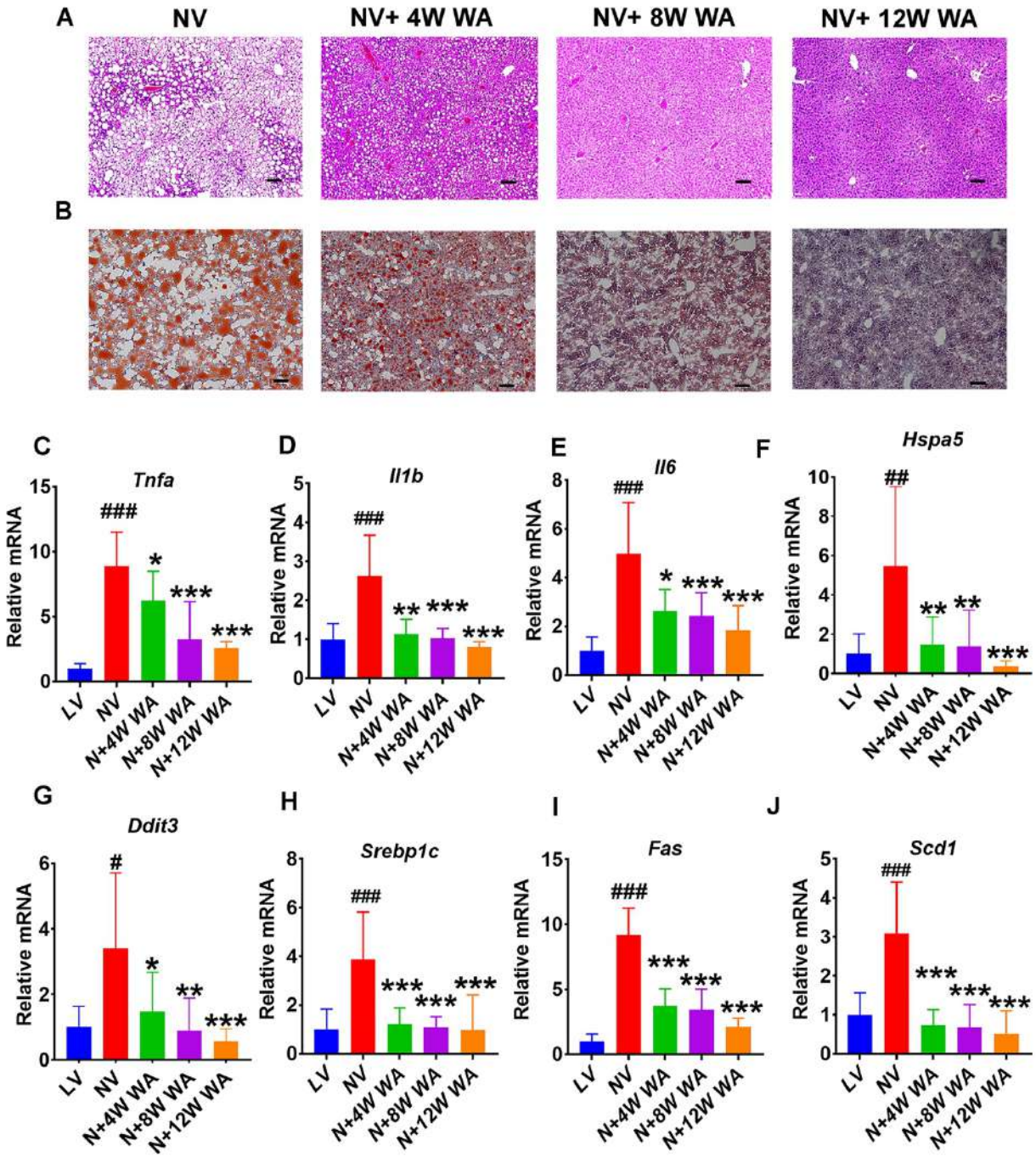

JPET Fast Forward. Published on August 16, 2019 as DOI: 10.1124/jpet.119.256792
This article has not been copyedited and formatted. The final version may differ from this version.

## Figure 8

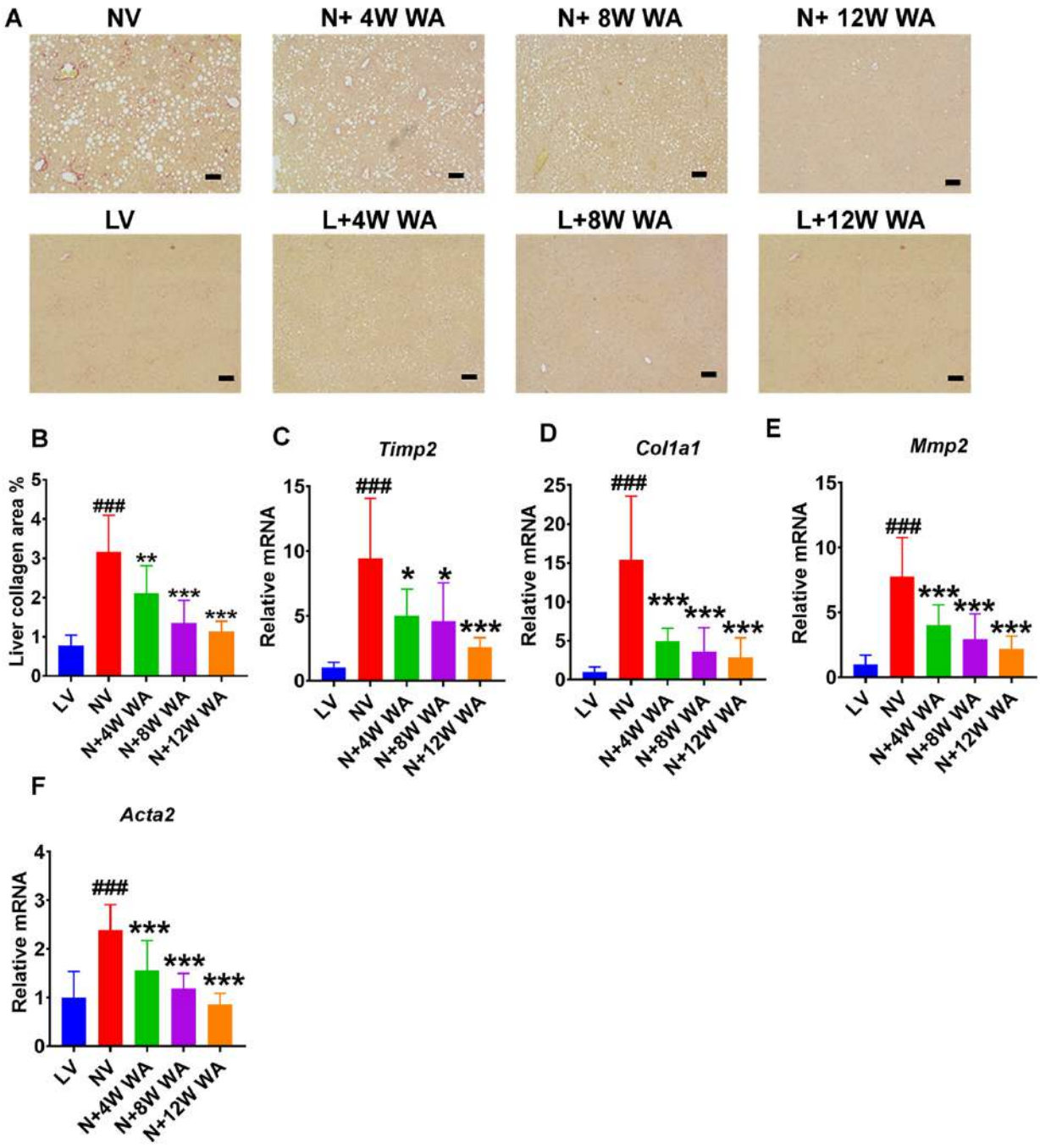

JPET Fast Forward. Published on August 16, 2019 as DOI: 10.1124/jpet.119.256792
This article has not been copyedited and formatted. The final version may differ from this version.

## Figure 9

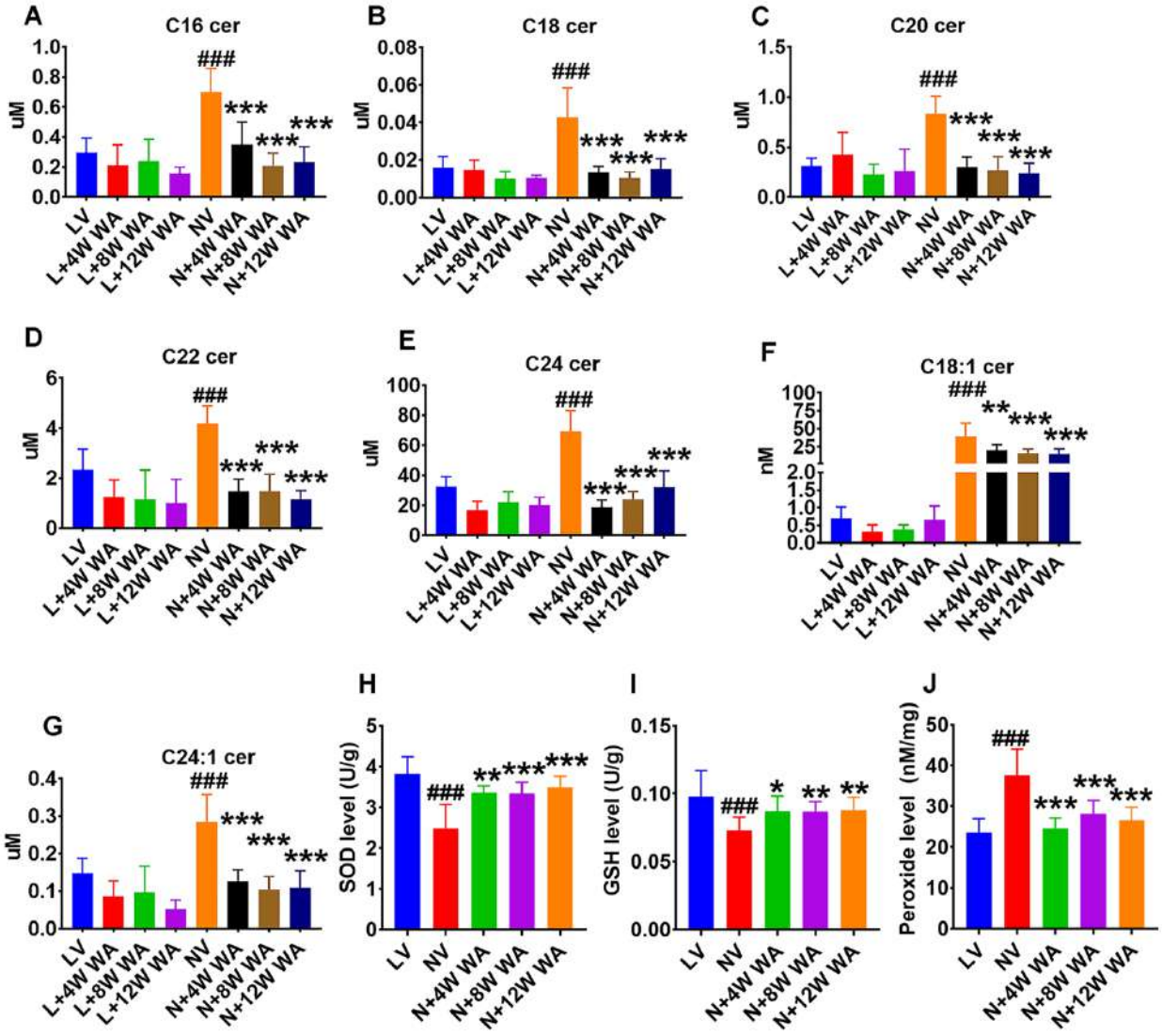

JPET Fast Forward. Published on August 16, 2019 as DOI: 10.1124/jpet.119.256792
This article has not been copyedited and formatted. The final version may differ from this version.

## Figure 10

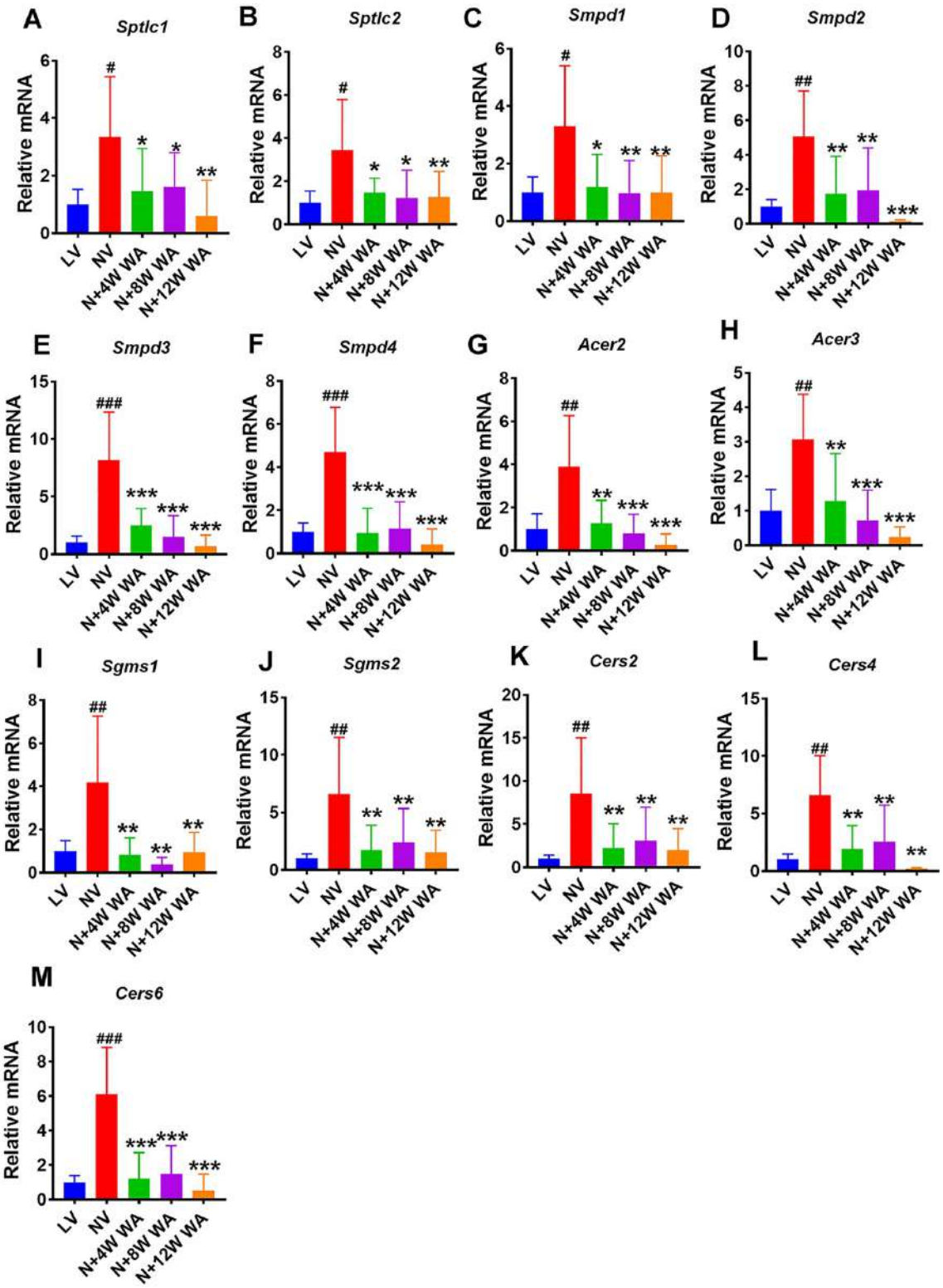

JPET Fast Forward. Published on August 16, 2019 as DOI: 10.1124/jpet.119.256792
This article has not been copyedited and formatted. The final version may differ from this version.

## Figure 11

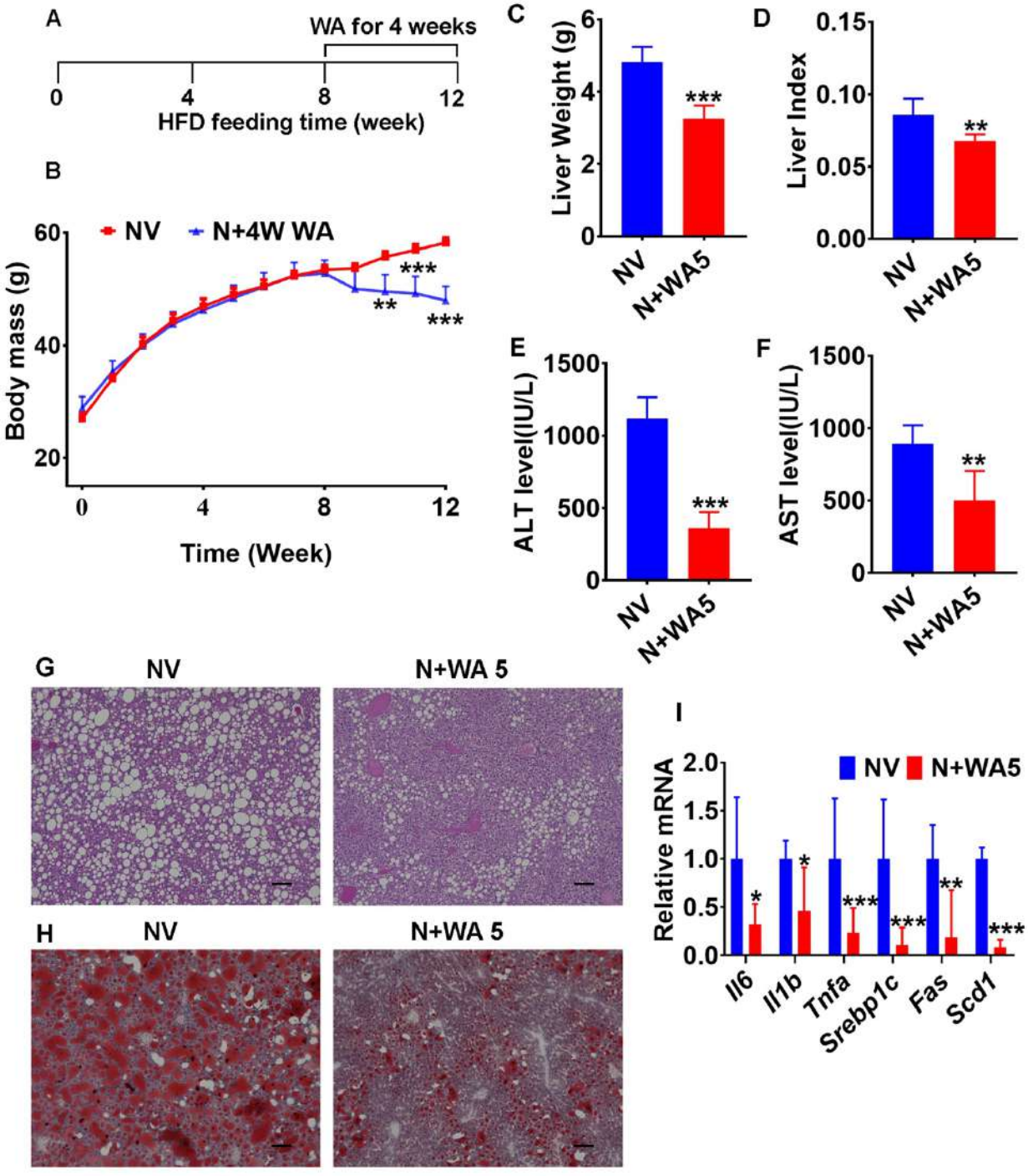

JPET Fast Forward. Published on August 16, 2019 as DOI: 10.1124/jpet.119.256792
This article has not been copyedited and formatted. The final version may differ from this version.

## Figure 12

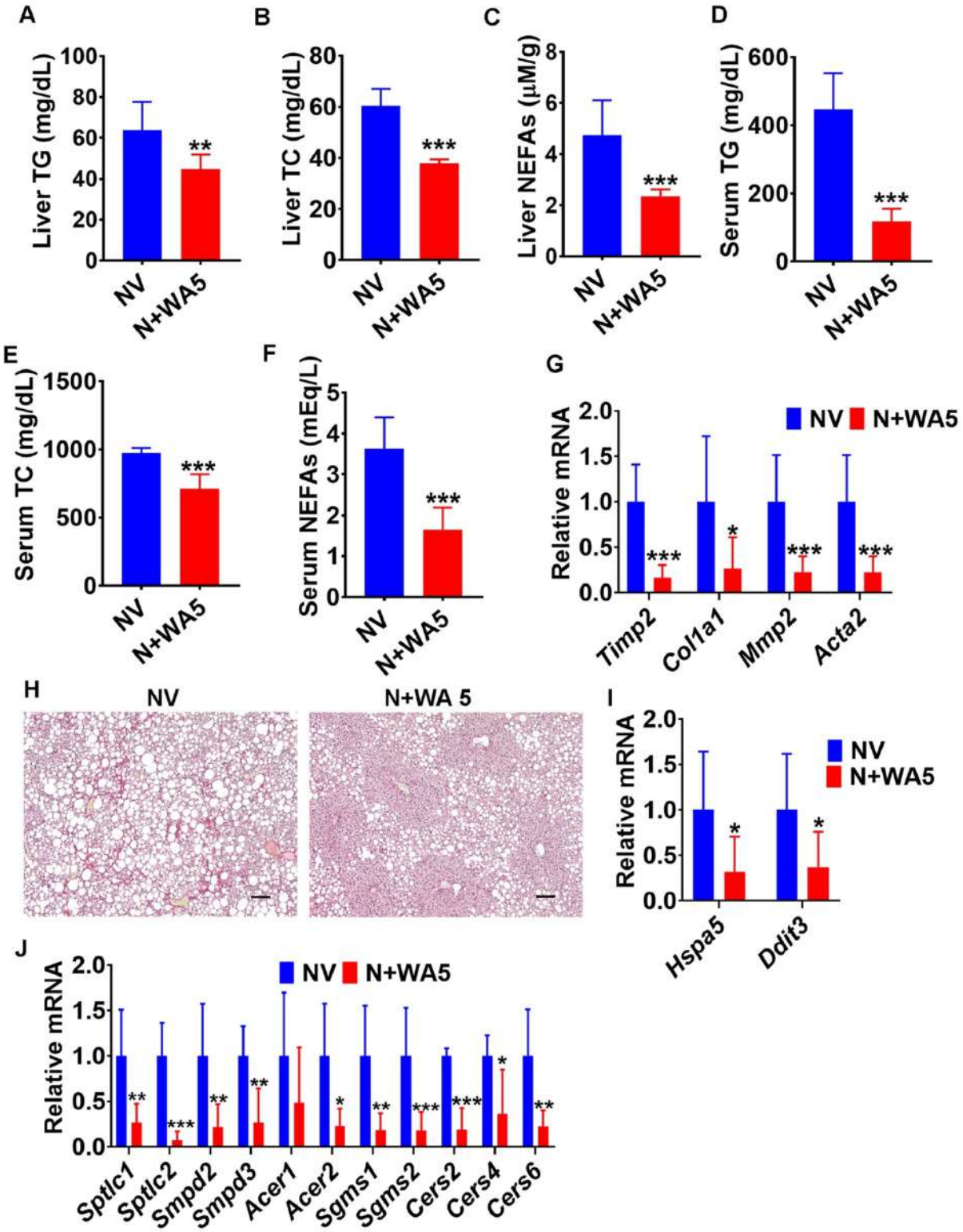

JPET Fast Forward. Published on August 16, 2019 as DOI: 10.1124/jpet.119.256792
This article has not been copyedited and formatted. The final version may differ from this version.

**Figure 13**